MASSACHUSETTS INSTITUTE OF TECHNOLOGY

HYDRODYNAMICS LABORATORY

DEPARTMENT OF CIVIL AND SANITARY ENGINEERING

TECHNICAL REPORT NO. 44

NON-LINEAR STANDING WAVES
IN A RECTANGULAR
TANK DUE TO FORCED OSCILLATION

by

J. D. LIN and L. N. HOWARD

OCTOBER 1960

HYDRODYNAMICS LABORATORY

Department of Civil and Sanitary Engineering

Massachusetts Institute of Technology

NON-LINEAR STANDING WAVES IN A RECTANGULAR

TANK DUE TO FORCED OSCILLATION

by

J. D. Lin and L. N. Howard

October 1960

Technical Report No. 44

BLANK PAGE

ACKNOWLEDGEMENT

ABSTRACT

This study is concerned with standing waves generated by a two-dimensional wave maker in a rectangular tank. The theoretical investigation was first based on the well-known linear theory of surface waves. The linearized version of the problem is basically two-dimensional and the solution of forced two-dimensional standing waves of small amplitude was obtained. Then, a system of equations, based on the exact free surface conditions, was derived for solutions of forced two-dimensional standing waves of finite amplitude. A non-linear solution corresponding to any mode of oscillation can in general be obtained by the method of iteration from the system of equations. However, only the fundamental mode was solved here for the velocity potential, free surface elevation and frequency-amplitude relation with the computation carried to the third order of approximation. The frequency-amplitude curves for two constant amplitudes of wave maker were found to consist of two non-intersecting branches of oscillation; the range of significant non-linear effects was also determined for the particular mode. Two profiles of standing waves were computed for the frequencies on each branch of the oscillation.

The stability of non-linear forced two-dimensional standing waves was studied by investigating the possibility of excitation of the fundamental mode of cross waves. A system of equations was again derived for solutions of

cross waves by extending the method used in the two-dimensional case. The solution corresponding to the first mode of the longitudinal component and the first mode of cross waves was solved by the method of iteration to the second order of approximation, and yields the following results:

(1) The half-frequency relation between the cross waves and wave maker,

(2) The frequency for excitation of the cross waves,

(3) The length/width ratios of the tank at which the cross waves can be excited by an infinitesimal amplitude of wave maker, and

(4) The phase relation between the cross waves and the wave maker.

The experimental investigation comprises essentially two parts: forced two-dimensional standing waves and cross waves. The experiment of two-dimensional standing waves serves as a verification of the theoretical solutions for both the frequency-amplitude relation and the profile of the standing waves. A satisfactory agreement was indicated in the comparison of the theoretical prediction and of the experimental results. For cross waves, the frequency-amplitude curve was obtained from the experiment in addition to confirming the results of the theoretical analysis above mentioned.

TABLE OF CONTENTS

-iv-

TABLE OF CONTENTS (cont'd.)

LIST OF FIGURES AND TABLES

LIST OF NOTATIONS

A_{mn}, a_n, c_n	dimensionless coefficients in Fourier's series for ζ
B_{mn}, b_n, d_n	dimensionless coefficients in Fourier's series for φ
A^*	total amplitude of standing waves, inches
A	dimensionless total amplitude of standing waves
E	function defined in Eqs. (4.4) or (A.10)
f_s	function defined in Eq. (B.21)
F	function defined in Eqs. (5.8) or (B.19)
h	depth of water, inches
k	wave number $= \dfrac{2\pi}{\lambda}$
K_n	coefficients defined in Eqs. (4.46) to (4.50)
ℓ	length/width ratio of the tank $= \dfrac{L}{W}$
L	effective length of the tank, inches
M,N,p m,n,s	positive integers
$\underline{q}^*$, $\underline{q}$	dimensional and dimensionless velocity vectors
S_N	functions defined in Eq. (A.6)
S_N	functions defined in Eq. (B.12)
T_N	functions defined in Eq. (B.7)
t^*, t	dimensional and dimensionless time
x^*, y^*, z^*	components of rectangular coordinates, inches
x, y, z	dimensionless components of rectangular coordinates

α^*	(alpha)	amplitude of wave maker on undisturbed free surface, inches
α		dimensionless amplitude of wave maker
β	(beta)	parameter for the frequency-amplitude curve of non-linear two-dimensional standing waves
γ^*, γ	(gamma)	dimensional and dimensionless coefficients in the argument of exponential function for the motion of wave maker, Eq. (2.9)
δ	(delta)	parameter for the frequency-amplitude curve of cross waves
ϵ	(epsilon)	phase angle
ζ^*	(zeta)	free surface elevation, inches
ζ		dimensionless free surface elevation
θ	(theta)	angle of oscillation of wave maker
λ, λ_c	(lambda)	dimensionless wave lengths of two-dimensional standing waves and cross waves
λ^*, λ_c^*		wave lengths of two-dimensional standing waves and cross waves, inches
λ, μ	(lambda, mu)	parameters
ν_n	(nu)	$= \sqrt{\ell^2 + n^2}$
σ^*	(sigma)	angular frequency of longitudinal waves and wave maker, $\sec^{-1}$
σ		dimensionless angular frequency of longitudinal waves and wave maker
σ_n		resonance frequency of the nth mode of longitudinal standing waves
σ_{mn}		resonance frequency of the mn^{th} mode of three-dimensional standing waves

LIST OF NOTATIONS (Cont'd.)

τ (tau)   correction factor for depth correction

Φ^* (phi)   velocity potential, ft.^{2}/sec.

Φ, φ dimensionless velocity potential

ω^* (omega)   angular frequency of cross waves, sec^{-1}

ω dimensionless angular frequency of cross waves

ω_n resonance frequency of the nth mode of cross waves

BLANK PAGE

I. INTRODUCTION

In the past decades the mathematical theory of water waves has been extensively developed. Experimental work becomes increasingly important to examine the theoretical analysis and to explore more facts for the development of more sophisticated problems in the field. In experimental investigations wave makers are generally used to generate different types of waves on the free surface of liquid for the study of wave motions under certain boundary conditions or of the interaction of waves with bodies in the liquid. Most frequently, there arise two-dimensional problems and two-dimensional progressive or standing waves are required for experimental investigations. It was observed that the two-dimensionality of the motion produced by a two-dimensional wave maker could not be preserved under certain circumstances due to lateral instability. This instability occurs in the form of standing waves with their crest lines normal to the wave maker [1, 2, 15](1). For a long channel with dissipation at the far end the standing waves appear only near the wave maker and their amplitudes decay rapidly along the channel; while for a finite-length channel with a vertical wall at the far end finite-amplitude standing waves of this type can be generated [3, 4]. The frequency of the standing waves was found to be only half that of wave maker as a subharmonic mode of forced oscillation. Hereafter, this type of standing waves is called cross waves.

As a general approach to the study of three-dimensional surface waves generated by two-dimensional wave maker, a rectangular channel of finite width and length is desirable for the energy in the system is finite and thus the assumption of a radiation condition at infinity can be avoided. Furthermore, in a slightly dissipative system, the effect of viscosity on three-dimensional waves in a long channel becomes significant. Ursell [3] showed that the amplitude of waves is exponentially damped along a semi-infinite channel of constant width and depth. A slightly dissipative system will be considered here; hence, a rectangular tank with a pair of wave makers parallel to each other and normal to the side walls is taken to be a mathematical model in this investigation. Here, we mean by a slightly dissipative system that the effect of viscosity can be neglected but there does exist slight dissipation to decay all modes of free oscillation and thus to ensure a periodic motion due to forced oscillation. For forced oscillation the motion in general consists of free modes of oscillation and a forced periodic motion due to forcing agency. The term, forced oscillation,

---

(1) Numbers in [ ] refer to References.

used in this study refers only to the forced periodic motion in a restricted sense as a result of slight dissipation in the system.

The objective of the present investigation is to study, both theoretically and experimentally, the stability of forced two-dimensional standing waves and the mechanics of excitation of cross waves by two-dimensional wave makers in a rectangular tank. A complete investigation of the problem of forced three-dimensional standing waves in a rectangular tank is not possible due to the fact that it is non-linear with infinitely-many degrees of freedom for oscillation. However, some particular solutions of practical significance can be investigated in a restricted manner. The problem of forced two-dimensional standing waves of finite amplitude will be solved as a family of particular solutions to the problem as a whole, and then the cross waves will be investigated. Therefore, the stability referred to here is in the sense that two-dimensional standing waves can be preserved without exciting the fundamental mode of cross waves.

1. Linear System

It is natural to begin the study by investigating the linearized version of the problem. The classical process of linearization will lead the problem to a linear two-dimensional one, the general solution of which is to be found as a system of forced two-dimensional standing waves of small amplitude. A spectrum of resonance frequencies of the two-dimensional system can then be obtained. As is known in the linear theory of oscillation, the linear solution is not valid when the system is in resonance, which is defined by the phenomenon that the amplitude predicted by the linear solution approaches infinity as the forcing frequency approaches a resonance frequency of the spectrum. However, the non-linearity and viscosity prevent the amplitude of standing waves from becoming infinite. Since the linear system is basically two-dimensional, the two-dimensional standing waves of small amplitude are always stable except in the neighborhood of each resonance frequency of the system. In order to investigate the range of stability in the system as a whole, non-linear solutions have to be investigated in each neighborhood of a resonance frequency. A non-linear solution of two-dimensional standing waves will first be obtained and then the non-linear solution of cross waves of the fundamental mode for the purpose of investigating stability.

2. Non-linear Two-dimensional System

Finite-amplitude progressive waves have been subject to numerous investigations since Russell's experiments [5]. The problem was first solved by Stokes in 1847 [6] and subsequently extended and refined by other authors [7-13] by the method of successive approximation based on the exact free

surface conditions. The existence theory was finally estab-
lished by a proof of Levi-Civita [10] for the infinite-depth
case and later extended to finite-depth case by Struik [11].
No analysis of similar kind was available for finite-ampli-
tude standing waves until in 1952 Penney and Price [14]
treated the problem of free two-dimensional standing waves
of finite amplitude. The difficulty involved here is that
for progressive waves of permanent form a uniform velocity
can be superposed on the system and then the problem is re-
duced to a steady two-dimensional motion. This mathematical
simplicity does not exist in standing waves. However, they
solved it by expressing the velocity potential and free sur-
face elevation as two Fourier series in x with coefficients
which are functions of t and then approximating to these
coefficients as Fourier series in t by the method of per-
turbation. The resulting solution is in the form of a
double Fourier series in x and t with coefficients which
are power series in a constant A (A/π is approximately
equal to the wave-height/wave-length ratio). In order to
investigate the highest standing waves, their solution for
the deep water case was carried to the fifth order. The
same problem was later investigated experimentally by
Taylor [1], who made a series of experiments to produce the
highest two-dimensional standing waves. The free standing
waves were produced approximately by a pair of wave makers
executing small-amplitude oscillatory motion in a rectangu-
lar tank near the resonance frequency of the fundamental
mode. The experimental results were in good agreement with
the profile predicted by Penney and Price; in particular,
the 90° angle at the crest of the highest standing waves
was verified. The frequency-amplitude curve of forced stand-
ing waves was found to consist of two non-intersecting
branches which are similar to those occurring in the theory
of non-linear mechanical oscillators. In his experiment,
lateral instability was observed to set in at the moment
when the standing waves reached a sufficiently high amplitude.

The approach adopted here to solve the problem of forced
two-dimensional standing waves of finite amplitude is similar
to Penney and Price's approach. Of course, the existence and
stability of two-dimensional waves has to be assumed for the
moment. A theoretical investigation of the two-dimensional
system will be carried out here. The non-linear solutions
in the forms of the velocity potential, free surface elevation
and frequency-amplitude relation will be obtained for small
amplitudes of the wave maker. The solution will also provide
quantitatively the range in which significant non-linear
effects occur. The experimental investigation in this case
will serve essentially as a verification of the theoretical
results. Due to the possibility of exciting cross waves in
the three-dimensional system, forced two-dimensional standing

waves may become unstable under certain circumstances; hence, the experiment would be difficult to carry out without a further understanding of possible non-linear solutions in the three-dimensional system.

3. Non-linear Three-dimensional System

A free surface of liquid under forced oscillation has long been the subject of investigation. Three-dimensional standing waves may be excited as a result of forced oscillation on the boundary of vessel which contains the liquid or by wave maker oscillating in the liquid. The half-frequency standing waves as a subharmonic mode of forced oscillation were most frequently observed. Faraday in 1831 [15] made a series of experiments concerning a layer of liquid on the surface of a vibrating plate. It was first found that the frequency of the minute standing waves was only half that of the plate. The problem was next investigated by Mathiessen [16], [17], but a synchronous vibration was found. In order to check the discrepancy Rayleigh in 1883 [18, 19] made another series of experiments similar to Faraday's and confirmed Faraday's results. Benjamin and Ursell [20] recently worked out a stability theory for a free surface under vertical vibration based on the solution of Mathieu's equation. Their theory, partly verified by experiments, can explain the above phenomena and shows that both half-frequency and full-frequency standing waves can be excited. All of the above investigations are limited to standing waves of small amplitude and the direction of oscillation more or less normal to the free surface. Nevertheless, these results should suggest that the half-frequency cross waves can be excited under certain circumstances.

Indeed, cross waves generated by a wave maker were first observed by Faraday in his experiment [15] and later by Schuler in 1933 [2], which again confirmed the half-frequency mode of oscillation. In the experiment for the study of the highest two-dimensional standing waves, Taylor [1] observed a type of instability which was formed by half-frequency standing waves in the transverse direction superposed on the two-dimensional standing waves. The crest of the three-dimensional waves became conical and so high that the free surface splashed violently. Finite-amplitude cross waves were generated on purpose in a towing tank by McKernan [4] and used to similate short crested seas for ship model experiments. Recently, Howard [21] worked out a theory, based on the second-order free surface conditions, that the excitation of half-frequency cross waves in a rectangular tank depends upon certain length/width ratio of the tank and a critical amplitude of the wave maker.

It is believed that three-dimensional standing waves can be excited in the system under consideration only due to the non-linearity in the free surface conditions since the linearized version of the system is basically two-dimensional. A non-linear solution for the fundamental mode of cross waves will be investigated based on the exact free surface conditions. The method used to solve the non-linear two-dimensional standing waves will be generalized for this purpose. The experimental part of the investigation for excitation of cross waves is expected to verify as well as to supplement the theoretical analysis since only the second-order solution will be carried out here.

As mentioned at the beginning the complexity involved in the theoretical and experimental investigations is due to the fact that it is a non-linear system with infinitely-many degrees of freedom for oscillation. The present investigation, however, will provide the linear solution of the system (forced two-dimensional standing waves of small amplitude); the non-linear solutions of the two-dimensional system (forced two-dimensional standing waves of finite amplitude); the range of significant non-linear effects in the two-dimensional system; and the general characteristics of cross waves.

II.   FORMULATION OF THE PROBLEM

2.1.   Dimensional Equations and Boundary Conditions

Finite-amplitude standing waves are generated in a rectangular tank by a pair of two-dimensional wave makers. The tank is taken to be of infinite depth.   The x-y plane of the rectangular coordinates coincides with the undisturbed free surface and the z-axis is vertically upwards.   The wave makers have a width W and are a distance 2L apart.   (See Fig. 2.1)
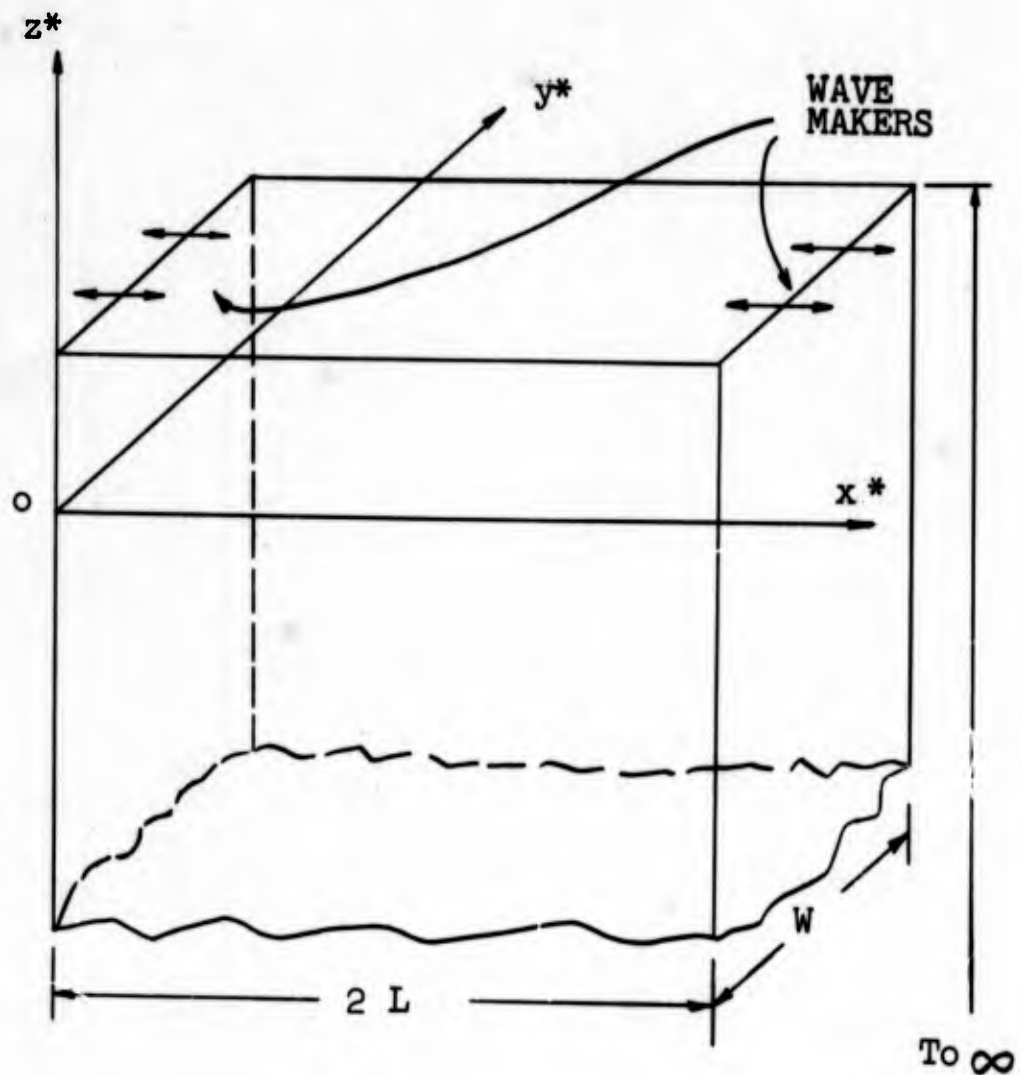
Figure 2.1

The fluid is assumed to be homogeneous, incompressible,
inviscid and moving irrotationally, hence there exists a
velocity potential, Φ^*[1], which describes a velocity field
[22] as

$$\underline{q}^* = -\nabla^*\Phi^* \quad , \tag{2.1}$$

and satisfies the Laplace equation

$$\nabla^{*2}\Phi^* = 0 \tag{2.2}$$

for $0 \leq x^* \leq 2L$, $0 \leq y^* \leq W$ and $z^* > -\infty$.

The free surface conditions,

$$\Phi^*_{t^*} - \tfrac{1}{2}\underline{q}^{*2} - g\zeta^* = 0 \qquad (2) \tag{2.3}$$

and

$$\zeta^*_{t^*} - \Phi^*_{x^*}\zeta^*_{x^*} - \Phi^*_{y^*}\zeta^*_{y^*} + \Phi^*_{z^*} = 0 \quad , \tag{2.4}$$

have to be satisfied on the free surface,

$$z^* = \zeta^*(x^*, y^*, t^*) \, , \tag{2.5}$$

where a zero atmospheric pressure is assumed and

$$\underline{q}^{*2} = \Phi^{*2}_{x^*} + \Phi^{*2}_{y^*} + \Phi^{*2}_{z^*} \, .$$

The boundary conditions are

for infinite depth case,

$$\Phi^* \longrightarrow \text{function of } t^* \text{ as } z^* \to -\infty ; \tag{2.6}$$

on the walls,

$$\frac{\partial\Phi^*}{\partial y^*} = 0 \qquad \text{at } y^* = 0 \text{ and } W ; \tag{2.7}$$

and on the wave makers,

$$\frac{\partial\Phi^*}{\partial x^*} = F(z^*)\sin\sigma^* t^* \tag{2.8}$$

---

(1) The asterisk on the upper right indicates a dimensional
     quantity.
(2) The subscript of an independent variable on the lower
     right indicates partial differentiation.

In his study of forced progressive waves of small amplitude, Havelock in 1929 [24] obtained, by means of an integral theorem, a general expression of the velocity potential for the function $F(z^*)$. The motion in general consists of a system of progressive waves far away from the wave maker and a local disturbance in the vicinity of the wave maker. However, he could simplify the expression of the velocity potential by an approximation that the motion of the wave maker is an exponential function with respect to the depth, i.e.

$$F(z^*) = Ae^{\gamma^* z^*} . \tag{2.9}$$

The motion of a plunger-type wave maker corresponds to $\gamma^* = 0$, but Havelock found that as $\gamma^* \to 0$, the local disturbance becomes infinite in the deep water case while the system of wave motion away from wave maker remains unchanged. The oscillatory motion of a flap-type wave maker can be approximated by the exponential function Eq. (2.9) by a proper choice of γ^* without the difficulty involved in the plunger type. A flap-type wave maker is adopted with its motion approximately described by an exponential function and then the boundary conditions on the wave makers become

$$\frac{\partial \Phi^*}{\partial x^*} = \alpha^* \sigma^* e^{\gamma^* z^*} \sin \sigma^* t^* \qquad \text{at} \quad x^* = 0 \tag{2.10}$$

and

$$\frac{\partial \Phi^*}{\partial x^*} = -\alpha^* \sigma^* e^{\gamma^* z^*} \sin \sigma^* t^* \qquad \text{at} \quad x^* = 2L . \tag{2.11}$$

In Eqs. (2.10) and (2.11), the amplitude of a wave maker at the undisturbed free surface, α^*, is assumed to be small and then the motion is limited at $x^* = 0$ and $2L$. Therefore, the motion of the wave maker is, in a sense, linearized and the non-linear waves are excited essentially due to resonance.

2.2 Dimensionless Equations and Boundary Conditions

By a choice of length unit L/π and time unit $(\frac{L}{g\pi})^{1/2}$, the following dimensionless quantities are defined:

$$x = \frac{\pi x^*}{L} , \quad y = \frac{\pi y^*}{L} , \quad z = \frac{\pi z^*}{L} , \quad t = (\frac{\pi g}{L})^{1/2} t^* , \quad \ell = \frac{L}{W}$$

$$\Phi = (\frac{\pi}{L})^{3/2} g^{-1/2} \Phi^* , \quad \sigma = (\frac{L}{\pi g})^{1/2} \sigma^* , \quad \alpha = \frac{\pi \alpha^*}{L} , \quad \gamma = \frac{L \gamma^*}{\pi} .$$

A set of dimensionless equations and boundary conditions can be derived from Eqs. (2.1) to (2.11) as follows:

$$\nabla^2 \Phi = 0 \qquad \text{for } 0 \le x \le 2\pi, 0 \le y \le \frac{\pi}{\ell} \text{ and } z > -\infty . \tag{2.12}$$

with $\quad \underline{q} = -\nabla \Phi$;

$$\left.\begin{array}{l} \zeta = \Phi_t - \frac{1}{2}q^2 \\ \zeta_t = \Phi_x \zeta_x + \Phi_y \zeta_y - \Phi_z \end{array}\right\} \quad \text{on} \quad z = \zeta(x,y,t) \; ; \qquad \begin{array}{l} (2.13) \\ (2.14) \end{array}$$

$$\Phi \to \text{function of } t \quad \text{as} \quad z \to -\infty \; ; \quad (2.15)$$

$$\frac{\partial \Phi}{\partial y} = 0 \quad \text{at} \quad y=0 \text{ and } \pi/\lambda \; ; \quad (2.16)$$

and $\quad \dfrac{\partial \Phi}{\partial x} = \alpha \sigma \sin \sigma t \, e^{z/2} \quad \text{at} \quad x = 0$

$$= -\alpha \sigma \sin \sigma t \, e^{z/2} \quad \text{at} \quad x = 2\pi \; . \quad (2.17)$$

The coefficient of z in the argument of the exponential function is chosen to be 1/2.

2.3 Transformation of Homogeneous Boundary Conditions

In order to have homogeneous boundary conditions for later Fourier series expressions of the velocity potential and free surface elevation, it is desirable to introduce a transformation

$$\Phi = 2\alpha \sigma \sin \frac{x}{2} \sin \sigma t \, e^{z/2} + \varphi \quad (2.18)$$

in which φ is the new velocity potential; hence φ satifies the Laplace equation

$$\nabla^2 \varphi = 0 \quad \text{for } 0 \leqslant x \leqslant 2\pi, 0 \leqslant y \leqslant \frac{\pi}{\lambda} \text{ and } z > -\infty \quad (2.19)$$

and the homogeneous boundary conditions,

$$\varphi \to \text{function of } t \qquad \text{as} \quad z \to -\infty \; , \quad (2.20)$$

$$\frac{\partial \varphi}{\partial x} = 0 \qquad \text{at } x=0 \text{ and } 2\pi \; , \quad (2.21)$$

and $\quad \dfrac{\partial \varphi}{\partial y} = 0 \qquad \text{at } y=0 \text{ and } \pi/\lambda . \quad (2.22)$

Substituting Eq. (2.18) for Φ in Eqs. (2.13) and (2.14), we have two transformed free surface conditions,

$$\zeta = \varphi_t - \frac{1}{2}q^2 - \alpha \sigma \sin \sigma t \, e^{z/2} (\varphi_x \cos \frac{x}{2} - \varphi_z \sin \frac{x}{2}) \quad (2.23)$$
$$+ 2\alpha \sigma \sin \frac{x}{2} \cos \sigma t \, e^{z/2} - \frac{1}{2}\alpha^2 \sigma^2 \sin^2 \sigma t \, e^{z}$$

and

$$\zeta_t = \varphi_x \zeta_x + \varphi_y \zeta_y - \varphi_z + \alpha \sigma \sin \sigma t \, e^{z/2} (\zeta_x \cos \frac{x}{2} - \sin \frac{x}{2}) \quad (2.24)$$

on the free surface, $z = \zeta(x,y,t)$,

where

$$\underline{q}^2 = \varphi_x^2 + \varphi_y^2 + \varphi_z^2 \; .$$

-9-

Now, the problem is to look for the possibility of a velocity potential, φ, and free surface elevation, ζ, as solutions of Eqs. (2.19), (2.23) and (2.24) and satisfying the homogeneous boundary conditions, Eqs. (2.20), (2.21) and (2.22).

III. LINEAR THEORY OF FORCED STANDING WAVES IN A RECTANGULAR TANK

3.1 Brief Review of Linear Theory

Since there is no general solution possible for the non-linear partial differential equation formulated in the previous section, approximate physical picture can be obtained, with the least mathematical effort, by solving the linearized equations. The additional assumption involved is that the amplitude of standing waves should be small in comparison with the wave length. The problem is then reduced to finding a velocity potential, Φ, as solution of the Laplace equation [22],

$$\nabla^2 \Phi = 0 \qquad \text{for } 0 \leq x \leq 2\pi, \, 0 \geq z \geq -\infty \qquad (3.1)$$

and satisfying the following linearized boundary conditions,

$$\Phi_{tt} + \Phi_z = 0 \qquad \text{on } z = 0 \, , \qquad (3.2)$$

$$\Phi \rightarrow \text{functions of } t \text{ as } z \rightarrow -\infty \, , \qquad (3.3)$$

and $\qquad \dfrac{\partial \Phi}{\partial x} = \pm \alpha \sigma \sin \sigma t \, e^{z/2} \qquad \text{at } x = 0 \text{ and } 2\pi. \qquad (3.4)$

After the solution of Φ is found, the free surface elevation can be obtained from

$$\zeta = \Phi_t \, . \qquad (3.5)$$

The normal modes of free standing waves of small amplitude satisfying the above system are given by the velocity potentials [23]

$$\Phi_{mn}(x, y, z) e^{i\sigma_{mn}t}$$
$$= C_{mn} \cos m\ell y \cos nx \, e^{\sqrt{m^2 \ell^2 + n^2} \, z + i\sigma_{mn}t} \, , \qquad (3.6)$$

where m, n are integers, C_{mn} is a complex constant,

$$\sigma_{mn}^2 = \sqrt{m^2 \ell^2 + n^2} \qquad (3.7)$$

and the real part on the right-hand-side of Eq. (3.6) is taken. The frequencies $\sigma_{mn}/2\pi$ given by Eq. (3.7) form the spectrum of natural frequencies of the three dimensional system, and it can be proved that

$$0 \leq \sigma_{m,n+1}^2 - \sigma_{m,n}^2 \leq 1 \qquad (3.8)$$

independent of the width π/ℓ , which would reduce to the two dimensional system, $\sigma_{n+1}^2 - \sigma_n^2 = 1$, if $m = 0$. Then, the free motion is of the form

$$\Phi(x,y,z;t) = \sum_m \sum_n \Phi_{mn}(x,y,z) e^{i\sigma_{mn} t} \qquad (3.9)$$

and a frequency analysis leads to the spectral frequencies Eq. (3.7) [3].

For forced oscillation, in general the motion consists of free modes of oscillation, Eq. (3.9), and a forced periodic motion having a frequency $\sigma/2\pi$ equal to the forcing frequency. The amplitude of forced motion approaches infinity as $\sigma/2\pi$ approaches a resonance frequency, while the other properties of the forcing agency are kept constant as generally recognized in the linear theory of oscillation. A measurement of resonance frequency provides the spectrum of the resonance frequencies. However, in the sense of forced motion defined in Sec. I for the dynamical system under investigation, the free modes are only transient and do not exist in the steady periodic motion due to slight dissipation. Hereafter, the solution of free modes of standing waves will be neglected and only the steady periodic solutions are to be investigated.

3.2 The Linear Solution of Forced Motion

The linearized version of the problem of forced oscillation is basically a two-dimensional one, since the linearized free surface condition, Eq. (3.2) and the motion of the wave maker, Eq. (3.4), are independent of y. Let the solution of two-dimensional standing waves of small amplitude be

$$\Phi = 2\alpha\sigma \sin\frac{x}{2} e^{z/2} \sin\sigma t + \sum_{n=0}^{\infty} a_n e^{nz} \cos nx \sin(\sigma t + \epsilon) \qquad (3.10)$$

satisfying all conditions except those on the free surface. The phase angle ϵ has to be 0 or π in order to have a solution. Substituting Eq. (3.10) for Φ in Eq. (3.2), leads to

$$\alpha\sigma(1-2\sigma^2)\sin\frac{x}{2}\sin\sigma t + \sum_{n=0}^{\infty} a_n(n-\sigma^2)\cos nx \sin(\sigma t + \epsilon) = 0$$

or

$$\sin\frac{x}{2} = \mp \frac{1}{\alpha\sigma(1-2\sigma^2)} \sum_{n=0}^{\infty} (n-\sigma^2) a_n \cos nx \qquad (3.11)$$

in which the negative sign is for $\epsilon = 0$ and the positive for $\epsilon = \pi$. In order to determine the coefficients A_n, $\sin x/2$ is expanded into a Fourier cosine series for $0 \leq x \leq 2\pi$, then

$$\sin\frac{x}{2} = \frac{2}{\pi} - \frac{4}{\pi} \sum_{n=1}^{\infty} \frac{\cos nx}{4n^2-1} \qquad . \qquad (3.12)$$

-12-

By comparing the coefficients of cosnx on the right-hand sides of Eqs.(3.11) and (3.12), it is found that:

$$a_0 = \pm \frac{2\alpha(1-2\sigma^2)}{\sigma\pi}$$

and

$$a_n = \pm \frac{4\alpha\sigma(1-2\sigma^2)}{\pi(4n^2-1)(n-\sigma^2)} \quad , \text{ for } n = 1, 2, 3, \cdots, \quad (3.13)$$

in which the positive sign is for $\varepsilon = 0$ and the negative for $\varepsilon = \pi$; but as we substitute both A_n and ε into Eq. (3.6), the sign becomes positive in front of the summation sign for either case.

It follows from Eq. (3.5) that the free surface elevation is

$$\zeta = \frac{2\alpha}{\pi}\left[1 - 2\sigma^2 \sum_{n=1}^{\infty} \frac{\cos nx}{(2n+1)(n-\sigma^2)}\right]\cos\sigma t \quad . \quad (3.14)$$

3.3 Numerical Computation

A numerical computation was carried out for the total amplitude of the linear standing waves at the point of symmetry in the tank, $x = \pi$. Since this is a simple harmonic motion, the total amplitude is

$$2|\zeta| = \frac{4\alpha}{\pi}\left|1 + 2\sigma^2 \sum_{n=1}^{\infty} \frac{(-1)^{n+1}}{(2n+1)(n-\sigma^2)}\right| \quad \text{at} \quad x = \pi \quad . \quad (3.15)$$

The frequency-amplitude relation based on Eq. (3.14) is shown in Fig. 3.1 for the wave maker amplitudes, $\alpha = 0.0194$ and 0.0388 and for the first mode of oscillation only, i.e. near $\sigma = 1$.

The spectrum of resonance frequencies can now be determined from the solution, Eq. (3.14) or Eq. (3.15) as the amplitude $|\zeta|$ approaches infinity at $\sigma = \sqrt{n}$, where n is an integer, hence, $\sigma_n^2 = n$.

3.4 Behavior of the Linear Solution

The spectrum of discrete resonance frequencies $\sigma_n^2 = n$ for the two-dimensional system is obtained when the amplitude of standing waves becomes infinite at $\sigma \rightarrow n$. The spacing of these resonance frequencies decreases as the mode of oscillation becomes higher and tends to zero at the highest mode. The spectra of resonance frequencies for both free and forced motions are identical. If the forcing frequency of the wave maker is away from the resonance frequency, the periodic solution obtained in

Sec. 3.2 is always stable since this is the only possible
solution based on the linear theory. In this case the fre-
quency of standing waves is equal to that of the wave maker
and the amplitude of standing waves is a function of frequency
at any location and linearly proportional to the amplitude
of the wave maker (see Eq. (3.14)). If the forcing frequency
is in the neighborhood of a resonance frequency, the linear
solution would contradict physical sense and thus is no
longer valid. Then, the non-linear solution for standing
waves of finite amplitude should be investigated in each
neighborhood of a resonance frequency of the spectrum of
the three-dimensional system. Although the two-dimensional
standing waves of finite amplitude are only a family of
particular solutions among the non-linear solutions of the
three dimensional system, an investigation of the transi-
tion from the two-dimensional linear to non-linear solu-
tion will lead to determine approximately the range of sig-
nificant non-linear effects in the neighborhood of a reson-
ance frequency. In this range the two-dimensional stand-
ing waves may be unstable for there is a possibility of ex-
citation of cross waves under certain circumstances.

In the case of free oscillation, the solution of
higher modes can be generalized from the fundamental one
by considering the higher mode as composed by a number of
fundamental ones, i.e. by using a wave-amplitude/wave-
length ratio based on the solution of the fundamental mode.
Physically, this is possible by putting a partition or false
wall vertically along the crest-trough line. This kind of
simple procedure does not exist in the forced motion and
each mode has to be solved individually. A simple demon-
stration for this is to compute approximately the wave-amp-
litude/wave-length ratio near the resonance frequency based
on Eq. (3.14), e.g.

$$\frac{|\zeta_1|}{|\zeta_2|} = \frac{5}{3} \qquad\qquad \frac{|\zeta_1|/\lambda_1}{|\zeta_2|/\lambda_2} = \frac{5}{6}$$

and

$$\frac{|\zeta_1|}{|\zeta_3|} = \frac{7}{3} \qquad\text{or}\qquad \frac{|\zeta_1|/\lambda_1}{|\zeta_3|/\lambda_3} = \frac{7}{9} \qquad \text{at} \quad x = \pi$$

in which $\lambda_1 \approx 2\lambda_2 \approx 3\lambda_3$. For free waves the ratios
should be 1 instead of 5/6 and 7/9. In addition, it
indicates that $|\zeta_n|/\lambda_n$ increases as n does.
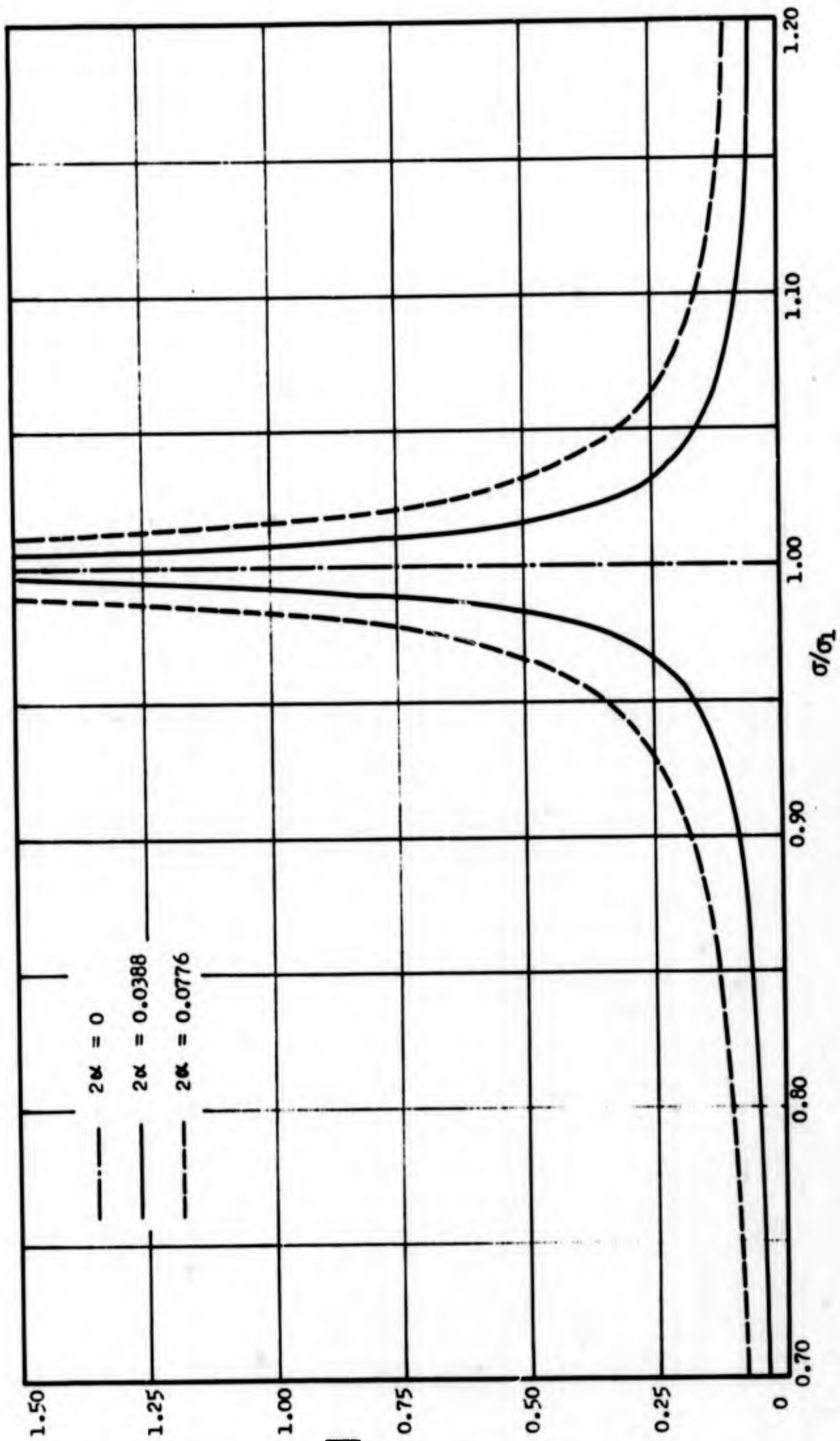
FIG. 3.1 Frequency-Amplitude Curves for the Linear Theory

IV. NON-LINEAR FORCED TWO-DIMENSIONAL STANDING WAVES IN A RECTANGULAR TANK

4.1 General Remarks

Forced standing waves of finite amplitude will be obtained as a non-linear solution of the two-dimensional problem as well as by investigation of the range of significant non-linear effects. In this range infinitely many solutions may possibly exist. Among them, two families of solutions are of significance, i.e. the non-linear two-dimensional standing waves and the fundamental mode of cross waves. The former will be treated in this section and together with the linear solution in Sec. III a complete solution is presented to the two-dimensional problem in the system as a whole provided that the stability criteria for two-dimensionality in the non-linear range can be established. At this moment, this problem is treated just as a two-dimensional one for the purpose mentioned above. An approach similar to Penney and Price's [14] is used here to find an approximate solution which is, in its final form, a double Fourier series in x and t. The velocity potential φ and free surface elevation ζ are expressed as two Fourier series in x with coefficients which are functions of t. Two sets of non-linear ordinary differential equations are derived from the free surface conditions for these coefficients. Then, a periodic solution is found by the method of iteration, which is generally applied to find the response curve (the frequency-amplitude relation) in non-linear mechanics [25, 26,27].

There are indeed two branches on the frequency-amplitude curve for forced standing waves of finite amplitude as found by Taylor [1]. They are on each side of the resonance curve (the frequency-amplitude curve of free oscillation) and disconnected due to neglecting of viscosity. It is found that the non-linear and linear frequency-amplitude curve are in good agreement in a wide overlapping range. The frequency-amplitude curves are computed to the third order for two different amplitudes of the wave maker. The coefficients are computed only to the second order. Finally, two profiles of standing waves with the frequencies on each branch of the frequency-amplitude curve are computed.

4.2 Fourier Series Expressions for φ and ζ

Assume the velocity potential to be expressible in a Fourier series in x with coefficients which are functions of t

$$\varphi = \sum_{n=0}^{\infty} b_n(t) e^{nz} \cos nx \ . \tag{4.1}$$

This series satisfies Eqs. (2.19) to (2.22) except the free surface conditions, Eqs. (2.23) and (2.24). If ζ is

-16-

eliminated in Eqs. (2.23) and (2.24), a partial differential equation is obtained with only one dependent variable, φ. But this would increase the order twice, and the multiplication of the series becomes very difficult to handle. Suppose that Eqs. (2.23) and (2.24) could be solved for ζ in terms of φ, then ζ would also be a Fourier series. Hence, assume

$$\zeta = \frac{a_0(t)}{2} + \sum_{n=1}^{\infty} a_n(t) \cos nx . \qquad (4.2)$$

These two series are considered as solutions of the free surface conditions, Eqs. (2.23) and (2.24). Substituting Eqs. (4.1) and (4.2) into Eqs. (2.23) and (2.24) and comparing the coefficients of Cosnx, two sets of non-linear ordinary differential equations are obtained with the dependent variables, a_n and b_n, and the independent variable, t. As seen in Eqs. (2.20) and (2.21), this process involves the multiplication of two Fourier series and an exponential function with its argument as a Fourier series. After two Fourier series have been multiplied, $e^{\lambda \zeta} \cos \mu x$ has to be expanded into another Fourier series. A special function was developed to handle this expansion (see Appendix A for details) [14] as follows:

$$e^{\lambda \zeta} \cos \mu x = E(\lambda, \mu) + \sum_{s=1}^{\infty} \cos sx \left[E(\lambda, s-\mu) + E(\lambda, s+\mu) \right] \qquad (4.3)$$

in which

$$E(\lambda, s) = E(\lambda, -s) = \sum_{N=0}^{\infty} \frac{\lambda^N}{2^N N!} S_N(s) . \qquad (4.4)$$

The function $S_n(s)$ is a series of a_n, and both $E(\lambda, s)$ and $S_n(s)$ were computed up to third order in Appendix A.

4.3 Two Sets of Non-Linear Ordinary Differential Equations for the Coefficients a_n and b_n of the Fourier Series

Substituting Eqs. (4.1) and (4.2) in Eqs. (2.23) and (2.24) and by the use of the expansions, Eq. (4.3), one obtains:

$$\frac{a_0}{2} + \sum_{s=1}^{\infty} a_s \cos sx$$

$$= \dot{b}_0 + \sum_{n=1}^{\infty} \dot{b}_n \left\{ E(n,n) + \sum_{s=1}^{\infty} \cos sx \left[E(n,s-n) + E(n,s+n) \right] \right\} \quad (1)$$

$$-\frac{1}{2}\sum_{m=1}^{\infty}\sum_{n=1}^{\infty} mn\, b_m b_n \left\{ E(m+n,m-n) + \sum_{s=1}^{\infty} \cos sx \left[E(m+n,s-m+n) + E(m+n,s+m-n) \right] \right\}$$

$$-\frac{2\alpha\sigma}{\pi}\sin\sigma t \left[\sum_{n=1}^{\infty} nb_n \left\{ E(n+\tfrac{1}{2},n) + \sum_{s=1}^{\infty}\cos sx \left[E(n+\tfrac{1}{2},s-n) + E(n+\tfrac{1}{2},s+n) \right] \right\} \right.$$

$$+ \sum_{m=1}^{\infty}\sum_{n=1}^{\infty} \frac{nb_n}{2m+1} \left\{ E(n+\tfrac{1}{2},m+n) + \sum_{s=1}^{\infty}\cos sx \left[E(n+\tfrac{1}{2},s-m-n) + E(n+\tfrac{1}{2},s+m+n) \right] \right\}$$

$$\left. -\sum_{m=1}^{\infty}\sum_{n=1}^{\infty} \frac{nb_n}{2m-1} \left\{ E(n+\tfrac{1}{2},m-n) + \sum_{s=1}^{\infty}\cos sx \left[E(n+\tfrac{1}{2},s-m+n) + E(n+\tfrac{1}{2},s+m-n) \right] \right\} \right]$$

$$-\frac{4\alpha\sigma^2}{\pi}\cos\sigma t \left[\sum_{n=1}^{\infty}\frac{2}{4n^2-1} \left\{ E(\tfrac{1}{2},n) + \sum_{s=1}^{\infty}\cos sx \left[E(\tfrac{1}{2},s-n) + E(\tfrac{1}{2},s+n) \right] \right\} - 2\sum_{s=1}^{\infty} E(\tfrac{1}{2},s)\cos sx - E(\tfrac{1}{2},0) \right]$$

$$-\frac{\alpha^2\sigma^2}{2}\sin^2\sigma t \left[E(1,0) + 2\sum_{s=1}^{\infty} E(1,s)\cos sx \right]$$

and $\qquad\qquad\qquad\qquad\qquad\qquad\qquad\qquad\qquad\qquad\qquad\qquad\qquad (4.5)$

$$\frac{\dot{a}_0}{2} + \sum_{s=1}^{\infty} \dot{a}_s \cos sx$$

$$= \frac{1}{2}\sum_{m=1}^{\infty}\sum_{n=1}^{\infty} mn\, a_m b_n \left\{ E(n,m-n) - E(n,m+n) + \sum_{s=1}^{\infty}\cos sx \left[E(n,s-m+n) + E(n,s+m-n) \right. \right.$$
$$\left. \left. - E(n,s-m-n) - E(n,s+m+n) \right] \right\}$$

$$- \sum_{n=1}^{\infty} nb_n \left\{ E(n,n) + \sum_{s=1}^{\infty} \cos sx \left[E(n,s-n) + E(n,s+n) \right] \right\}$$

$$+ \frac{4\alpha\sigma}{\pi}\sin\sigma t \left[\sum_{n=1}^{\infty}\frac{1}{4n^2-1} \left\{ E(\tfrac{1}{2},n) + \sum_{n=1}^{\infty}\cos sx \left[E(\tfrac{1}{2},s-n) + E(\tfrac{1}{2},s+n) \right] \right\} \right.$$

$$\left. - \sum_{m=1}^{\infty}\sum_{n=1}^{\infty} \frac{mn\,a_n}{4m^2-1} \left\{ E(\tfrac{1}{2},m-n) - E(\tfrac{1}{2},m+n) + \sum_{s=1}^{\infty}\cos sx \left[E(\tfrac{1}{2},s-m+n) + E(\tfrac{1}{2},s+m-n) \right. \right. \right.$$
$$\left. \left. \left. - E(\tfrac{1}{2},s-m-n) - E(\tfrac{1}{2},s+m+n) \right] \right\} \right]$$

$$- \frac{2\alpha\sigma}{\pi}\sin\sigma t \left[E(\tfrac{1}{2},0) + 2\sum_{s=1}^{\infty} E(\tfrac{1}{2},s)\cos sx \right] . \qquad\qquad (4.6)$$

(1) The dot on top indicates a differentiation with respect to time, t.

Comparing the coefficients of Cossx, then

$$\frac{a_0}{2} = \dot{b_0} + \sum_{n=1}^{\infty} \dot{b_n} E(n,n) - \frac{1}{2}\sum_{m=1}^{\infty}\sum_{n=1}^{\infty} mn\, b_m b_n E(m+n, m-n) + \frac{4\alpha\sigma^2}{\pi}\cos\sigma t\left[E(\tfrac{1}{2},0) - 2\sum_{n=1}^{\infty}\frac{E(\tfrac{1}{2},n)}{4n^2-1}\right]$$

$$- \frac{2\alpha\sigma}{\pi}\sin\sigma t\left\{\sum_{n=1}^{\infty} n b_n E(n+\tfrac{1}{2},n) + \sum_{m=1}^{\infty}\sum_{n=1}^{\infty}\frac{n b_n}{4m^2-1}\left[2(m-1)E(n+\tfrac{1}{2},m+n) - 2(m+1)E(n+\tfrac{1}{2},m-n)\right]\right\}$$

$$- \frac{1}{2}\alpha^2\sigma^2\sin^2\sigma t\, E(1,0) \tag{4.7}$$

for $S \geq 1$,

$$a_S = \sum_{n=1}^{\infty} \dot{b_n}\left[E(n,s-n) + E(n,s+n)\right] - \frac{1}{2}\sum_{m=1}^{\infty}\sum_{n=1}^{\infty} mn\, b_m b_n\left[E(m+n,s-m+n) + E(m+n,s+m-n)\right]$$

$$- \frac{2\alpha\sigma}{\pi}\sin\sigma t\left\{\sum_{n=1}^{\infty} n b_n\left[E(n+\tfrac{1}{2},s-n) + E(n+\tfrac{1}{2},s+n)\right] + \sum_{m=1}^{\infty}\sum_{n=1}^{\infty}\frac{n b_n}{2m-1}\left[E(n+\tfrac{1}{2},s-m-n) + E(n+\tfrac{1}{2},s+m+n)\right]\right.$$

$$\left. - \sum_{m=1}^{\infty}\sum_{n=1}^{\infty}\frac{n b_n}{2m-1}\left[E(n+\tfrac{1}{2},s-m+n) + E(n+\tfrac{1}{2},s+m-n)\right]\right\}$$

$$+ \frac{8\alpha\sigma^2}{\pi}\cos\sigma t\left\{E(\tfrac{1}{2},s) - \sum_{n=1}^{\infty}\frac{1}{4n^2-1}\left[E(\tfrac{1}{2},s-n) + E(\tfrac{1}{2},s+n)\right]\right\} - \alpha^2\sigma^2\sin\sigma t\, E(1,s) \tag{4.8}$$

and

$$\frac{\dot{a_0}}{2} = \frac{1}{2}\sum_{m=1}^{\infty}\sum_{n=1}^{\infty} mn\, a_m b_n\left[E(n,m-n) - E(n,m+n)\right] - \sum_{n=1}^{\infty} n b_n E(n,n)$$

$$+ \frac{4\alpha\sigma}{\pi}\sin\sigma t\left\{\sum_{n=1}^{\infty}\frac{E(\tfrac{1}{2},n)}{4n^2-1} - \sum_{m=1}^{\infty}\sum_{n=1}^{\infty}\frac{mn\, a_n}{4m^2-1}\left[E(\tfrac{1}{2},m-n) - E(\tfrac{1}{2},m+n)\right]\right.$$

$$\left. - \frac{1}{2}E(\tfrac{1}{2},0)\right\} \tag{4.9}$$

for $S \geq 1$,

$$\dot{a_S} = \frac{1}{2}\sum_{m=1}^{\infty}\sum_{n=1}^{\infty} mn\, a_m b_n\left[E(n,s-m+n) + E(n,s+m-n) - E(n,s-m-n) - E(n,s+m+n)\right]$$

$$- \sum_{n=1}^{\infty} n b_n\left[E(n,s-n) + E(n,s+n)\right] \tag{4.10}$$

$$+ \frac{4\alpha\sigma}{\pi}\sin\sigma t\left\{\sum_{n=1}^{\infty}\frac{1}{4n^2-1}\left[E(\tfrac{1}{2},s-n) + E(\tfrac{1}{2},s+n)\right] - E(\tfrac{1}{2},s)\right.$$

$$\left. - \sum_{m=1}^{\infty}\sum_{n=1}^{\infty}\frac{mn\, a_n}{4m^2-1}\left[E(\tfrac{1}{2},s-m+n) + E(\tfrac{1}{2},s+m-n) - E(\tfrac{1}{2},s-m-n) - E(\tfrac{1}{2},s+m+n)\right]\right\} .$$

4.4 Solution by the Method of Iteration

The equation obtained in the previous section will be solved by the method of iteration. A consideration of the order of magnitude of the coefficients, a_s and b_s, is essential for the solution. Penney and Price, in their treatment of non-linear free standing waves [14], had successfully shown that a_s is of the order A^s and b_s of the same order or higher, where A is the amplitude of

linear free standing waves. For this problem, there does
exist a small parameter, i.e. the amplitude of the wave
maker α. It is necessary to use caution in taking a simi-
lar approach, because in free standing waves one may solve
for a fundamental mode of oscillation and the solution of
higher modes can be obtained by considering the motion with-
in each wave length as a fundamental mode. By contrast,
in forced standing waves the wave maker can be operated at
a frequency of any mode, and higher modes cannot be obtained
in this way as discussed in Sec. 3.4 and have to be solved
individually. Therefore, the order of magnitude of a_s and
b_s depends on the mode of the desired solution. From
Sec. 3.4, it was shown that the non-linear effect is con-
fined to the neighborhood of a resonance frequency of
the spectrum, $\sigma_n^2 = n$ for $n = 1,2,3,\ldots$ in the dimension-
less form, which corresponds to a natural frequency of
free standing waves. Examining the sets of Eqs. (4.7) to
(4.10) for linear free oscillation by neglecting those non-
linear and forcing terms, it is found that

$$a_s = \dot{b}_s \quad \text{and} \quad \dot{a}_s = -sb_s ,$$

or
$$\ddot{b}_s + sb_s = 0 \qquad\qquad\qquad (4.11)$$

with the solutions

$$b_s = \beta_s \sin(\sqrt{s}\, t + \epsilon_s) \qquad \text{for } s = 1,2,3,\cdots . \quad (4.12)$$

For a periodic solution, not all of these components can
be present since their frequencies in general, are not
exact multiples. The frequency, $\sigma_s = \sqrt{s}$, is also the reson-
ance frequency of the system as s is an integer. There-
fore, one has to confine himself in finding a solution
which belongs to one of these modes. When the wave maker
is operated in the neighborhood of one of these modes, a
solution exists with the frequency of the wave maker as a
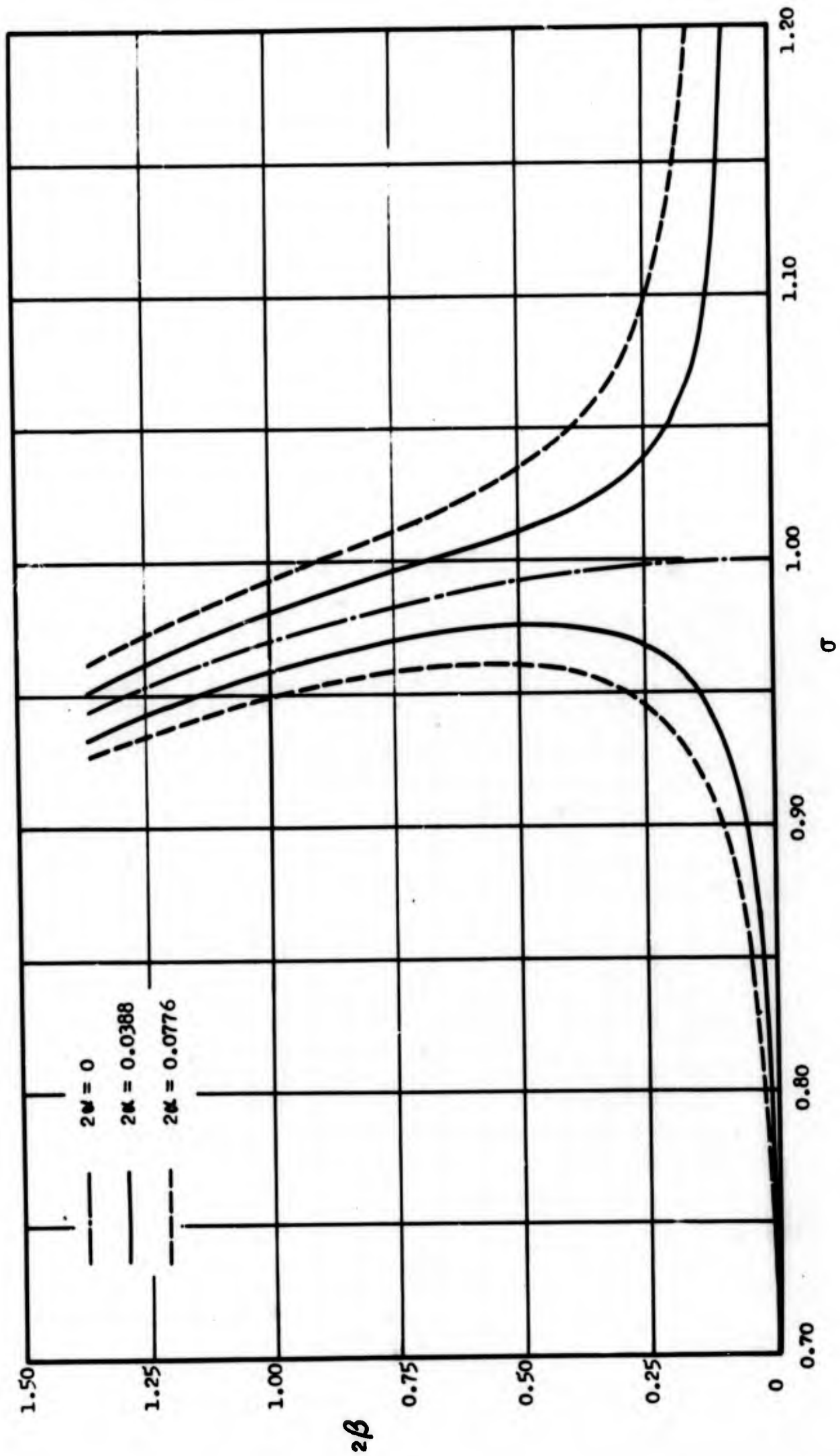fundamental frequency.

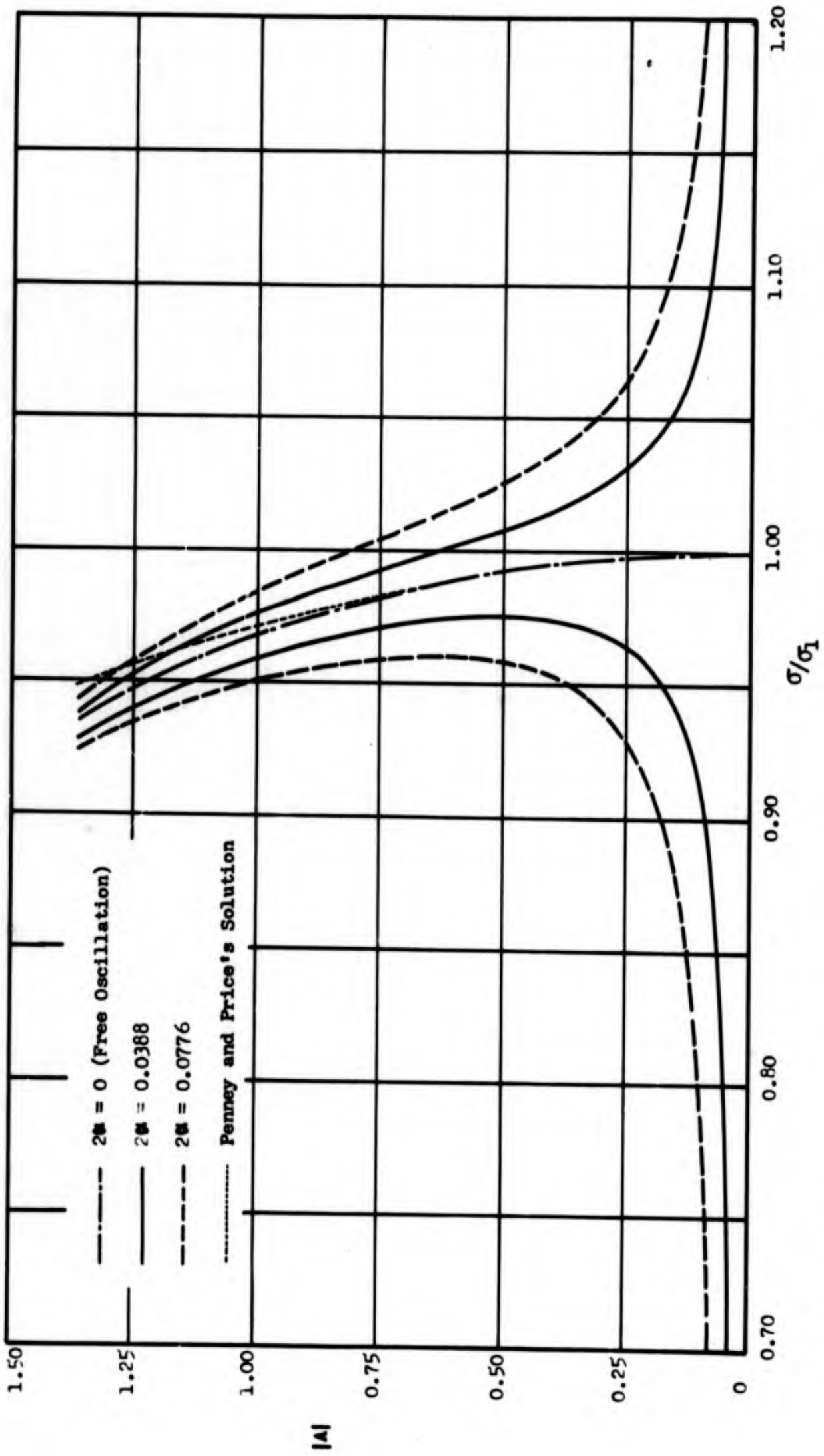FIG. 4.2 σ-β Curves for the Non-linear Two-dimensional Solution

FIG. 4.3 Frequency-Amplitude Curves for Forced Two-dimensional Standing Waves of Finite Amplitude

-22-

However, for forced oscillation there are some forcing terms on the right of Eq. (4.11) with the linear term of the order of α; then, there do exist the particular integrals for those values of b_s in which $\sqrt{s}$ is not a multiple of the forcing frequency σ. The set of equations for linear forced oscillation is obtained from Eqs. (4.7) to (4.10) as follows:

$$a_0 = 2\dot{b}_0 + \frac{8\alpha\sigma^2}{\pi}\cos\sigma t$$

$$\dot{a}_0 = -\frac{4\alpha\sigma}{\pi}\sin\sigma t$$

$$a_n = \dot{b}_n - \frac{8\alpha\sigma^2}{\pi(4n^2-1)}\cos\sigma t$$

$$\left.\dot{a}_n = b_n + \frac{4\alpha\sigma}{\pi(4n^2-1)}\sin\sigma t \right\} \qquad \text{for} \quad n \geq 1$$

(4.13)

by assuming that α is of the same order as all co-efficients. The solution of Eq. (4.13) yields exactly the same results obtained in Sec. III based on the linear theory.

For the moment, a solution is to be found for the fundamental mode of forced two-dimensional standing waves, i.e. a solution with the fundamental frequency in the neighborhood of $\sigma = 1$. Then, the iteration process may be started from an approximate solution

$$b_1 = \beta \sin(\sigma t + \epsilon)$$

where β is more or less the ratio of wave amplitude / wave-length of the standing waves corresponding to Penney and Price's A, which is proportional to α as the frequency is far away from $\sigma = 1$ and becomes much larger than α near $\sigma = 1$; hence, α is of the order of β or higher. In the light of the linear solution obtained in Sec. III, a_0 and b_0 are always of $O(\alpha)$; a_1 and b_1 of $O(\alpha/(\sigma^2-1))$; a_n and b_n

$(n \geq 2)$ of $O(\alpha/(\sigma^2-n))$. Now considering the order of magnitude of the coefficients separately with respect to α and β

$$
\begin{array}{cccc}
a_0, b_0 & a_1, b_1 & a_2, b_2 & a_3, b_3 \quad \cdots \\
O(\alpha) & O(|\frac{\alpha}{\sigma^2-1}|,\beta) & O(|\frac{\alpha}{\sigma^2-2}|,\beta^2) & O(|\frac{\alpha}{\sigma^2-3}|,\beta^3) \quad \cdots
\end{array}
$$

where $\sigma^2 \approx 1$ because of the first mode of oscillation. The order of magnitude of the coefficients with respect to α cannot be expressed in integral powers similar to β, but the magnitude of $\left|\frac{\alpha}{\sigma^2-n}\right|$

decreases rapidly as $n \geq 2$ in comparison with $\left|\frac{\alpha}{\sigma^2-1}\right|$

for $\sigma^2 \approx 1$. Therefore, for the sake of simplifying the computation, it is assumed that

$$a_0, b_0 \qquad a_1, b_1 \qquad a_2, b_2 \qquad a_3, b_3 \quad \cdots$$
$$0\,(\beta) \qquad\quad 0\,(\beta) \qquad\quad 0\,(\beta^2) \qquad 0\,(\beta^3) \cdots$$

and α is of $0(\beta)$ or higher; during the process of iteration the contribution of $\left| \dfrac{\alpha}{\sigma^{2-n}} \right|$ to a_n and b_n will be recovered in the nth order of approximation while those involved in the terms higher than the nth are neglected.

If solutions corresponding to any higher mode, say, the nth mode, are desired, it can be assumed that a_0, b_0, a_n, b_n are of $0(\beta)$; a_{n-1}, b_{n-1}, a_{n+1}, b_{n+1} are of $0(\beta^2)$ and so forth.

Now, the problem will be solved for the first mode of oscillation, i.e. in the neighborhood of $\sigma = 1$. $S_n(s)$ and $E(\lambda, \mu)$ required in the computation are listed in Appendix A. As a result of expanding Eqs. (4.7) to (4.10) by keeping terms to the third order, eight equations are obtained for a_s and b_s ($s = 0,1,2$ and 3) as follows:

$$a_0 = 2\dot{b}_0 + (1+\tfrac{1}{2}a_0)a_1\dot{b}_1 - (1+a_0)b_1^2 + \tfrac{4\alpha\sigma}{\pi}\sin\sigma t\left[(1+\tfrac{3}{4}a_0-\tfrac{1}{2}a_1)b_1 + \tfrac{2}{3}b_2\right] \qquad (4.14)$$
$$+ \tfrac{8\alpha\sigma^2}{\pi}\cos\sigma t\left[(1+\tfrac{1}{4}a_0+\tfrac{1}{32}a_0^2)-\tfrac{1}{6}(1+\tfrac{1}{4}a_0)a_1-\tfrac{1}{30}a_2+\tfrac{7}{120}a_1^2\right] - \tfrac{1}{2}\alpha^2\sigma^2\sin^2\sigma t(1+\tfrac{1}{2}a_0)$$

$$a_1 = \dot{b}_1\left[(1+\tfrac{1}{2}a_0+\tfrac{1}{8}a_0^2)+\tfrac{1}{2}a_2+\tfrac{3}{8}a_1^2\right] + a_1b_1^2 - 2b_1b_2 - \tfrac{4\alpha\sigma}{3\pi}\sin\sigma t\left[(1+\tfrac{3}{4}a_0)-\tfrac{21}{10}a_1b_1-\tfrac{18}{5}b_2\right]$$
$$- \tfrac{8\alpha\sigma^2}{3\pi}\cos\sigma t\left[(1+\tfrac{1}{4}a_0+\tfrac{1}{32}a_0^2)-\tfrac{7}{10}(1+\tfrac{1}{4}a_0)a_1+\tfrac{19}{70}a_2+\tfrac{27}{280}a_1^2\right] - \tfrac{1}{2}\alpha^2\sigma^2\sin^2\sigma t\,a_1 \quad (4.15)$$

$$a_2 = \dot{b}_2 + a_0\dot{b}_2 + \tfrac{1}{2}(1+\tfrac{1}{2}a_0)a_1\dot{b}_1 - \tfrac{4\alpha\sigma}{15\pi}\sin\sigma t\left[(1+\tfrac{3}{4}a_0)b_1+\tfrac{90}{7}b_2+\tfrac{19}{14}a_1b_1\right]$$
$$- \tfrac{8\alpha\sigma^2}{15\pi}\cos\sigma t\left[(1+\tfrac{1}{4}a_0+\tfrac{1}{32}a_0^2)+\tfrac{19}{14}(1+\tfrac{1}{4}a_0)a_1-\tfrac{155}{42}a_2-\tfrac{67}{168}a_1^2\right] \qquad (4.16)$$

$$a_3 = \dot{b}_3 + a_1\dot{b}_2 + \tfrac{1}{2}a_2\dot{b}_1 + \tfrac{1}{8}a_1^2\dot{b}_1 - \tfrac{4\alpha\sigma}{35\pi}\sin\sigma t\left[(1+\tfrac{3}{4}a_0)b_1+\tfrac{13}{6}a_1b_1+\tfrac{70}{9}b_2\right]$$
$$- \tfrac{8\alpha\sigma^2}{35\pi}\cos\sigma t\left[(1+\tfrac{1}{4}a_0+\tfrac{1}{32}a_0^2)+\tfrac{13}{18}(1+\tfrac{1}{4}a_0)a_1+\tfrac{545}{198}a_2+\tfrac{347}{792}a_1^2\right] \qquad (4.17)$$

$$\dot{a}_0 = -\tfrac{4\alpha\sigma}{\pi}\sin\sigma t\left[(1+\tfrac{1}{4}a_0+\tfrac{1}{32}a_0^2)+\tfrac{1}{2}(1+\tfrac{1}{4}a_0)a_1+\tfrac{1}{4}a_2+\tfrac{1}{8}a_1^2\right] \qquad (4.18)$$

$$\dot{a}_1 = -b_1\left[1+\tfrac{1}{2}a_0+\tfrac{1}{8}a_0^2-\tfrac{1}{2}a_2+\tfrac{1}{8}a_1^2\right]-a_1b_2 \qquad (4.19)$$
$$+ \tfrac{4\alpha\sigma}{3\pi}\sin\sigma t\left[(1+\tfrac{1}{4}a_0+\tfrac{1}{32}a_0^2)-\tfrac{11}{10}(1+\tfrac{1}{4}a_1)a_1-\tfrac{157}{70}a_2-\tfrac{61}{280}a_1^2\right]$$

$$\dot{a}_2 = -2b_2 - 2a_0 b_2 - (1 + \tfrac{1}{2}a_0)a_1 b_1$$
$$+ \tfrac{4\alpha\sigma}{15\pi} \sin\sigma t \left[(1 + \tfrac{1}{4}a_0 + \tfrac{1}{32}a_0^2) + \tfrac{71}{14}(1 + \tfrac{1}{4}a_0)a_1 - \tfrac{235}{42}a_2 - \tfrac{107}{168}a_1^2\right] \quad (4.20)$$

$$\dot{a}_3 = -3b_3 - 3a_1 b_2 - \tfrac{3}{2}a_2 b_1 - \tfrac{3}{8}a_1^2 b_1$$
$$+ \tfrac{4\alpha\sigma}{35\pi} \sin\sigma t \left[(1 + \tfrac{1}{4}a_0 + \tfrac{1}{32}a_0^2) + \tfrac{19}{6}(1 + \tfrac{1}{4}a_0)a_1 + \tfrac{4515}{148}a_2 + \tfrac{2307}{742}a_1^2\right]$$
$$(4.21)$$

4.4.1 First-order Solution

By taking only the first-order terms in Eqs. (4.14), (4.15), (4.18) and (4.19), and eliminating a_0 and a_1, one has

$$\ddot{b}_0 = - \frac{2\alpha\sigma(1 - 2\sigma^2)}{\pi} \sin\sigma t \qquad (4.22)$$

and

$$\ddot{b}_1 + b_1 = \frac{4\alpha\sigma(1 - 2\sigma^2)}{3\pi} \sin\sigma t \qquad (4.23)$$

Then, the integration of Eq..(4.22) leads to a periodic solution,

$$b_0 = \frac{2\alpha(1 - 2\sigma^2)}{\pi\sigma} \sin\sigma t \qquad (4.24)$$

and

$$a_0 = \frac{4\alpha}{\pi} \cos\sigma t \qquad (4.25)$$

from Eq. (4.14). It can easily be computed that the coefficient, a_0, is the variation of the undisturbed free surface due to the volume of fluid displaced by the wave maker in motion.

Eq. (4.23) can be rewritten as the following [26]:

$$\ddot{b}_1 + \sigma^2 b_1 = (\sigma^2 - 1)b_1 + \frac{4\alpha\sigma(1 - 2\sigma^2)}{3\pi} \sin\sigma t \qquad (4.26)$$

Since the interest is centered on a periodic solution with the frequency σ of the forcing function, one starts with an approximation solution

$$b_1 = \beta \sin(\sigma t + \epsilon) \qquad (4.27)$$

where the amplitude β will serve as a parameter in higher order of approximation and the phase angle ε indicates that the standing waves do not necessarily have the same phase as the wave maker. Substituting Eq. (4.27) into the right-hand-side of Eq. (4.26), one has

$$\ddot{b}_1 + \sigma^2 b_1 = (\sigma^2-1)\beta \sin(\sigma t + \epsilon) + \frac{4\alpha\sigma(1-2\sigma^2)}{3\pi} \sin\sigma t \qquad (4.28)$$

where ε has to be 0 or π in order to have a solution. Then,

$$\ddot{b}_1 + \sigma^2 b_1 = \left[\pm(\sigma^2-1)\beta + \frac{4\alpha\sigma(1-2\sigma^2)}{3\pi}\right] \sin\sigma t \qquad (4.29)$$

For a periodic solution, the secular term [25], which is the particular integral due to the term on the right-hand-side of Eq. (4.29), must vanish. Hence, the first-order solution is

$$b_1 = \beta \sin(\sigma t + \epsilon) \qquad (4.30)$$

with
$$(\sigma^2-1)\beta \pm \frac{4\alpha\sigma(1-2\sigma^2)}{4\pi} = 0 \qquad (4.31)$$

and
$$a_1 = \left(\pm\beta - \frac{8\alpha\sigma}{\pi}\right)\sigma \cos\sigma t \qquad (4.32)$$

where the positive sign is for $\varepsilon = 0$ and the negative for $\varepsilon = \pi$.

The phase relationship between the wave maker and two-dimensional forced standing waves was found experimentally by Taylor [1] as shown in Fig. 4.1. A theoretical interpretation is that the motion of a fluid particle in the neighborhood of the wave maker has to be the same as that of the wave maker in the direction normal to it, and thus the wave maker must always be in phase with the motion of a fluid particle. Comparing the direction of streamlines with the motion of the wave maker sketched in Fig. 4.1, the phase relationship is evident. This can also be applied to any higher mode of oscillation.
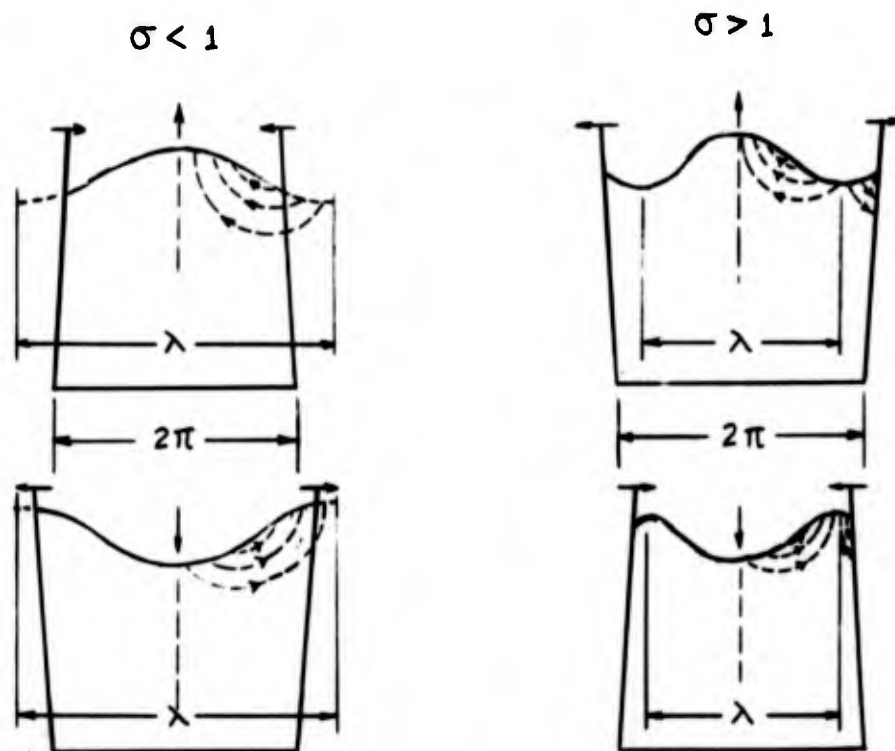
Fig. 4.1 Phase Relation

The first-order amplitude of standing waves at $x = \pi$ is

$$\zeta_{x=\pi} = (\frac{4\alpha}{\pi} \mp \beta\sigma + \frac{8\alpha\sigma^2}{\pi}) \cos\sigma t \qquad (4.33)$$

Hence, the negative sign should be used for $\varepsilon = 0$ and $\sigma > 1$, while the positive sign for $\varepsilon = \pi$ and $\sigma < 1$. For convenience in the later computation, the sign is absorbed in β such that β is positive for $\sigma > 1$ and negative for $\sigma < 1$ and ε is always equal to zero. Then, only the upper sign is used in Eqs. (4.29) to (4.33) from here on.

4.4.2 Second-order Solution

By taking the terms up to second order and eliminating the linear term of a_0 in Eqs. (4.14) and (4.18), one has

$$\ddot{b}_0 = -\frac{2\alpha\sigma(1-2\sigma^2)}{\pi}\sin\sigma t - \frac{1}{2}a_1\ddot{b}_1 + \dot{b}_1(b_1 - \frac{1}{2}\dot{a}_1) - \frac{2\alpha\sigma}{\pi}\sin\sigma t [\dot{b}_1 + \frac{1}{4}(1-2\sigma^2) + \frac{1}{6}(3+2\sigma^2)a_1]$$

$$- \frac{2\alpha\sigma^2}{\pi}\cos\sigma t (b_1 + \frac{1}{2}\dot{a}_0 - \frac{1}{3}\dot{a}_1) + \frac{1}{4}\alpha^2\sigma^3\sin 2\sigma t \qquad (4.34)$$

-27-

The solution of Eq. (4.34) is obtained by substituting the first-order solution from the previous section on the right-hand-side and integrating twice:

$$b_0 = \frac{2\alpha(1-2\sigma^2)}{\pi\sigma} \sin\sigma t \qquad (4.35)$$

$$-\frac{1}{8}\left[\beta^2(1+\sigma^2)/\sigma - \frac{\alpha\beta}{\pi}(5+4\sigma^2) - \frac{2\alpha^2}{9\pi^2\sigma^2}(9-48\sigma^2-46\sigma^4) + \frac{1}{2}\alpha^2\sigma\right]\sin2\sigma t$$

with the integration constants equal to zero for the periodic solution. Also,

$$a_0 = \frac{1}{2}\left[\beta^2(\sigma^2-1) + \frac{4\alpha\beta\sigma(1-\sigma^2)}{\pi} + \frac{8\alpha^2\sigma^2(9+4\sigma^2)}{9\pi^2} - \frac{1}{2}\alpha^2\sigma^2\right] + \frac{4\alpha}{\pi}\cos\sigma t$$

$$+ \frac{1}{2}\left[\frac{\alpha\beta\sigma}{\pi} + \frac{2\alpha^2(3-4\sigma^2)}{3\pi^2}\right]\cos2\sigma t$$

$$(4.36)$$

by using Eq. (4.35) for the linear term of b_0 and the first order solutions on the right-hand-side of Eq. (4.18).

With a similar procedure to that used in obtaining Eq. (4.34),

$$\ddot{b}_1 + b_1 = \frac{4\alpha\sigma(1-2\sigma^2)}{3\pi}\sin\sigma t - \frac{1}{2}a_0 b_1 - \frac{1}{2}\dot{a}_0\dot{b}_1 + \frac{4\alpha\sigma}{\pi}\sin\sigma t\left[b_1 + \frac{1}{4}(1-2\sigma^2)a_0 - \frac{1}{10}(11-14\sigma^2)a_1\right]$$

$$+ \frac{4\alpha\sigma^2}{3\pi}\cos\sigma t\left[b_1 + \frac{1}{2}\dot{a}_0 - \frac{7}{5}\dot{a}_1\right] - \frac{1}{2}a_0\ddot{b}_1 \qquad (4.37)$$

or

$$\ddot{b}_1 + \sigma^2 b_1 = \left[(\sigma^2-1)\beta + \frac{4\alpha\sigma(1-2\sigma^2)}{3\pi}\right]\sin\sigma t$$

$$+ \left[\frac{\alpha\beta}{15\pi}(28\sigma^4+39\sigma^2-15) - \frac{2\alpha^2\sigma}{45\pi^2}(112\sigma^4+16\sigma^2-15)\right]\sin2\sigma t \qquad (4.38)$$

Again, the secular term must vanish for a periodic solution. Then one obtains

$$b_1 = \beta\sin\sigma t - \frac{1}{3\sigma^2}\left[\frac{\alpha\beta}{15\pi}(28\sigma^4+39\sigma^2-15) - \frac{2\alpha^2\sigma}{45\pi^2}(112\sigma^4+16\sigma^2-15)\right]\sin2\sigma t \qquad (4.39)$$

with

$$(\sigma^2-1)\beta + \frac{4\alpha\sigma(1-2\sigma^2)}{3\pi} = 0 \qquad (4.40)$$

and

$$a_1 = \left[\frac{\alpha\beta\sigma}{15\pi}(5+14\sigma^2) - \frac{4\alpha^2\sigma^2}{45\pi^2}(15+28\sigma^2)\right] + \left(\beta - \frac{8\alpha\sigma}{3\pi}\right)\sigma\cos\sigma t$$

$$+ \left[\frac{\alpha\beta}{45\pi\sigma}(30-3\sigma^2-14\sigma^4) - \frac{4\alpha^2}{135\pi^2}(15+29\sigma^2-28\sigma^4)\right]\cos2\sigma t$$

$$(4.41)$$

Finally, it follows from Eqs. (4.16) and (4.20) that

$$\ddot{b}_2 + 2b_2 = \frac{4\alpha\sigma(1-2\sigma^2)}{15\pi}\sin\sigma t - a_1 b_1 - \frac{1}{2}\dot{a}_1\dot{b}_1 - \frac{1}{2}a_1\ddot{b}_1 \qquad (4.42)$$

$$- \frac{4\alpha\sigma}{15\pi}\sin\sigma t\left[\dot{b}_1 + \frac{1}{4}(1-2\sigma^2)a_0 + \frac{1}{14}(71-38\sigma^2)a_1\right] + \frac{4\alpha\sigma^2}{15\pi}\cos\sigma t\left(b_1 + \frac{1}{2}\dot{a}_0 + \frac{19}{7}\dot{a}_1\right)$$

$$= \frac{4\alpha\sigma(1-2\sigma^2)}{15\pi}\sin\sigma t$$

$$+ \frac{1}{2}\left[\beta^2\sigma(\sigma^2-1) + \frac{\alpha\beta\sigma^2}{105\pi}(478-432\sigma^2) + \frac{4\alpha^2\sigma}{15\pi^2}(1-\frac{368}{21}\sigma^2 + \frac{304}{21}\sigma^4)\right]\sin 2\sigma t$$

with the solutions,

$$b_2 = \frac{4\alpha\sigma(1-2\sigma^2)}{15\pi(2-\sigma^2)}\sin\sigma t \qquad (4.43)$$

$$+ \frac{1}{4(1-2\sigma^2)}\left[\beta^2\sigma(\sigma^2-1) + \frac{2\alpha\beta\sigma^2}{105\pi}(239-216\sigma^2) + \frac{4\alpha^2\sigma}{315\pi^2}(21-368\sigma^2+304\sigma^4)\right]\sin 2\sigma t$$

and

$$a_2 = \frac{1}{4}\left[\beta^2\sigma^2 - \frac{8\alpha\beta\sigma(7+54\sigma^2)}{105\pi} - \frac{16\alpha^2\sigma^2(21-76\sigma^2)}{315\pi^2}\right] - \frac{4\alpha\sigma^2}{5\pi(2-\sigma^2)}\cos\sigma t$$

$$- \frac{1}{4(1-2\sigma^2)}\left[\beta^2\sigma^2 - \frac{4\alpha\beta\sigma(14+103\sigma^2)}{105\pi} + \frac{8\alpha^2\sigma^2(21+132\sigma^2)}{315\pi^2}\right]\cos 2\sigma t$$

$$(4.44)$$

Only the particular integral due to the forcing terms is taken since the solution with $\sigma=\sqrt{2}$ will disappear for the steady periodic motion. Note that Eq. (4.40) is identical with Eq. (4.31) of the first-order solution, i.e. the frequency-amplitude relation near $\sigma = 1$ remains the same as for the linear theory in Sec. 3.2. Therefore, in order to get the non-linear characterisitc of the frequency-amplitude curve, the third-order solution has to be investigated.

4.4.3 Third-order Solution for the frequency-amplitude relation

As mentioned in Sec. 4.1, the third-order solution only deals with the non-linear characteristic of the frequency-amplitude relation, which is then used for the computation of the second-order solution in the previous section. To do this, only the secular term of the following equation has to be computed from Eqs. (4.15) and (4.19) by elimination of a_1.

$$\ddot{b}_1 + b_1 = -\frac{1}{2}\ddot{b}_1(a_0 + \frac{1}{4}a_0^2 + a_2 + \frac{3}{4}a_1^2) - \frac{1}{2}\dot{b}_1(\dot{a}_0 + \frac{1}{2}a_0\dot{a}_0 + \dot{a}_2 + \frac{3}{2}a_1\dot{a}_1) - \frac{1}{2}b_1(a_0 + \frac{1}{4}a_0^2 - a_2 + \frac{1}{4}a_1^2)$$

$$- a_1\ddot{b}_2 - \dot{a}_1\dot{b}_2 - a_1 b_2 + \dot{a}_1 b_1^2 + 2a_1 b_1\dot{b}_1 + 2b_1 b_2 + 2b_1\dot{b}_2$$

$$+ \frac{4\alpha\sigma}{\pi}\sin\sigma t\left[(1-2\sigma^2)(1+\frac{1}{4}a_0 + \frac{1}{32}a_0^2) - \frac{1}{10}(11-14\sigma^2)(1+\frac{1}{4}a_0)a_1 - \frac{1}{70}(157+38\sigma^2)a_2\right.$$

$$\left. - \frac{(61+54\sigma^2)}{280}a_1^2 + (1+\frac{3}{4}a_0 - \frac{21}{10}a_1)\dot{b}_1 + (\frac{3}{4}\dot{a}_0 - \frac{21}{10}\dot{a}_1)b_1 - \frac{18}{5}b_2\right]$$

-29-

$$+ \frac{2\alpha\sigma^2}{\pi} \cos\sigma t \left[2(1+\tfrac{3}{4}a_0 - \tfrac{21}{10}a_1)b_1 - \tfrac{36}{5}b_2 + (1+\tfrac{1}{4}a_0 - \tfrac{7}{10}a_1)\dot{a}_0 \right.$$
$$\left. - \tfrac{7}{10}(1+a_0 - \tfrac{54}{49}a_1)\dot{a}_1 + \tfrac{38}{35}\dot{a}_2 \right]$$

$$+ \tfrac{1}{2}\alpha^2\sigma^2\left[\sigma a_1 \sin 2\sigma t + \dot{a}_1 \sin^2\sigma t\right] \tag{4.45}$$

The second-order solutions of a_n and b_n are put into the right-hand-side of Eq. (4.45), and the coefficient of $\sin\sigma t$ provides the third-order frequency-amplitude relation as follows:

$$(\sigma^2-1)\beta + \frac{4\alpha\sigma(1-2\sigma^2)}{3\pi} + K_0\beta^3 + K_1(\tfrac{\alpha}{\pi})\beta^2 + K_2(\tfrac{\alpha}{\pi})^2\beta + K_3(\tfrac{\alpha}{\pi})^3 \tag{4.46}$$

where

$$K_0 = \frac{1}{4} - \frac{\sigma^2(1-\sigma^2)(34\sigma^2-27)}{32(2\sigma^2-1)} \tag{4.47}$$

$$K_1 = -\frac{\sigma(651-1327\sigma^2-2413\sigma^4)}{840} + \frac{\sigma(14+8420\sigma^2-8250\sigma^4)}{420(2\sigma^2-1)} \tag{4.48}$$

$$K_2 = (3{,}082{,}880\sigma^6 + 1{,}376{,}280\sigma^4 - 132{,}300\pi^2\sigma^4 - 743{,}904\sigma^2 + 66{,}150\pi^2\sigma^2 + 8820)\big/_{520}$$
$$- (560\sigma^6 + 500\sigma^4 - 690\sigma^2 + 15)\big/45\sigma^2 - (5{,}131\sigma^2 + 79{,}147\sigma^4 + 88{,}160\sigma^6)\big/22{,}050(1-2\sigma^2)$$
$$- (45 - 177\sigma^2 - 12\sigma^4 - 368\sigma^6 + 280\sigma^8)\big/675(2-\sigma^2) \tag{4.49}$$

$$K_3 = -\sigma(2{,}416{,}000\sigma^6 + 2{,}553{,}088\sigma^4 - 198{,}450\pi^2\sigma^4 - 2{,}167{,}536\sigma^2 + 33{,}075\pi^2\sigma^2 + 202{,}860)\big/_{396{,}900}$$
$$+ (30 - 92\sigma^2 - 160\sigma^4 - 448\sigma^6)\big/135\sigma + (86{,}640\sigma^4 - 49{,}692\sigma^2 + 11{,}886)\sigma^3\big/33{,}075(1-2\sigma^2)$$
$$+ \sigma(3{,}136\sigma^8 - 4{,}784\sigma^6 - 1{,}624\sigma^4 + 156\sigma^2 + 90)\big/2{,}025(2-\sigma^2) \tag{4.50}$$

4.5 Numerical Computation

4.5.1 The Frequency-amplitude Curves

Eq. (4.46) is rewritten as the following:

$$\sigma^2 = 1 - \frac{4\alpha\sigma(1-2\sigma^2)}{3\pi\beta} - K_0\beta^2 - K_1(\tfrac{\alpha}{\pi})\beta - K_2(\tfrac{\alpha}{\pi})^2 - K_3(\tfrac{\alpha}{\pi})^3/\beta \qquad (4.51)$$

Here the frequency of non-linear two-dimensional standing waves is considered as a function of β with α as a parameter on the σ-β plane. Since it is non-linear in both σ and β, Eq. (4.51) is again solved numerically by the method of iteration. Only two wave maker amplitudes, $\alpha = 0.0194$ and 0.0388, were computed. For the range of magnitude of α, the last term is small in comparison with the second term on the right-hand-side of Eq. (4.51). For $\alpha = 0.0388$ and $\sigma = 1$,

$$K_3 = -5.1631 \quad \text{and} \quad (\alpha/\pi)^2 = 0.00003813$$

while $\dfrac{4\sigma(1-2\sigma^2)}{3} = -1.3333$;

hence, $\left| \dfrac{4\alpha\sigma(1-2\sigma^2)}{3\pi} \right| \gg \left| K_3(\tfrac{\alpha}{\pi})^3 \right|$

and the last term was neglected in the computation. With a small variation of σ in the neighborhood of $\sigma = 1$, Eq. (4.51) consists essentially of two parts: one is a hyperbola with the asymptotes, $\sigma^2 = 1$ and $\beta = 0$ and the other is a parabola with its vertex at $\sigma^2 = -K_2(\tfrac{\alpha}{\pi})^2$ in the σ^2-β plane. In Sec. 4.4.1, it was assumed that β takes a positive value for $\sigma > 1$ and a negative for $\sigma < 1$ to take account of the phase relation between the wave maker and standing waves. For non-linear standing waves, $\sigma < 1$ should imply that the oscillation is on the branch on the left of the resonance curve and $\sigma > 1$ on the right branch for the first mode. The resonance curve (the frequency-amplitude curve for free oscillation) of the third order can be obtained by letting $\alpha = 0$ in Eq. (4.51); then,

$$\sigma^2 = 1 - K_0\beta^2 \qquad (4.52)$$

where K_0 is given by Eq. (4.47). The procedure of computation is to break Eq. (4.51) into two parts:

$$\chi_1 = 1 \pm \frac{4\alpha\sigma(1-2\sigma^2)}{3\pi\beta} \qquad (4.53)$$

and

$$\chi_2 = -K_0\beta^2 \pm K_1(\tfrac{\alpha}{\pi})\beta - K_2(\tfrac{\alpha}{\pi})^2 \qquad (4.54)$$

in which the upper positive sign is for $\sigma < 1$ and the lower negative for $\sigma > 1$ and β is an absolute value again for both cases. The iteration was started with $\sigma = 1$ for different β's and $\alpha = 0.0194$ and 0.0388 until the final χ_1 and χ_2 were in agreement with their previous trials within the fourth place after the decimal, i.e. less than 0.1% in error. Then, $\sigma = \sqrt{\chi_1 + \chi_2}$ was plotted against β as shown in Fig. 4.2.

Based on the solution of b_0, b_1 and b_2 in Sec. 4.4.4, the free surface is at rest at $\sin n\sigma t = 0$, or $t = n\pi/\sigma$. The free surface elevation to the second order can be obtained from Eq. (4.2) by using a_0, a_1 and a_2 of Eqs. (4.36), (4.41) and (4.44). Then, the total amplitude, $|A|$, at $X = \pi$ as a function of σ is

$$|A| = \left| \zeta_{t=\pi/\sigma} - \zeta_{t=0} \right|$$
$$= \left| \mp 2\beta\sigma - \frac{4\alpha}{\pi} - \frac{8\alpha\sigma^2(17-10\sigma^2)}{15\pi(2-\sigma^2)} \right| \tag{4.55}$$

in which the negative sign in front of β is for $\sigma < 1$ and the positive for $\sigma > 1$. The computed $\sigma - |A|$ curves are shown in Fig. 4.3 for $\alpha = 0.0194$ and $\alpha = 0.0388$.

4.5.2 The Profiles of Forced Standing Waves

The profiles of the free surface at rest were computed for $\sigma = 0.965$ and 1.000 with $\alpha = 0.0194$. The free surface elevation, Eq. (4.2), to the second order leads to

$$\zeta = \frac{a_0}{2} + a_1 \cos X + a_2 \cos 2X \tag{4.56}$$

in which a_0, a_1 and a_2 are given by Eqs. (4.36), (4.41) and (4.44). The parameter, β, in the coefficients may be obtained from Fig. 4.2

as $\qquad 2\beta = 0.217 \qquad$ for $\qquad \sigma = 0.965$

and $\qquad 2\beta = 0.694 \qquad$ for $\qquad \sigma = 1.000$

The computed profiles are shown in Fig. 4.4
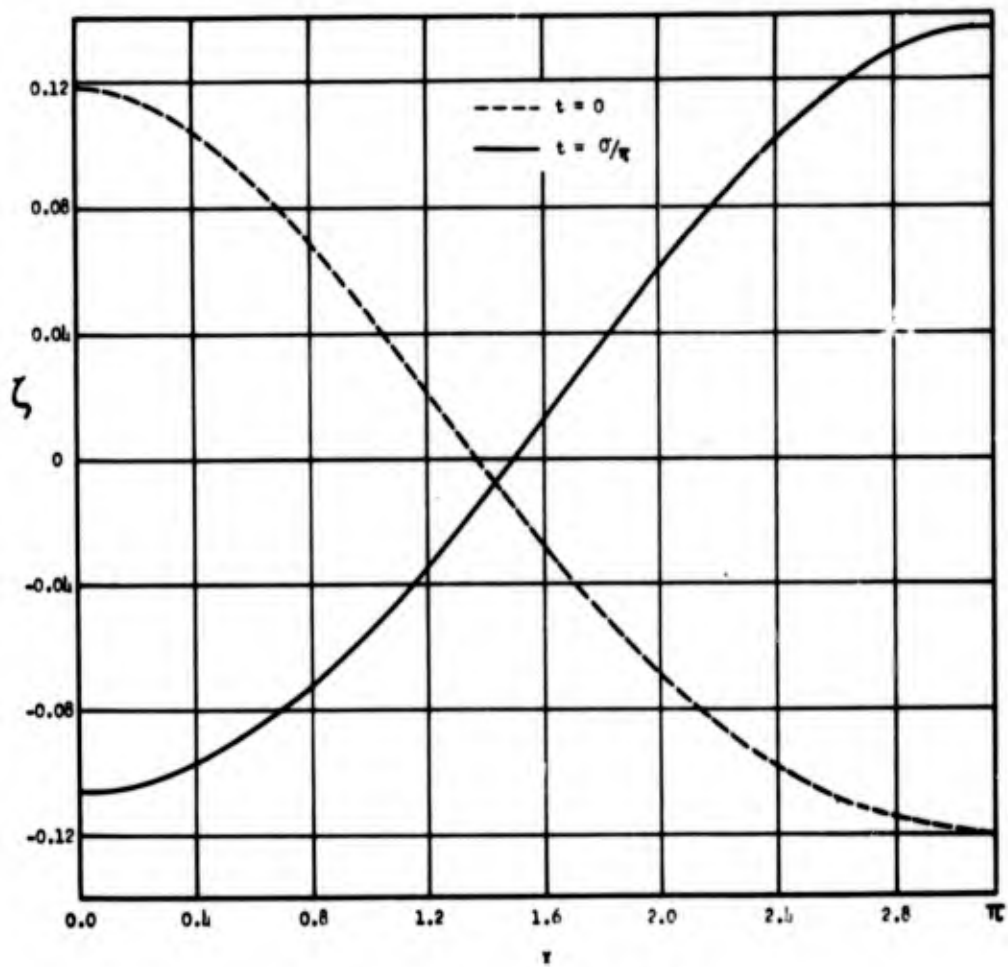
(a) $\sigma = 0.965$
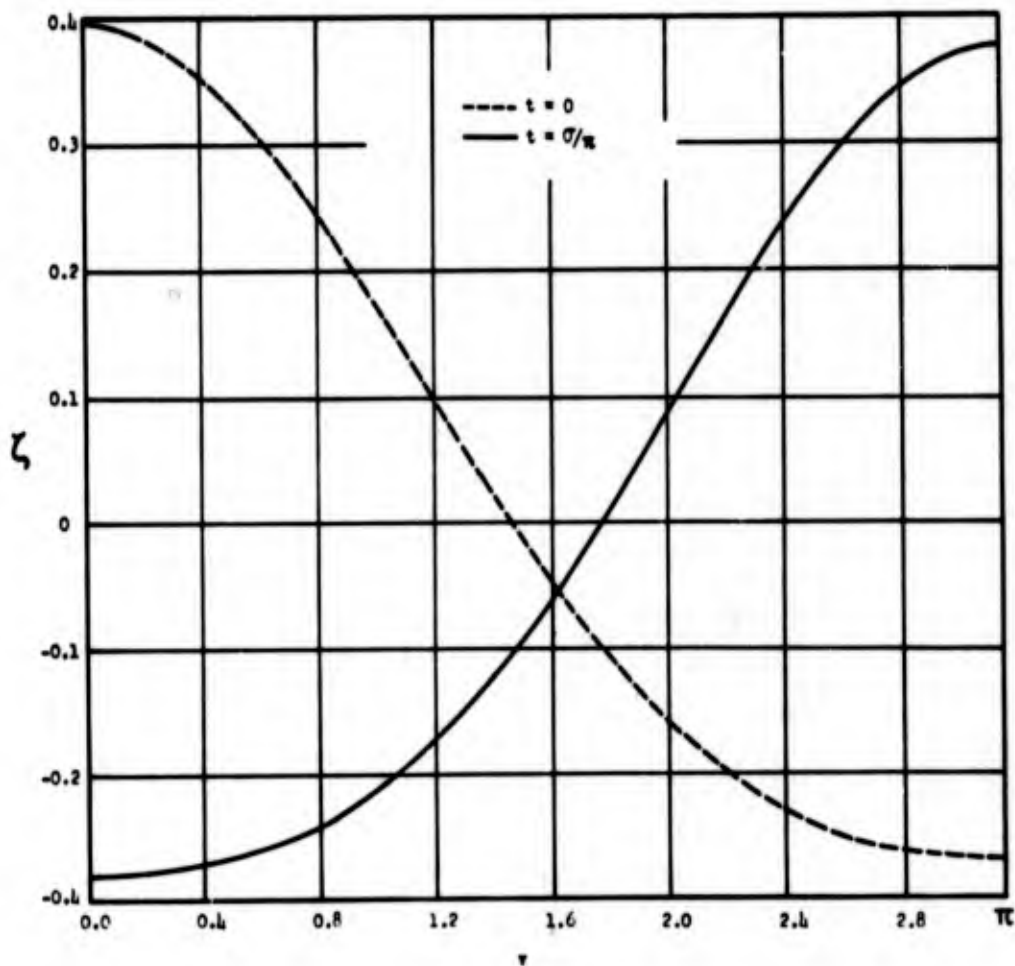
(b) $\sigma = 1.000$

FIG. 4.4 Profiles of Forced Two-dimensional Standing Waves
for $\sigma = 0.0194$

4.6 Higher Modes of Forced Two-Dimensional Standing Waves

The procedure to find a solution for any higher mode is exactly the same as for the fundamental mode presented in previous sections. The assumption of the order of magnitude of the coefficient made in Sec. 4.3 provides a starting point to compute $S_n(s)$ and $E(\lambda, \mu)$ and then a set of equations can be obtained from Eqs. (4.7) to (4.10) to any desired order of magnitude. The non-linear frequency-amplitude relation will appear in the secular term of the solution belonging to the equation with the frequency near the wave maker frequency at the third order of approximation. The final forms of the coefficients will be a Fourier series in t with its fundamental frequency the same as the one of the wave maker and the coefficient as a function of α, β and σ. The β is determined explicitly from the σ-β curve for a particular β. It will also be noted that the resonance curve of free oscillation ($\alpha = 0$) should remain the same for all modes of oscillation.

4.7 Comparison of the Linear and Non-linear Solutions

A comparison of the non-linear frequency-amplitude curves obtained in Sec. 4.5.1 with those of the linear theory in Sec. 3.3 is made in Fig. 4.5. The agreement is surprisingly good for the region with the frequency far away from $\sigma = 1$. These results indicate that the non-linear effect is essentially confined to the neighborhood of the resonance frequency, the range depends on the amplitude of the wave maker and also provides the range of significant non-linear effects as far as these two values of α are concerned. These ranges determined from Fig. 4.5 are

$$0.93 < \sigma/\sigma_1 < 1.05 \qquad \text{for } \alpha = 0.0194$$

$$0.92 < \sigma/\sigma_1 < 1.08 \qquad \text{for } \alpha = 0.0388$$

A comparison of the resonance curve with Penney and Price's indicates good agreement for $|A| < 0.75$. The discrepancy at high amplitude may be on account of the following two reasons: (1) The present solution is based on the third-order σ-β curves and second-order Eq. (4.55), while their result is of the fifth order; (2) In Penney and Price's computation the second term of Eq. (4.47) for K_0 is missing as a result of approximating all σ values on the right of the equation for the frequency-amplitude curve which is equivalent to letting $\sigma = 1$ in Eqs. (4.47) to (4.50) and (4.55).
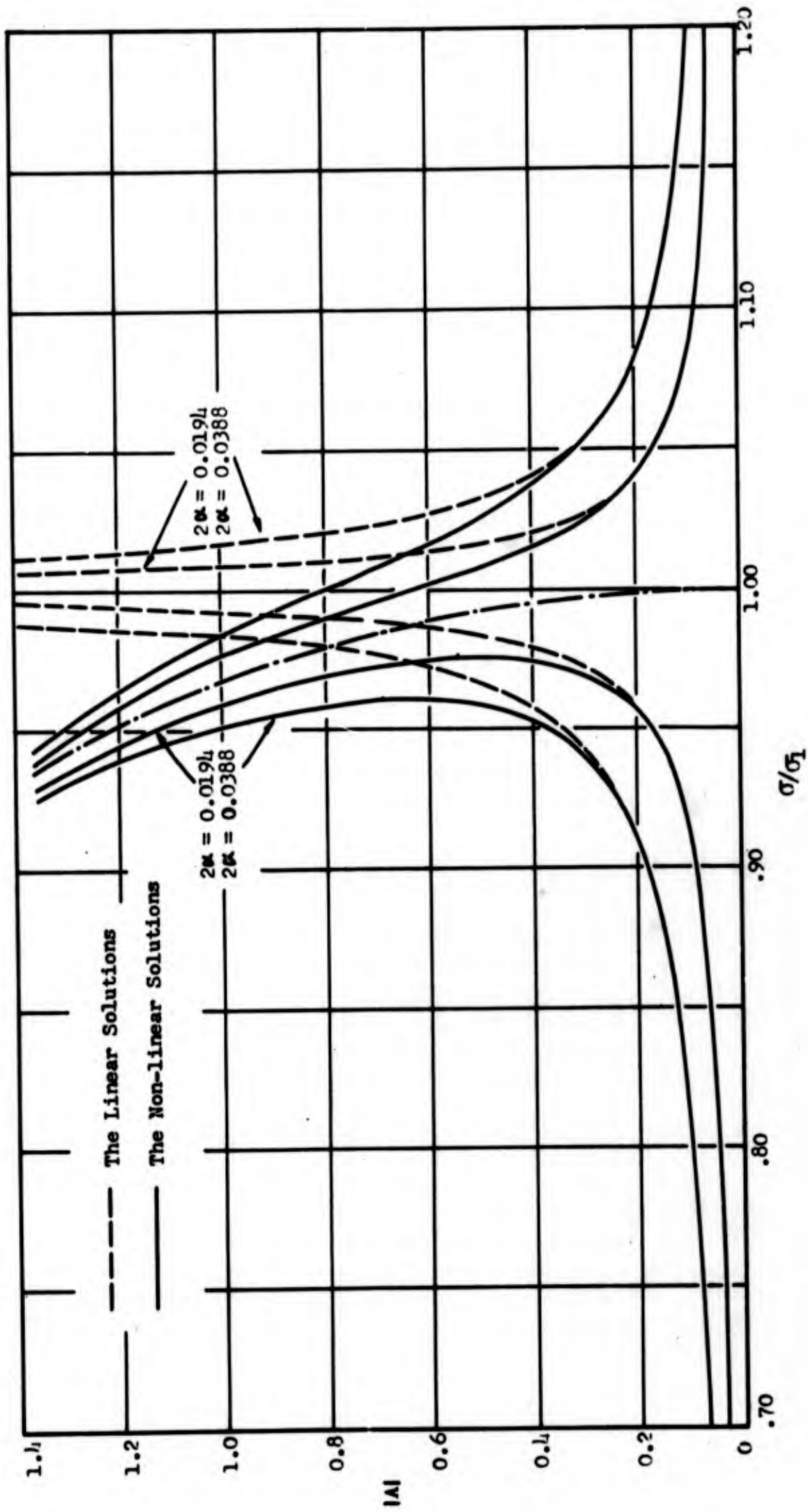
FIG. 4.5 Comparison of Frequency-Amplitude Curves of Forced Two-dimensional Linear and Non-linear Solutions

V. NON-LINEAR FORCED THREE-DIMENSIONAL STANDING WAVES IN A RECTANGULAR TANK

5.1 General Remarks

The preliminary investigation based on the linear theory in Section III shows that the linearized version of the problem under consideration is basically two-dimensional. The forced two-dimensional standing waves of small amplitude are from the linear solution of the system and are always stable except in the neighborhood of a resonance frequency. This result leads to the general conviction that three-dimensional standing waves in the system can be generated only due to the non-linearity in the exact free surface conditions (See Eqs. (2.23) and (2.24))in the range of non-linear effects and hence the forced standing waves must be of finite amplitude. The non-linear solution of forced two-dimensional standing waves obtained in the previous section provides the range of stability for the linear solution and also represents a family of particular solutions to the problem as a whole. The present section is to investigate the underlying mechanics of exciting the fundamental mode of cross waves based on the exact free surface conditions. In addition to generalizing the expansion of the product of an exponential of a Fourier series and another Fourier series into the three-dimensional case, the approach is essentially similar to Sec. IV, but the degrees of freedom for the solutions are doubled. A system of non-linear ordinary differential equations will be derived for the coefficients of the double Fourier series in x and y of φ and ζ. These equations can be solved by the method of iteration to any desired order of approximation. Only the second-order solution is found here and thus the result will be qualitative. However, a quantitative result can be obtained if the elaborate computation is to be carried on to a higher order of approximation. With the second order solution, it is found that the half-frequency mode of subharmonic oscillations is indeed the fundamental mode of cross waves and the favorable condition to excite cross waves depends on the length/width ratio of the tank and the amplitude of motion of the wave maker. It is expected that some quantitative description of cross waves is to be obtained from the experimental investigation in the later part of the investigation.

5.2 Fourier Series Expressions for φ and ζ

Assume

$$\varphi = \sum_{m=0}^{\infty} \sum_{n=0}^{\infty} B_{mn}(t) \cos m\ell y \cos nx \, e^{\sqrt{m^2\ell^2 + n^2} \, z} \tag{5.1}$$

which satisfies the Laplace equation, Eq. (2.19), and the homogeneous boundary conditions, Eqs. (2.20) to (2.22); and also assume

$$\zeta = \sum_{m=0}^{\infty} \sum_{n=0}^{\infty} A_{mn}(t) \cos m\ell y \cos nx \quad \text{for} \quad z = \zeta(x,y,t) \tag{5.2}$$

which together with φ, Eq. (5.1), satisfies the free surface conditions, Eqs. (2.23) and (2.24). Then, neglecting all harmonics higher than $\cos \ell y$, approximately

$$\varphi = \sum_{n=0}^{\infty} B_{0n} \cos nx \, e^{nz} + \sum_{n=0}^{\infty} B_{1n} \cos nx \, e^{\sqrt{\ell^2 + n^2} \, z} \cos \ell y$$

$$= \sum_{n=0}^{\infty} b_n \cos nx \, e^{nz} + \sum_{n=0}^{\infty} d_n \cos nx \, e^{\nu_n z} \cos \ell y \tag{5.3}$$

where $b_n = B_{0n}$, $d_n = B_{1n}$ and $\nu_n = \sqrt{\ell^2 + n^2}$; and

$$\zeta = \sum_{n=0}^{\infty} A_{0n} \cos nx + \sum_{n=0}^{\infty} A_{1n} \cos nx \cos \ell y$$

$$= \frac{a_0}{2} + \sum_{n=1}^{\infty} a_n \cos nx + \left(\frac{c_0}{2} + \sum_{n=1}^{\infty} c_n \cos nx\right) \cos \ell y \tag{5.4}$$

where $a_0 = 2A_{00}$, $c_0 = 2A_{10}$ and $a_n = A_{0n}$, $c_n = A_{1n}$ for $n \geqslant 1$.

Therefore, the solution of three-dimensional waves is desired with only the fundamental mode of cross waves. Let

$$\zeta = \zeta_1 + \zeta_2 \tag{5.5}$$

with

$$\zeta_1 = \frac{a_0}{2} + \sum_{n=1}^{\infty} a_n \cos nx = \frac{1}{2} \sum_{n=-\infty}^{\infty} a_n e^{inx} \; ; \; a_n = a_{-n} \tag{5.6}$$

and

$$\zeta_2 = \left(\frac{c_0}{2} + \sum_{n=1}^{\infty} c_n \cos nx\right) \cos \ell y = \frac{1}{2} \sum_{n=-\infty}^{\infty} c_n e^{inx} \cos \ell y \; ; \tag{5.7}$$

$$c_n = c_{-n}$$

5.3 The System of Non-Linear Ordinary Equations for the Coefficients, a_n, b_n, c_n and d_n.

The general procedure of solution is to substitute φ and ζ above into the free surface conditions, Eqs. (2.23) and (2.24); first to obtain four equations in terms of $\cos nx$ by comparing the coefficients of $\cos m\ell y$ for $m = 0$ and 1; and then to obtain four sets of ordinary differential equations in a_n, b_n, c_n and d_n for $n = 0,1,2,\cdots$. by comparing the coefficients of $\cos nx$ for $n = 0,1,2,\cdots$. These equations can be solved by the method of iteration to any desired order of approximation, as in the previous section. The present problem differs from the two-dimensional one by containing two parameters, one of which is for cross waves and the other for the longitudinal component. There exist two frequency-amplitude relations in the fundamental modes of the two components to determine these two parameters. Prior to the above-mentioned procedure, $e^{\lambda \zeta_2} \cos \mu \ell y$ is to be expanded in addition to $e^{\lambda \zeta_1} \cos \mu x$ which appears in the free surface conditions, Eqs. (2.23) and (2.24). The expansion $e^{\lambda \zeta_1} \cos \mu x$ developed in Appendix A is again used in this section. The expansion

$$e^{\lambda \zeta_2}\cos\mu\ell y = F(\lambda,\mu)+ \sum_{s=1}^{\infty} \cos s\ell y \left[F(\lambda,s-\mu)+ F(\lambda,s+\mu)\right]$$

where

$$F(\lambda,\mu)= F(\lambda,-\mu) = \sum_{s=-\infty}^{\infty} f_s(\lambda,\mu)\cos sx \qquad (5.8)$$

and the related functions are developed in Appendices B and C and computed to the third order.

The system of equations in terms of the functions $E(\lambda,\mu)$ and $f_s(\lambda,\mu)$ are given in Appendix D.

5.4 Solution by the Method of Iteration

The system of Eqs. (D.1) to (D.8) in Appendix D is based on the dimensionless equations formulated in Sec. II. An examination of the mode of oscillation in the three-dimensional system is necessary before any assumption of the order of magnitude of the coefficients a_n, b_n, c_n and d_n can be made. Since the interest is only in the fundamental mode of cross waves, the component mode in the transverse direction is fixed. The resonance frequency corresponding to this mode, $\omega_1^*/2\pi$, depends only on the width of the tank for the infinite-depth case, and

$$\omega_1^{*2} = \frac{2\pi g}{\lambda_c} = \frac{\pi g}{W} = \frac{\pi g}{L}\left(\frac{L}{W}\right) \qquad (5.9)$$

where the cross wave length is $\overset{*}{\lambda}_0 = 2\pi$ for the fundamental mode of cross waves. In dimensionless form,

$$\omega_1^2 = L/w = \ell .$$

(5.10)

Hence, we are looking for a solution of cross waves with a frequency ω in the neighborhood of $\omega_1 = \sqrt{\ell}$ but the corresponding longitudinal mode of oscillation still remains to be determined, for there are infinitely many discrete resonance frequencies. The unit L/π used in the derivation of the dimensionless system in Sec. II implies in this case that $\lambda = 2L$ for the assumed φ and ζ in Eqs. (5.1) and (5.2) because the cos nx in the summation should in general be $\cos\frac{2n\pi x^*}{\lambda^*}$, where λ^* is the wave length of the longitudinal component. This means that the fundamental mode in the longitudinal component has been chosen and the frequency relation between these components and the length/width ratio remains to be determined. The resonance frequency of the longitudinal mode $\sigma_1 = \ell$ can easily be verified. The generalization to higher longitudinal modes will be treated later. It is natural to consider that β and δ are of the same order, which leads to the assumption that a_0, b_0, c_0, d_0, a_1 and b_1 are of $O(\beta \text{ or } \delta)$ while c_1, d_1, a_2, b_2 of $O(\beta^2 \text{ or } \delta^2)$ and so forth. In general the order of magnitude of c_s and d_s is fixed relative to a_s and b_s which depend on the longitudinal mode of oscillation to be solved for in a manner similar to the two-dimensional case.

The next step is to compute the function $f_s(\lambda,\mu)$ to the third order as given in Appendix B and also to use $E(\lambda,\mu)$ in Appendix A for the expansion of the system of Eqs. (D.1) to (D.8) in Appendix D to the third order. The system of second-order equations is given as follows.

$$a_0 = 2\dot{b}_0 + a_1\dot{b}_1 - b_1^2 + \tfrac{1}{2}\ell c_0 \dot{d}_0 - \ell^2 d_0^2 + \tfrac{4\alpha\sigma}{\pi}b_1\sin\sigma t + \tfrac{8\alpha\sigma^2}{\pi}(1+\tfrac{1}{4}a_0 - \tfrac{1}{6}a_1)\cos\sigma t - \tfrac{1}{2}\alpha^2\sigma^2\sin^2\sigma t$$

(5.11)

$$a_1 = \dot{b}_1 + \tfrac{1}{2}a_0\dot{b}_1 - \tfrac{4\alpha\sigma}{3\pi}b_1\sin\sigma t - \tfrac{8\alpha\sigma^2}{3\pi}(1+\tfrac{1}{4}a_0 - \tfrac{7}{10}a_1)\cos\sigma t$$

(5.12)

$$a_2 = \dot{b}_2 + \tfrac{1}{2}a_1\dot{b}_1 - \tfrac{4\alpha\sigma}{15\pi}b_1\sin\sigma t - \tfrac{8\alpha\sigma^2}{15\pi}(1+\tfrac{1}{4}a_0 + \tfrac{19}{14}a_1)\cos\sigma t$$

(5.13)

$$c_0 = 2\dot{d}_0 + \ell a_0\dot{d}_0 - \tfrac{4\alpha\sigma}{\pi}\ell d_0\sin\sigma t$$

(5.14)

$$c_1 = \dot{d}_1 + \tfrac{1}{2}\dot{b}_1 c_0 + \ell a_1\dot{d}_0 - \ell b_1 d_0 + \tfrac{4\alpha\sigma}{3\pi}\ell d_0\sin\sigma t - \tfrac{\alpha\sigma^2}{3\pi}c_0\cos\sigma t$$

(5.15)

$$\dot{a}_0 = -\frac{4\alpha\sigma}{\pi}\sin\sigma t(1+\tfrac{1}{4}a_0+\tfrac{1}{2}a_1) \tag{5.16}$$

$$\dot{a}_1 = -b_1 - \tfrac{1}{2}a_0 b_1 + \frac{4\alpha\sigma}{3\pi}\sin\sigma t(1+\tfrac{1}{4}a_0+\tfrac{11}{10}a_1) \tag{5.17}$$

$$\dot{a}_2 = -2b_2 - a_1 b_1 + \frac{4\alpha\sigma}{15\pi}\sin\sigma t(1+\tfrac{1}{4}a_0+\tfrac{71}{14}a_1) \tag{5.}$$

$$\dot{c}_0 = -2\ell d_0 - \ell^2 a_0 d_0 - \frac{\alpha\sigma}{\pi}c_0\sin\sigma t \tag{5}$$

$$\dot{c}_1 = -\nu_1 d_1 - \tfrac{1}{2}b_1 c_0 - \ell^2 a_1 d_0 + \frac{\alpha\sigma}{3\pi}c_0\sin\sigma t \tag{5.20}$$

First, the pair of Eqs. (5.14) and (5.19) is solved again by Duffing's method of iteration. By eliminating c_0, then

$$\ddot{d}_0 + \ell d_0 = -\tfrac{1}{2}a_0(\ddot{d}_0+\ell d_0) - \tfrac{1}{2}\ell \dot{a}_0 \dot{d}_0 + \frac{\alpha\sigma}{2\pi}[4\ell \dot{d}_0 - c_0(1-2\sigma^2)]\sin\sigma t$$
$$+ \frac{\alpha\sigma^2}{\pi}(2\ell d_0 - \dot{c}_0)\cos\sigma t \tag{5.21}$$

The equation of the linear free oscillation as the first-order approximation is

$$\ddot{d}_0 + \ell d_0 = 0 \tag{5.22}$$

which yields the solution,

$$d_0 = \delta \sin(\omega t + \epsilon) \tag{5.23}$$

and

$$c_0 = 2\delta\omega\cos(\omega t + \epsilon) \tag{5.24}$$

where δ is a parameter, ϵ is the phase difference with the wave maker and $\omega_0^2 \approx \ell$. Then, substituting Eqs. (5.23) and (5.24) and also $a_0 = -4\alpha\sigma/\pi \sin\sigma t$, which is the first-order a_0 from Eq.(5.16), into the right-hand-side of Eq. (5.21), there results:

$$\ddot{d}_0 + \omega^2 d_0 = (\omega^2-\ell)\delta\sin(\omega t+\epsilon) + \frac{\alpha\delta\sigma}{2\pi}[\omega(4\ell-1+2\sigma^2)-2\sigma(\ell+\omega^2)]\sin(\sigma t-\omega t-\epsilon)$$
$$+ \frac{\alpha\delta\sigma}{2\pi}[\omega(4\ell-1+2\sigma^2)+2\sigma(\ell+\omega^2)]\sin(\sigma t+\omega t+\epsilon) \tag{5.25}$$

Note that the lowest frequency of the forcing function on the right-hand-side of Eq. (5.25) is equal to $\sigma-\omega$, which has to be the fundamental frequency of cross waves for the

existence of a steady periodic solution. Therefore, it has been proved that

$$\omega = \sigma/2 \tag{5.26}$$

and the phase difference ϵ has to be zero or $\pi/2$.
As far as the analysis up to this stage is concerned, the phase angle either zero or $\pi/2$ will satisfy the conditions required to yield a periodic solution. However, the result of experimental measurements in Sec. VIII indicated that the phase angle should be $\pi/2$; and the following computation will be based on $\epsilon = \pi/2$.

Eq. (5.25) becomes

$$\ddot{d}_0 + \omega^2 d_0 = \delta \left[\omega^2 - \ell - \frac{\alpha\omega^2}{\pi}(4\omega^2 - 1) \right] \cos \omega t$$
$$+ \frac{\alpha\delta\sigma}{\pi}(8\ell - 1 + 12\omega^2) \cos 3\omega t \tag{5.27}$$

which gives

$$d_0 = \delta \cos \omega t - \frac{\alpha\delta}{8\pi}(8\ell - 1 + 12\omega^2) \cos 3\omega t \tag{5.28}$$

with the secular term

$$\omega^2 - \ell - \frac{\alpha\omega^2}{\pi}(4\omega^2 - 1) = 0 \tag{5.29}$$

For $\omega^2 \approx \ell$, $\omega \approx 1/2$ and $\sigma \approx 1$ which is the frequency of the wave maker or the corresponding longitudinal mode in agreement with what has been chosen. Furthermore, the ratio of length/width of the tank for exciting this three-dimensional mode with $\alpha \to 0$ as a limit is

$$\ell = 1/4 \tag{5.30}$$

From Eq. (5.14), one has

$$C_0 = -2\delta\omega \left[1 - \frac{\alpha}{\pi}(4\omega^2 - 1) \right] \sin \omega t + \frac{\alpha\delta\omega}{4\pi}(4\omega^2 - 3) \sin 3\omega t \tag{5.31}$$

by use of Eqs. (5.28), (5.23) and (5.24) together with the solution of $a_0 = \frac{4\alpha}{\pi} \cos \sigma t$.

For the fundamental mode of the longitudinal component, the pair of Eqs. (5.12) and (5.17) lead to

$$\ddot{b}_1 + b_1 = -\frac{1}{2}a_0(\ddot{b}_1 + b_1) - \frac{1}{2}\dot{a}_0\dot{b}_1 + \frac{4\alpha\sigma^2}{3\pi}\cos\sigma t (b_1 + \frac{1}{4}\dot{a}_0 - \frac{7}{10}\dot{a}_1)$$

$$+ \frac{4\alpha\sigma}{3\pi}\sin\sigma t \left[(1 - \sigma^2)(1 + \frac{1}{4}a_0) - \frac{11}{10}(1 - \frac{14}{11}\sigma^2)a_1 + \dot{b}_1 \right] \tag{5.32}$$

independent of c_n and d_n, and identical with Eq. (4.37) in the two-dimensional case. Hence, the solutions are

$$b_1 = \beta \sin\sigma t - \frac{1}{3\sigma^2}\left[\frac{\alpha\beta}{15\pi}(28\sigma^4+39\sigma^2-15) - \frac{2\alpha^2\sigma}{45\pi^2}(112\sigma^4+16\sigma^2-15)\right]\sin 2\sigma t \tag{5.33}$$

with the secular term

and
$$(\sigma^2-1)\beta + \frac{4\alpha\sigma(1-2\sigma^2)}{3\pi} = 0 \tag{5.34}$$

$$a_1 = \left[\frac{\alpha\beta\sigma}{15\pi}(5+14\sigma^2) - \frac{4\alpha^2\sigma^2}{45\pi^2}(15+28\sigma^2)\right] + \left(\beta - \frac{8\alpha\sigma}{3\pi}\right)\sigma\cos\sigma t$$
$$+ \left[\frac{\alpha\beta}{45\pi\sigma}(30-3\sigma^2-14\sigma^4) - \frac{4\alpha^2}{135\pi^2}(15+29\sigma^2-28\sigma^4)\right]\cos 2\sigma t \tag{5.35}$$

from Eqs. (4.39), (4.40) and (4.41). Note that there are two parameters δ and β in this problem for the determination of the frequency-amplitude relations of cross waves and of the longitudinal component of standing waves. For the second-order solutions obtained here, β appears in Eq. (5.34) which is still linear in characteristic and independent of δ; while the absence of δ in Eq. (5.29) means that there are no cross waves in the linear relation of frequency and amplitude. Therefore, the quantitative results of the non-linear solution cannot be obtained unless a higher order of approximation is carried out for the frequency-amplitude relation similar to the two-dimensional case presented in Sec. IV.

The rest of the coefficients are also solved to the second order and given in the following:

$$a_0 = \frac{1}{2}\left[\beta^2(\sigma^2-1) + \frac{4\alpha\beta(1-\sigma^2)\sigma}{\pi} + \frac{8\alpha^2\sigma^2(9+4\sigma^2)}{9\pi^2} - \frac{1}{2}\alpha^2\sigma^2 + \frac{1}{4}\delta^2\lambda(\sigma^2-4\lambda)\right]$$
$$+ \frac{4\alpha}{\pi}\cos\sigma t + \frac{1}{2}\left[\frac{\alpha\beta\sigma}{\pi} + \frac{2\alpha^2(3-4\sigma^2)}{3\pi^2}\right]\cos 2\sigma t \tag{5.36}$$

$$b_0 = \frac{2\alpha(1-2\sigma^2)}{\pi\sigma}\sin\sigma t - \frac{1}{8}\left[\beta^2(1+\sigma^2)/\sigma - \frac{\alpha\beta}{\pi}(5+4\sigma^2) - \frac{2\alpha^2}{9\pi^2\sigma}(9-48\sigma^2-46\sigma^4)\right.$$
$$\left.+ \frac{1}{2}\alpha^2\sigma - \frac{1}{2}\delta^2\lambda(\sigma^2+4\lambda)/\sigma\right]\sin 2\sigma t \tag{5.37}$$

$$a_2 = \frac{1}{4}\left[\beta^2\sigma^2 - \frac{8\alpha\beta\sigma(7+54\sigma^2)}{105\pi} - \frac{16\alpha^2\sigma^2(21-76\sigma^2)}{315\pi^2}\right] - \frac{4\alpha\sigma^2}{5\pi(2-\sigma^2)}\cos\sigma t$$
$$- \frac{1}{4(1-2\sigma^2)}\left[\beta^2\sigma^2 - \frac{4\alpha\beta\sigma^2(14+103\sigma^2)}{105\pi} + \frac{8\alpha^2\sigma^2(21+132\sigma^2)}{315\pi^2}\right]\cos 2\sigma t \tag{5.38}$$

$$b_2 = \frac{4\alpha\sigma(1-2\sigma^2)}{15\pi(2-\sigma^2)}\sin\sigma t + \frac{1}{4(1-2\sigma^2)}\left[\beta^2\sigma(\sigma^2-1) + \frac{2\alpha\beta\sigma^2}{105\pi}(234-216\sigma^2)\right.$$
$$\left.+ \frac{4\alpha^2\sigma}{315\pi^2}(21-368\sigma^2+304\sigma^4)\right]\sin 2\sigma t \tag{5.39}$$

$$C_1 = \left\{ \frac{\omega^2}{2(\nu_1 - \omega^2)} \left[\delta\beta(\ell + 2\omega^2 - 4\ell\omega^2) - \frac{4\alpha\delta\omega}{3\pi}(2\ell - 2\omega^2 - 16\ell\omega^2 + 1) \right] \right.$$

$$\left. + \frac{1}{2} \left[\beta\delta(2\ell\omega^2 + 2\omega^2 - \ell) - \frac{8\alpha\delta\omega}{3\pi}(4\ell\omega^2 + \omega^2 - \ell) \right] \right\} \sin\omega t$$

$$+ \left\{ \frac{3\omega^2}{2(\nu_1 - 9\omega^2)} \left[\beta\delta(4\ell\omega^2 + 2\omega^2 + 3\ell) - \frac{4\alpha\delta\omega}{3\pi}(6\ell + 6\omega^2 + 16\ell\omega^2 - 1) \right] \right.$$

$$\left. - \frac{1}{2} \left[\beta\delta(2\ell\omega^2 + 2\omega^2 + \ell) - \frac{8\alpha\delta\omega}{3\pi}(4\ell\omega^2 + \omega^2 + \ell) \right] \right\} \sin 3\omega t \qquad (5.40)$$

$$d_1 = \frac{1}{2(\nu_1 - \omega^2)} \left[\beta\delta\omega(\ell + 2\omega^2 - 4\ell\omega^2) - \frac{4\alpha\delta\omega^2}{3\pi}(2\ell - 2\omega^2 - 16\ell\omega^2 + 1) \right] \cos\omega t$$

$$+ \frac{1}{2(\nu_1 - 9\omega^2)} \left[\beta\delta\omega(4\ell\omega^2 + 2\omega^2 + 3\ell) - \frac{4\alpha\delta\omega^2}{3\pi}(6\ell + 6\omega^2 + 16\ell\omega^2 - 1) \right] \cos 3\omega t$$

$$\qquad (5.41)$$

5.5 Higher Modes in the Longitudinal Component of Standing Waves

For higher modes in the longitudinal component, the half-frequency relation between the wave maker and cross waves remains the same, while the length/width ratio of the tank ℓ found in Sec. 5.4 is different for having cross waves with $\alpha \to 0$. The ratio for any longitudinal mode can be obtained by the following consideration. Write the velocity potential in dimensional form as

$$\varphi^* = \sum_{m=0}^{\infty} \sum_{n=0}^{\infty} B_{mn}^*(t) \cos\frac{2m\pi y^*}{\lambda_c^*} \cos\frac{2n\pi x^*}{\lambda^*} e^{\sqrt{(\frac{2m\pi}{\lambda_c^*})^2 + (\frac{2n\pi}{\lambda^*})^2} \, z^*} \qquad (5.42)$$

in which $\frac{2m\pi y^*}{\lambda_c^*}$ corresponds to $m\ell y$ in the dimensionless form used in the last section. Now, instead of L/π let the unit be chosen as $\lambda^*/2\pi$, and

$$\varphi = \sum_{m=0}^{\infty} \sum_{n=0}^{\infty} B_{mn} \cos m\ell'y \cos nx \, e^{\sqrt{m^2\ell'^2 + n^2} \, z} \qquad (5.43)$$

where $\ell' = \frac{\lambda^*}{\lambda_c^*}$. By using the new unit, Eqs. (5.21) to (5.31) remain unchanged, then Eq. (5.30) gives

$$\ell' = 1/4$$

therefore,

$$\ell' = \frac{\lambda^*}{\lambda_c^*} = \frac{2L/n}{2W} = \frac{L}{nW} = \frac{1}{4}$$

or

$$\ell = L/W = \frac{n}{4} \qquad (5.44)$$

where n is integer corresponding to the nth mode of the longitudinal component.

With only the second-order solution, the results are summarized in the following:

(1) The fundamental mode of cross waves has a frequency which is half that of the wave maker (Eq. 5.26).

(2) The frequency which can excite the cross waves is $\frac{\omega}{2\pi}$ in the neighborhood of $\omega^2 = \ell$ only. Note that (Eq. (5.29) differs from Eq. (5.34) which is identical to the two-dimensional case of the same order of approximation. In Eq. (5.34), the term $4\alpha\sigma(1-2\sigma^2)/3\pi\beta$ gives essentially the two-dimensional standing waves of small amplitude as the frequency is away from the resonance frequency (See Sec. 4.5). The absence of the corresponding term in Eq. (5.29) indicates that there are no linear cross waves and the cross waves exist only in the neighborhood of $\omega^2 = \ell$.

(3) The most favorable condition to excite cross waves exists for the length/width ratio of the tank $\ell = \frac{n}{4}$, when the amplitude of the wave maker is very small. However, as $\ell \neq \frac{n}{4}$, the excitation depends on a critical value of α (See Eq. (5.29)), where n is the mode of the longitudinal component of standing waves.

(4) The phase angle between the cross waves is 0 or $\pi/2$. By using the experimental result obtained in Sec. VIII $\varepsilon = \pi/2$.

Since the non-linear characteristic does not appear in Eqs. (5.29) and (5.34) at the second order, similar to the two-dimensional case in Sec. IV, the quantitative result cannot be obtained. The relation between the frequency and the two parameters (β and δ) remains yet to be determined. A higher order of approximation has to be carried out for this purpose. As mentioned in the Introduction, the interest is centered only on the mechanics of the excitation of cross waves, an elaborate process would be involved in the computation of a higher-order solution. It is expected that the experiment will provide some information of the frequency-amplitude relation of the cross waves.

VI. EXPERIMENTAL EQUIPMENT

6.1 General Description

The experimental investigation was carried out in the Hydrodynamics Laboratory of Massachusetts Institute of Technology. A rectangular tank, 3 feet 6 1/4 inches long, 2 feet 3/16 inches wide and 3 feet deep with glass sides and ends was built for this purpose. Due to the symmetry of the problem, only one wave maker was used. The flap-type wave maker is located inside the tank on the rails, which are parallel to the side walls, and hence the distance between the wave maker and the end is adjustable. An adjustable connecting rod is used to transmit the circular motion of the eccentric cam to oscillatory motion of the wave maker. An AMES dial gage and a displacement gage (Linearsyn Model S2) are located at the top of wave maker to measure the amplitude of the wave maker and to record the motion of the wave maker for the determination of the phase relation. The amplitude of standing waves is measured by a resistance-type wave gage, which is fixed into a point-gage staff mounted on a cross beam. The whole unit can be slid along the cross beam. The output of the wave gage and of the displacement gage is recorded on a four-channel Sanborn Model 150 Oscillograph. The frequency of the wave maker is measured by an electronic counter system. An aluminum circular plate is mounted on the fly wheel with 400 holes on its periphery with a light source on one side and a photoelectric tube on the other. The tube is connected with an electronic counter. When one side of the wave maker is in use, aluminum wool is put in the other side to absorb the waves generated. The overall arrangement is shown in a schematic diagram and a photograph (Figs. 6.1 and 6.2).

6.2 The Driving Unit and Wave Maker

The driving unit consists of the following parts:

(1)   A 3-h.p. U.S. Motor Varidrive with a continuous speed range of 44.5 to 310 rpm, i.e. 0.742 to 5.167 c.p.s. The speed was roughly calibrated with the counter on the motor, which was used as a guide to the range of frequency needed for an experiment. After the motor is warmed up, the variation of speed is usually less than 0.05% near 2 c.p.s. and even less for lower speed. (Fig. 6.3).

(2)   A fly wheel, 2 feet in diameter and 1 inch thick, on which an eccentric sliding block and its guiding frame are bolted. The eccentric sliding block is driven by a motor and thus its position can be
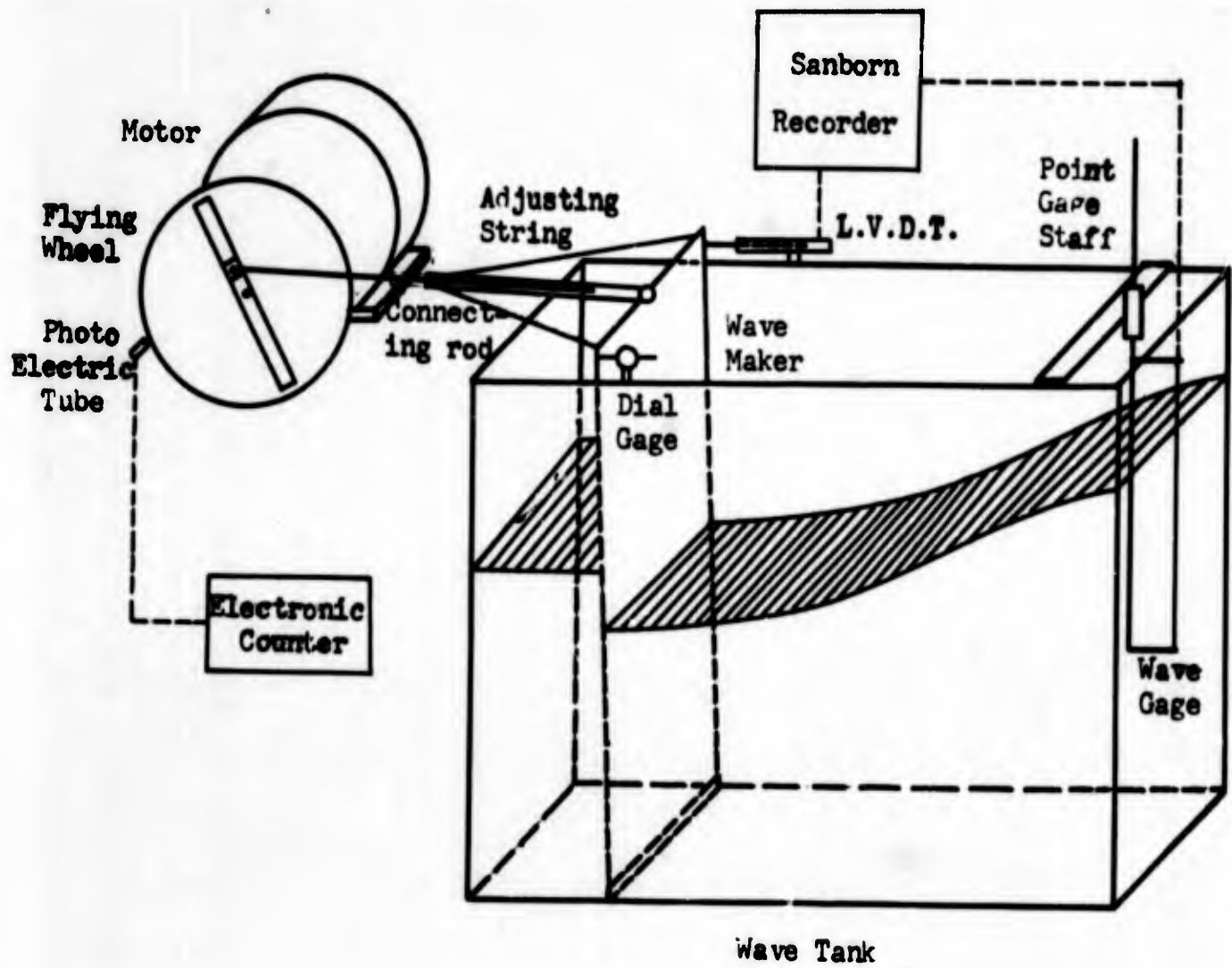
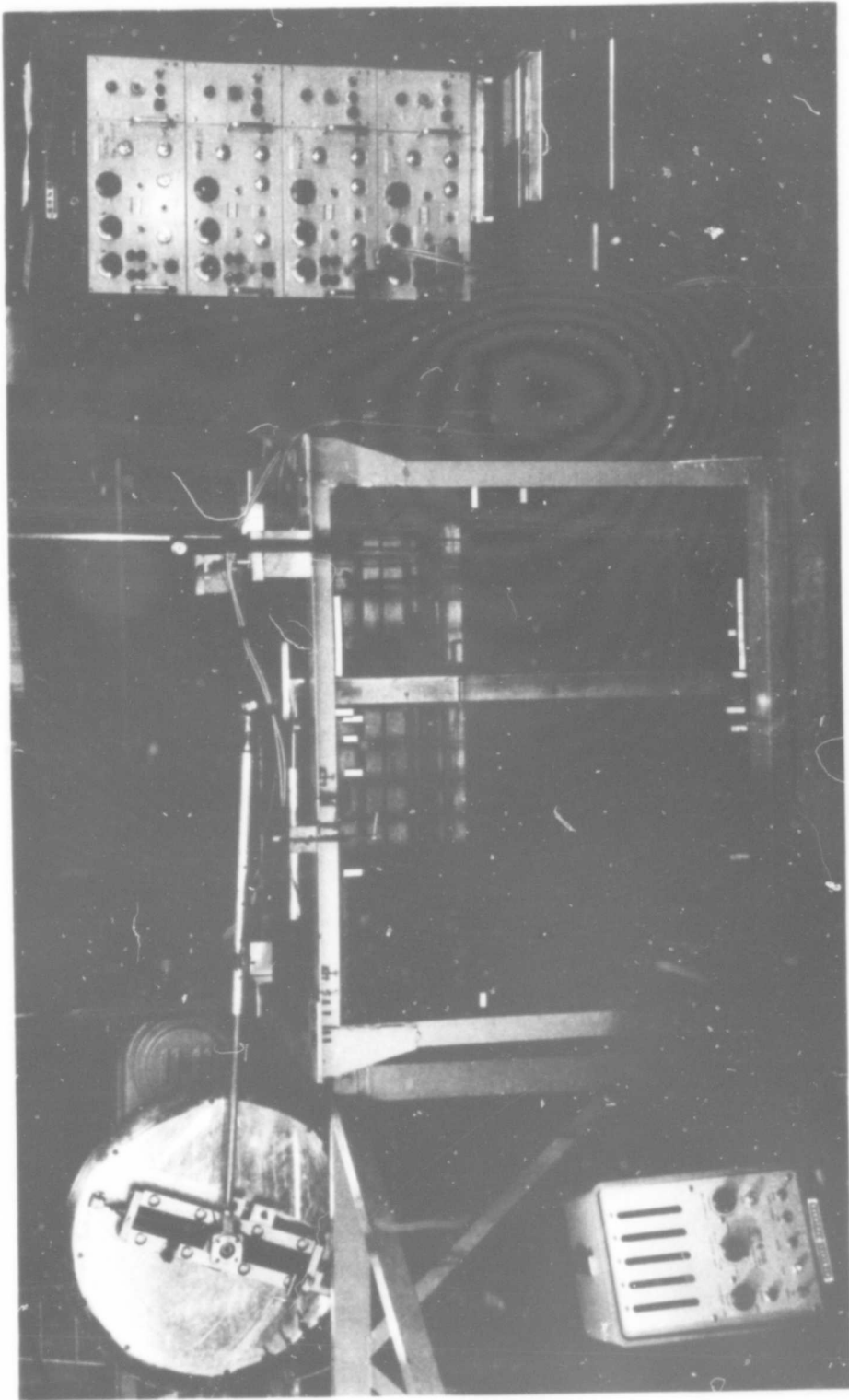FIG. 6.1 Schematic Diagram of Experimental Setup

FIG. 6.2 Photograph of Overall Experimental Setup

varied during a run. The eccentricity is recorded on a counter on the wheel. Owing to an error in construction, there exists a minimum eccentricity or minimum wave maker amplitude of about 0.14 degree. A circular aluminum plate with holes on its periphery is bolted on the fly wheel and used as a light-beam cutting device for the electronic counter system (Fig. 6.4).

(3)   An adjustable connecting rod, made of a brass rod of 3/4-inch diameter and steel tubing of 3/4-inch I.D. The rod runs inside the tubing and is fixed by four setscrews to suit the neutral position of wave maker. A ball joint connects the rod at the center to the top of wave maker. Two adjustable steel wires run from the middle of the rod to each end on the top of wave maker to adjust the wave maker and to keep it parallel to the end of the tank.

The Wave Maker

The wave maker is made of a plexiglass plate of 3/4-inch thickness and of 3-foot height. At its lower edge, a brass hinge of the same width is screwed on and rests on a movable cross beam. The center of the hinge is 1 37/64 inches above the floor. The top and two sides of the wave maker are reinforced by three aluminum angles. There is a clearance between the wave maker and the side wall of about 3/32 inch. A spring-loaded hard rubber seal is used for the wave maker (Fig. 6.5). The upper part of the seal was usually lubricated with water brought up by high-amplitude waves; but when the amplitude of waves was small, water was injected periodically into the seal.

6.3 Wave Gage

A resistance wave gage is made of two platinum wires, 0.008 inch in diameter, spaced 1/4 inch apart. The wires, insulated from each other, are stretched on a bow-shaped frame, which is fixed into the point gage staff (Fig. 6.6a). During measurements, about one half of the length of wires was submerged vertically in water. The wires were connected to one branch of the bridge circuit (Fig. 6.6b). The output of the gage depends on the amount of submergence (nearly a linear function) and was recorded by a Sanborn Recorder. Before each run, the wires were wiped with a damp cloth and foreign matter was removed from the water surface. Static calibrations were made before and after each run by moving the gage up and down.
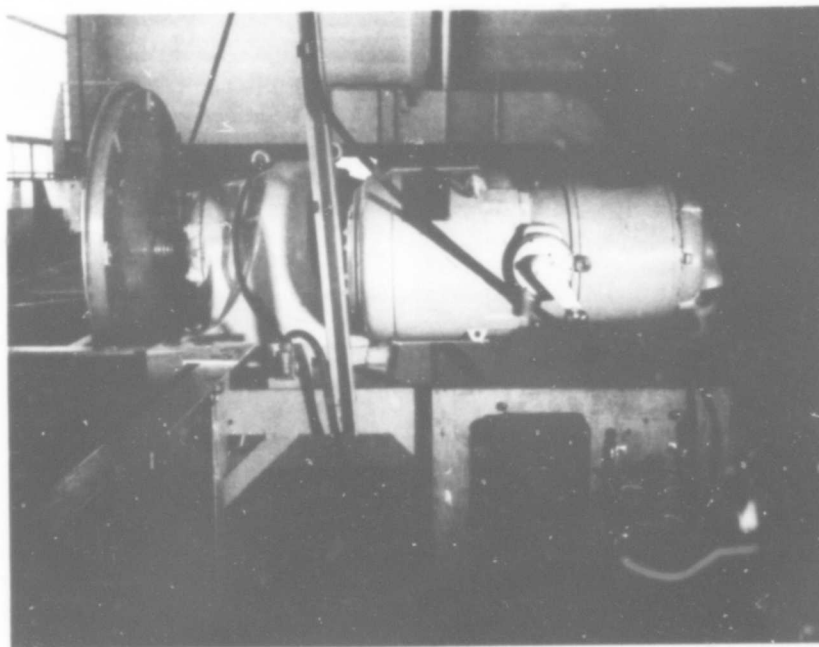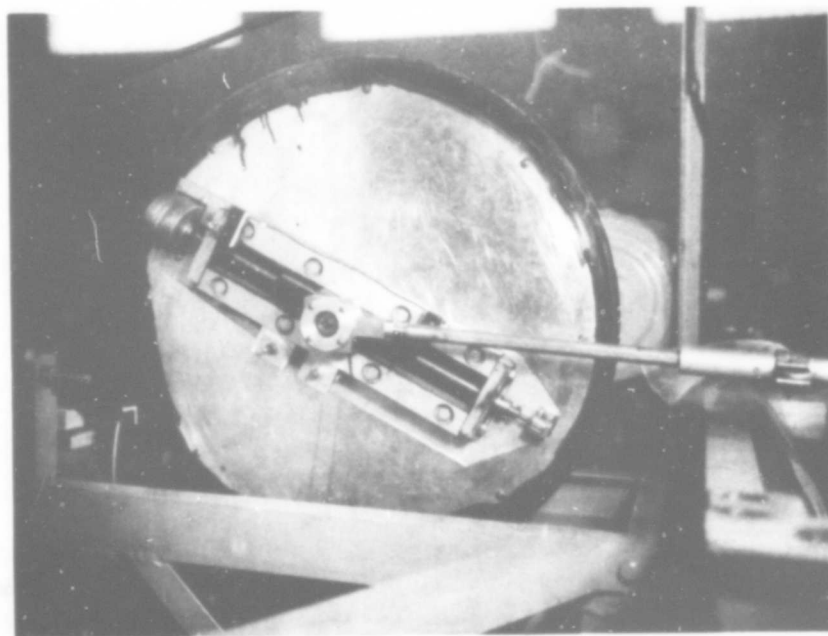
FIG. 6.3 Photograph of Motor

FIG. 6.4 Photograph of Fly Wheel

During a run, the gage gave continuous recording of total
wave amplitude with respect to time at a point. The over-
all error for the gage recording system was found to be
less than 3-5% [28].

6.4 Dial Gage and Displacement Gage

An AMES dial gage with 0.001" graduation was used to
measure the amplitude of the wave maker at the top of the
wave maker, 3 feet from the hinge. The measurement was
made for each run when the wave maker was oscillating at
a low speed (Fig. 6.7a).

The motion of the wave maker was also measured with
a displacement gage, a linear variable differential trans-
former (Linearsyn Model S2), the output of which is
directly proportional to the displacement. In order to
investigate the phase relation between the wave maker and
the standing waves, the motion was recorded simultaneously
with the wave amplitude on two-channel Permapaper in a
Sanborn Recorder. This device has two parts: a coil
assembly, 11·1/8 inches long, 0.312 inch I.D. and 3/4-inch
O.D., and a magnetic assembly. The transformer has a full
range of 4-inch stroke and an excitation voltage of 6 volts.
(Fig. 6.7 a,b). The gage was located at the top of the
wave maker.

6.5 Electronic Counter System

The electronic counter system consists of four parts:
1. an electronic counter, 2. a photo-electric tube, 3. light
source and 4. a light-beam cutting device. (Fig. 6.8)

A Hewlett-Packard Model 521C electronic counter and
a RCA 1P41 photo-electric tube were used. The light source
was supplied by a 200-watt projector lamp of two-parallel-
filament type which was focussed on the photo-electric tube
through a light-beam cutting device. A circular aluminum
disk of 26-inch diameter was provided with 400 holes of
3/32-inch diameter equally spaced at 19/64 inch near its
periphery and was mounted concentrically on the fly wheel
with the light source on one side and the photo-electric
tube on the other. The light beam, the holes and the
photo-electric tube were properly lined up. The focus of
the light source was adjusted in such a way that the tube
could receive maximum intensity and area of the light
through the holes.

Hard Rubber Rectangular
Strip of 3/8" Thick

1/4" 1/4" 1/8"

5/8"

Section A-A

Details of Seal

1/8" Thick Aluminum Strip

Hinge

Cross Beam

3"x3"x1/4" Angle

WAVE   MAKER   BACK

1/4" Holes for Spring
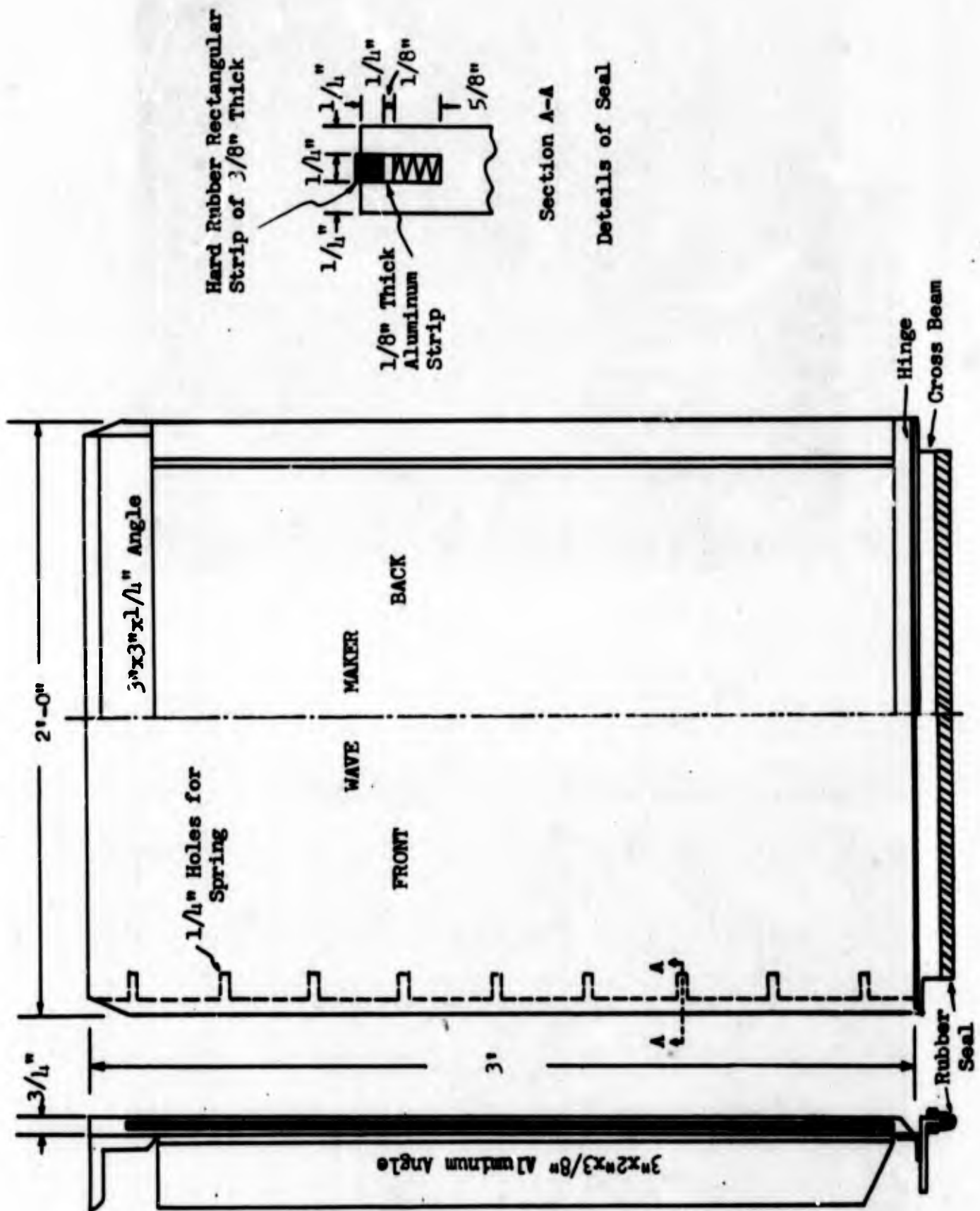
WAVE   FRONT   MAKER
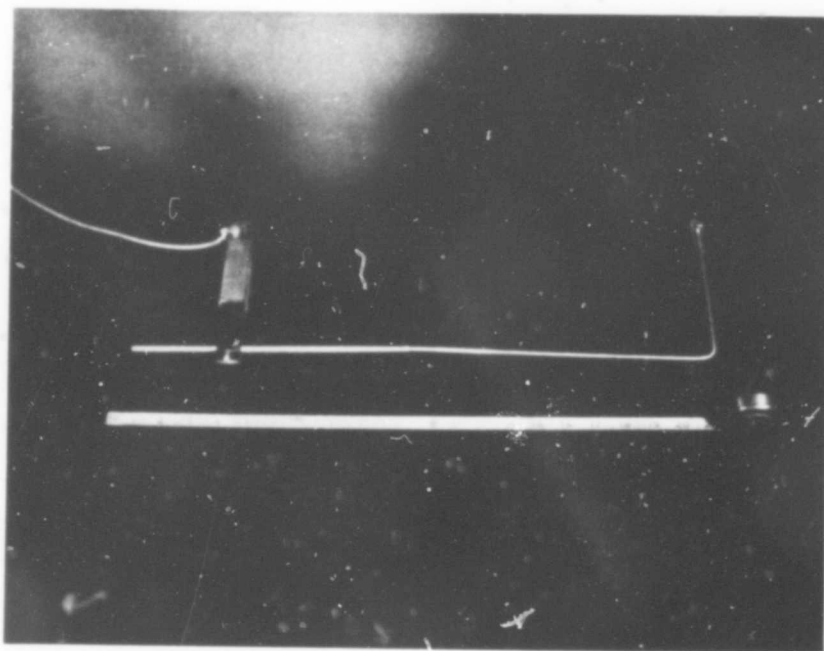
2'-0"

3/4"

3'

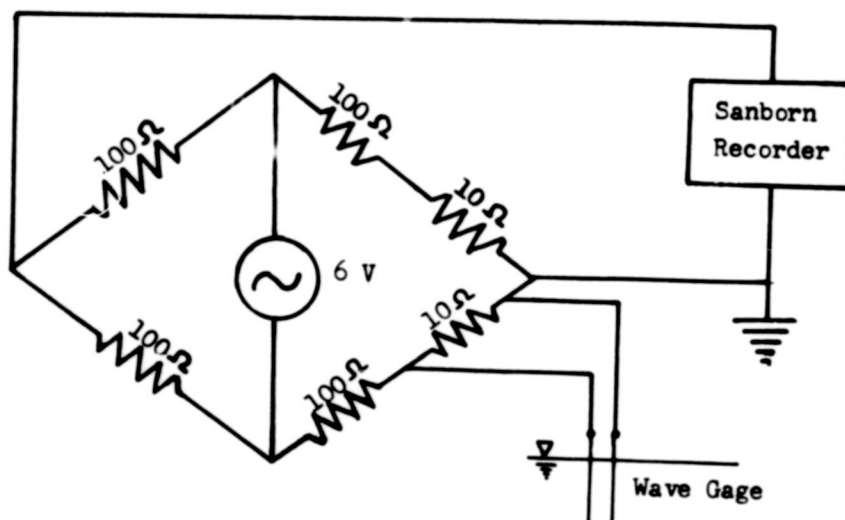3"x2"x3/8" Aluminum Angle

Rubber Seal

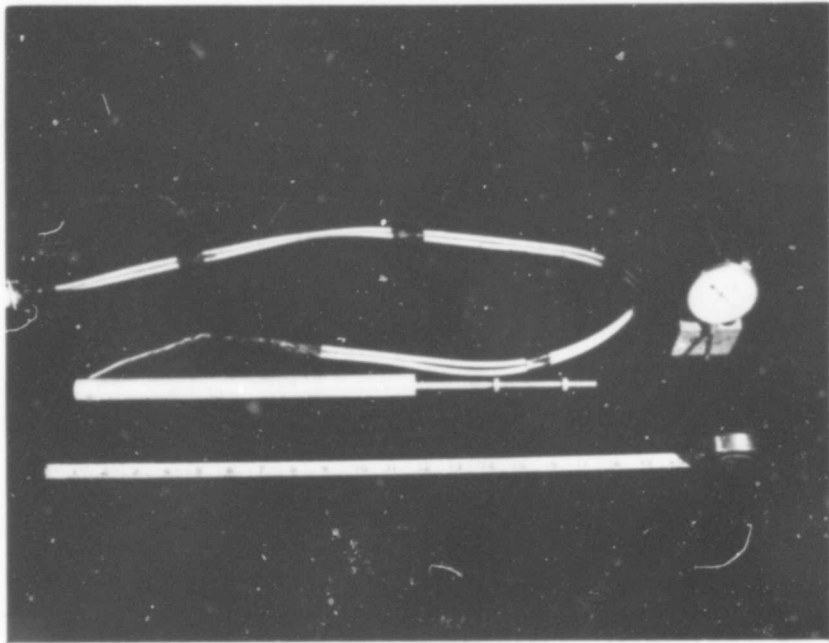FIG. 6.5 Drawing of Wave Maker
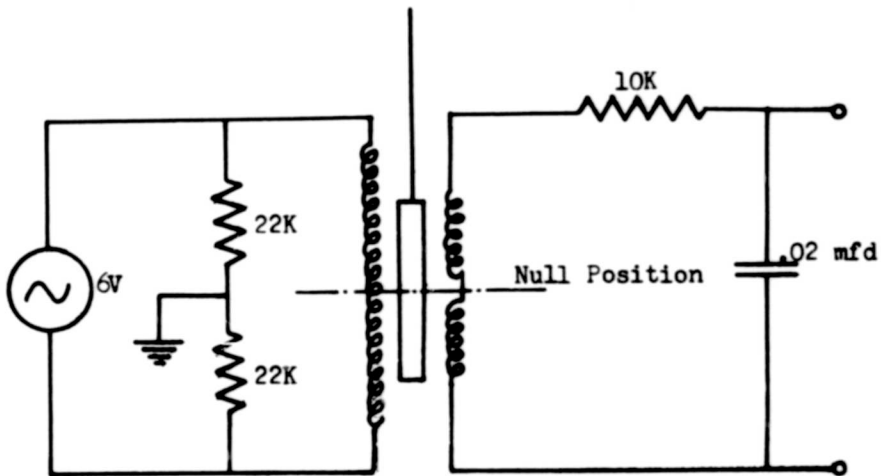
-51-

(a) Photograph

(b) Bridge Circuit

FIG. 6.6 Wave Gage

(a) Photograph

(b) Circuit Diagram of Linear Variable
Differential Transformer

FIG. 6.7 Dial Gage and Linear Variable Differential Transformer
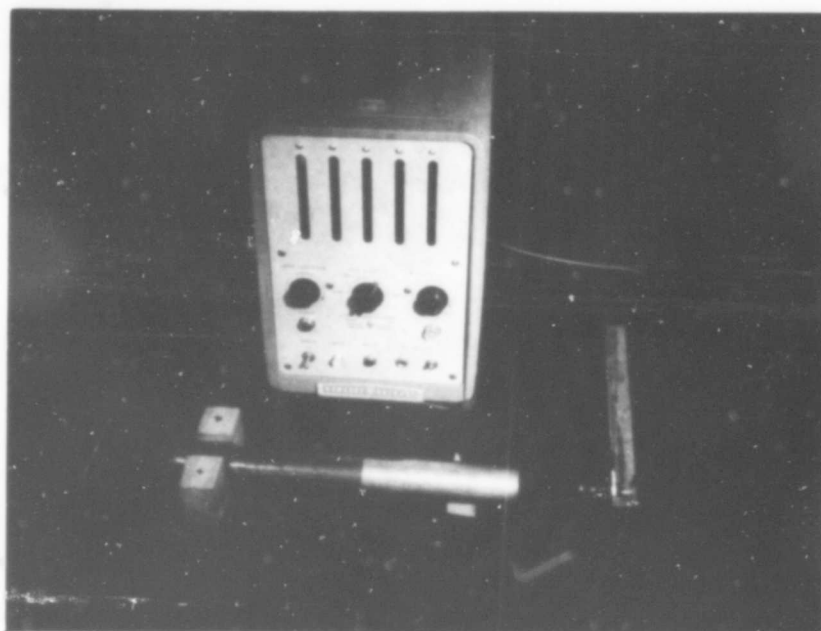
FIG. 6.8 Electronic Counter System

VII. METHODS OF MEASUREMENT

7.1 Depth of Water

The depth of water was measured directly by a scale submerged in the tank. All runs were made at a depth of two feet except two runs which were used to study the depth effect on the finite-amplitude standing waves. The depth was used as a check of the deep-water assumption; hence a correction of resonance frequency was made for runs with insufficient depth of water. The error involved in measurement is negligible since the value of the hyperbolic tangent, nearly equal to one, is not sensitive to this error.

7.2 Frequency of Wave Maker

There are 400 holes on the rim of the circular disk mounted on the fly wheel. The light beam was cut 400 times in a revolution and a counting period of 10 seconds was usually used. The total number of electric pulses sensed by the tube due to the cutting of the light beam was automatically recorded by the counter in a period of 10 seconds and can be read off directly. The error of the counter is ± 1 count. Hence, for a frequency of, say, 2 c.p.s., the system may have an error $\pm 0.0125\%$, which is smaller than the variation of speed due to the motor. The total error involved in frequency measurement was estimated at less than 0.05% (including the speed variation of the motor).

7.3 Wave Height

Wave height was measured in centimeters by a resistance wave gage. Before and after each run the gage was calibrated to check the error in the recording system. The calibration was made by moving the gage up or down. The direction and amount of displacement were recorded on the permapaper in the Sanborn recorder and the corresponding value was taken from the scale on the point gage staff. Usually more than one attenuation was used to measure high amplitude standing waves. For the measurement of the frequency-amplitude relation of two-dimensional standing waves, the wires were located at the middle of the tank about 3/8 inch from the end wall, which is the point of symmetry for all modes of oscillation (Fig. 7.1). For cross waves, the wires were set about 3/8 inch from the side wall at the point where the crest of longitudinal waves was located and the composite waves were later analyzed (Fig. 7.2). The 3/8 inch distance between the wires and the wall are necessary
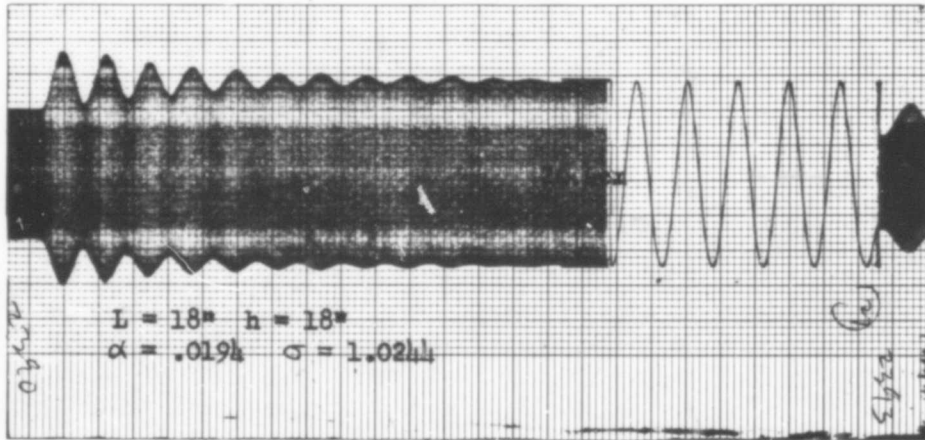
FIG. 7.1 Sample of Measurement on Two-dimensional Standing Waves
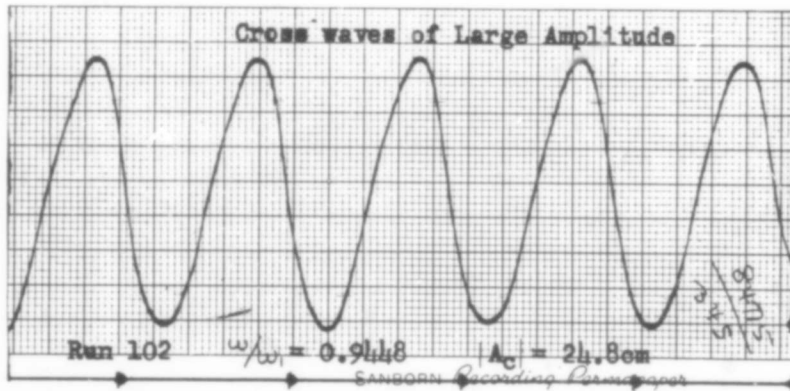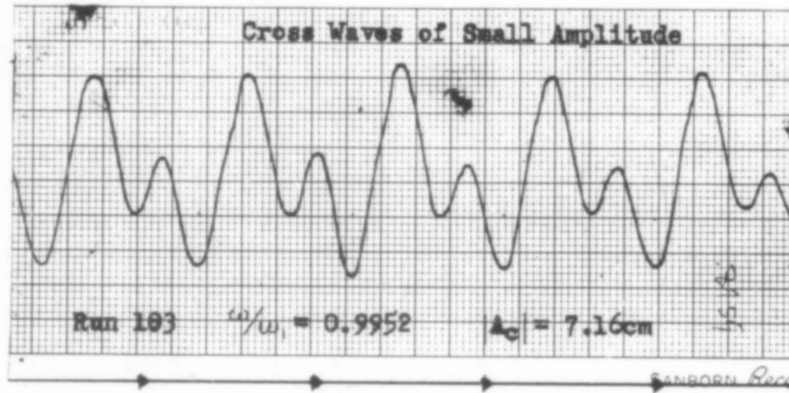

FIG. 7.2 Sample of Measurement on Three-dimensional Standing Waves

to avoid the capillary effect as well as to keep the part
of the wires above the free surface well insulated from
each other. The error due to the wire not being exactly
located at the crest can be estimated, for example, from
the computed profiles of the two-dimensional standing
waves given in Fig. 4.4. If L = 18 inches (the smallest
length used), it is about 2% off the exact location of
crest. The error of the amplitude is negligible as shown
in Fig. 4.4, since the slopes are small both at the crest
and trough in this case. When the standing waves are at
the greatest height, the error can be approximately computed
as follows. Let the angle made by the free surface with
the vertical near the crest be $45°$ and the free surface
near the trough be horizontal, then the amplitude $|A|$ is
0.063 too small for $|A|_{max.}$ = 1.367, hence the error is
always less than 5%.

The wave gage and point gage staff were fixed on a
sliding block on a traversing beam for the measurement of
the profile of two-dimensional standing waves. The beam
was carefully leveled and the position of the gage could
be read on the scale of the beam the relative position of
which was determined before and after each run.

7.4 Amplitude of Wave Maker

An AMES dial gage was clamped on the angle at the
top of the side wall and its sliding shaft touched the
wave maker at a distance of 3 feet from the hinge. All
measurements were made visually as the wave maker oscil-
lated at a low frequency. The graduation on the gage
is 0.001 inch.

The linear variable differential transformer was
sometimes used to measure the amplitude of the wave
maker in addition to its phase relative to that of the
standing waves. A calibration is required by means of
the dial gage.

7.5 Phase Relation

The phase relation between the wave maker and the
standing waves at the location of the wave gage could
be obtained from the two-channel Permapaper in the San-
born recorder by recording the outputs from the wave
gage and linear variable differential transformer
simultaneously. The directions of oscillation for the
standing waves and wave maker had to be calibrated. For
two-dimensional standing waves, the relation could be
directly determined from the graph, but an analysis is
necessary to get the cross wave components from the
composite waves recorded by the system. (See Figs. 7.3
and 7.4)

7.6   Analysis of Composite Standing Waves for the Components

Since the wave gage measures the oscillation of the free surface at a point on the horizontal plane with respect to time, the record shows the composite standing waves with components of different frequencies. It is assumed here that the composite standing waves are composed of only two modes, the full-frequency mode and the half-frequency mode with all of their higher harmonics neglected. The former is essentially that of the longitudinal standing waves and the latter that of the cross waves. A graphical method was adopted for decomposition. With $\frac{\omega}{2\pi}$ and T as the frequency and period of the cross waves, the composite standing waves are given by

$$Z_1 = A \sin \omega t + B \sin(2\omega t + \epsilon)$$

where A and B are amplitudes of cross and longitudinal standing waves respectively, and ϵ is the phase difference. Shifting the profile in either direction by a quarter of a period of cross waves,

$$Z_2 = A \sin \omega(t + \tfrac{T}{4}) + B \sin\left[2\omega(t + \tfrac{T}{4}) + \epsilon\right]$$

$$= A \cos \omega t - B \sin(2\omega t + \epsilon)$$

Hence

$$\tfrac{1}{2}(Z_1 + Z_2) = \tfrac{1}{2}A(\sin \omega t + \cos \omega t)$$

$$= \tfrac{1}{\sqrt{2}} A \sin(\omega t + \tfrac{\pi}{4})$$

or

$$|A| = \tfrac{1}{\sqrt{2}}|Z_1 + Z_2|$$

If we shift the profile by a half period of cross waves, then

$$Z_2 = A \sin \omega(t + \tfrac{T}{2}) + B \sin(2\omega t + \omega T + \epsilon)$$

$$= -A \sin \omega t + B \sin(2\omega t + \epsilon)$$

Hence

$$\tfrac{1}{2}(Z_1 + Z_2) = B \sin(2\omega t + \epsilon)$$

or

$$|B| = \tfrac{1}{2}|Z_1 + Z_2|$$

Note that the component of the cross waves can be obtained by Eq. (8.4) with a shift of its phase, $T/4$, and the total amplitude can then be computed by Eq. (8.5). A similar procedure can be applied to obtain the longitudinal component by a phase shift of $T/2$.
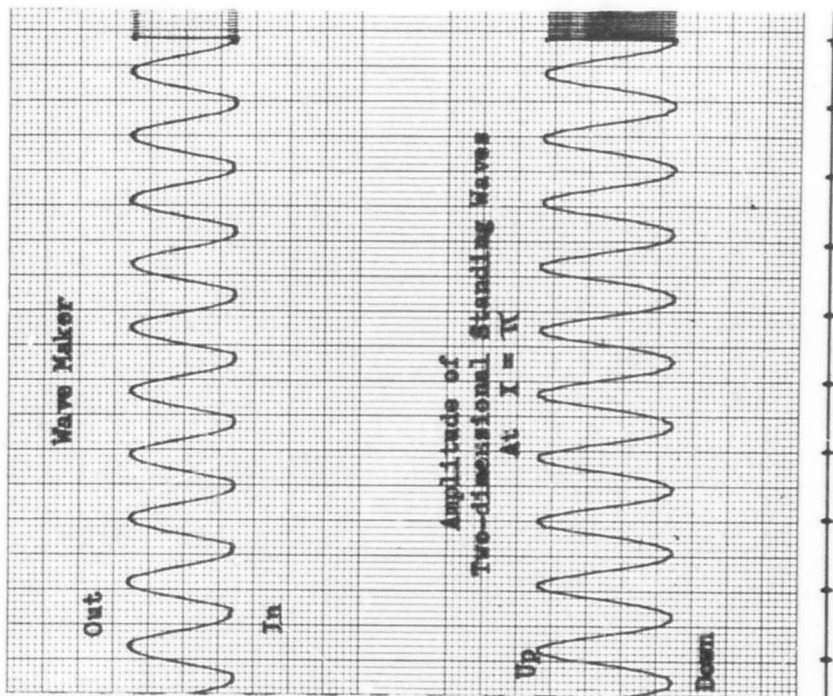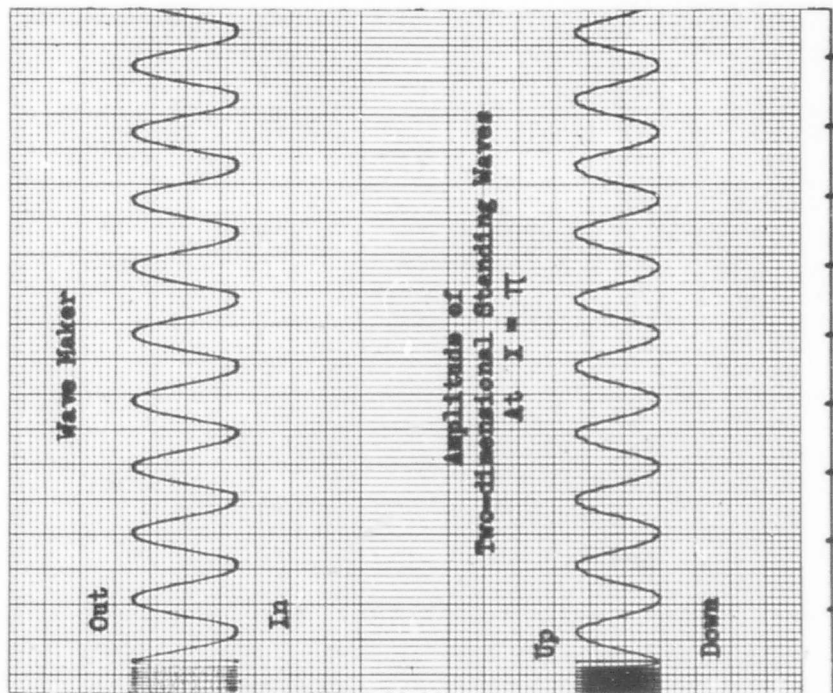
(a) $\sigma < \sigma_1$ (b) $\sigma > \sigma_1$

FIG. 7.3 Phase Relation for the First Mode Two-dimensional Standing Waves
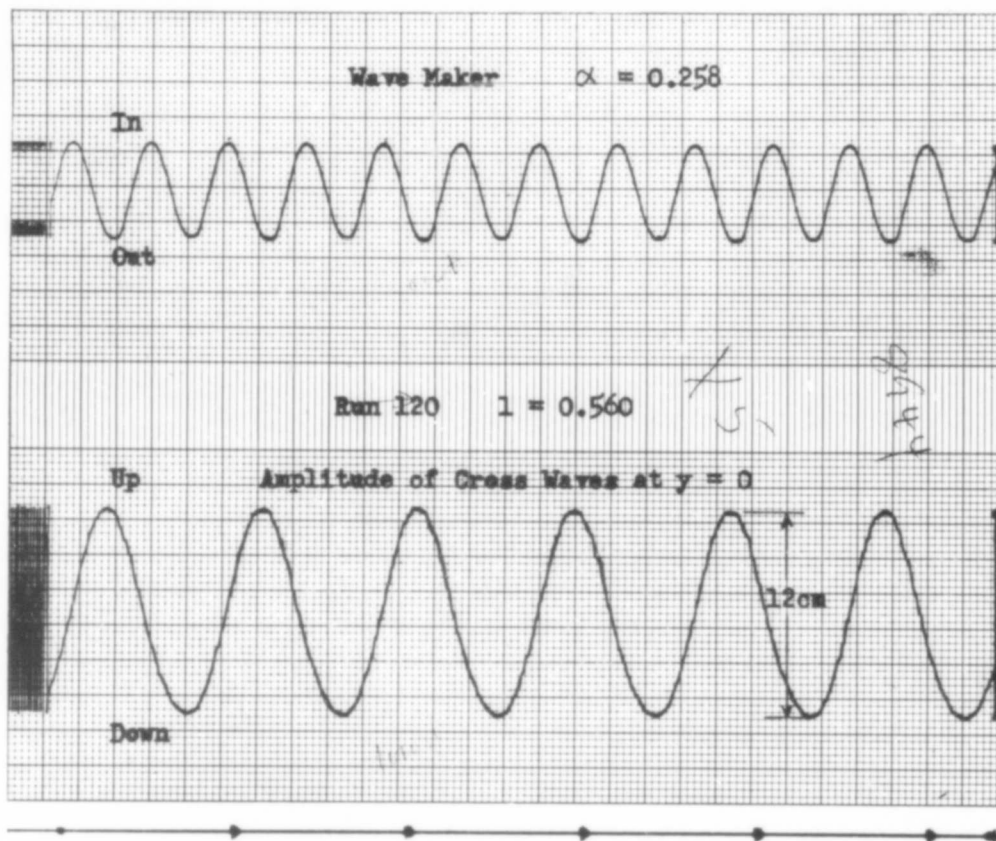
FIG. 7.4 Phase Relation for Cross Waves

VIII. EXPERIMENTAL RESULTS AND DISCUSSION

The experimental program of the investigation consists mainly of two parts:

(1) Two-dimensional standing waves for the study of the finite-depth effect and the verification of the theoretical solution obtained in Sec. IV. (See Table 8.1 for the summary of experiments); and

(2) Cross waves for study of their excitation at different length/width ratios of the tank as well as frequency-amplitude curves. (See Table 8.2)

8.1 Limitations of Experimental Equipment

Due to the symmetry of the problem, only one wave maker was used in the experiment and this has no limitation in general except for the highest two-dimensional standing waves due to the significant wall effect as the angle between the free surface and end wall tends to 45° near the crest. The depth of water was kept at 2-feet, which is very close to the infinite-depth case; however, the high accuracy of frequency required for the study of non-linear waves still demands a frequency correction which will be discussed in detail in the next section. There are no limitations on the frequency of the wave maker for the range under investigation but the lower limit of the eccentricity on the fly wheel as mentioned in Sec. 6.2 gives the smallest amplitude of the wave maker at about 0.14°. For the study of excitation of cross waves a smaller amplitude of the wave maker is desired for the small value of length/width ratio. The range of length/width ratio available is $0 < \ell < 1.5$ which is satisfactory both for two-dimensional waves and cross waves. For cross waves, the effect of viscosity becomes significant for large values of ℓ. The viscosity was neglected in the analysis, hence the investigation is limited to small values of ℓ.

8.2 The Effect of Finite Depth

The analysis is based on the assumption of infinite depth. For free waves of finite amplitude, Penney and Price [14] concluded that the difference between infinite-depth and finite-depth cases could be neglected if the depth is greater than one quarter of the wave length, i.e. $h/\lambda > 1/4$ corresponding to $\pi h/L > \pi/2$ for the first two-dimensional mode. The smallest value of $\pi h/L$ in the experiment is 2.443, which is 63% greater than Penney and Price's value. The discrepency is still shown in the correlation of the frequency-amplitude curve for most cases; perhaps the high accuracy of frequency required in non-linear waves was overlooked by them. A finite-depth analysis has not been attempted here, however, it was found that a frequency correction based on the linear theory yields good correlation of the data. As is well known in the classical theory of small amplitude water waves, the frequency $\sigma^* / 2\pi$ can be predicted by the formula:

$$\sigma^{*2} = g k^* \tanh k^* h \qquad \text{where} \quad k^* = 2\pi/\lambda^* \qquad (8.1)$$

for the finite-depth case. Hence, a frequency correction factor is defined as

$$\tau = \tanh \frac{2\pi h}{\lambda^*} = \tanh \frac{n\pi h}{L} \qquad (8.2)$$

where $2L = n\lambda^*$ and $n = 1, 2, 3, \ldots$ for 1st, 2nd, 3rd, ... normal mode of oscillation. Due to the height of the tank being insufficient to provide a depth which gives $\tau \to 1$ within the accuracy required, a series of experiments (Runs 1 to 3) was made to test the correction factor used in the non-linear case. The results (Fig. 8.1) indicate that the correction yields good correlation for the three depth/length ratios and the data are also in good agreement with the computed curve based on the theoretical solution of the infinite-depth case. The remaining runs have a depth of 2 feet and the frequency correction factors are listed in Tables 8.1 and 8.2. Therefore, the correction factor $\tanh(\pi h/L)$ based on the linear theory was used throughout the analysis and Penney and Price's $h/\lambda > 1/4$ is not sufficient as far as the frequency of standing waves of finite amplitude is concerned.
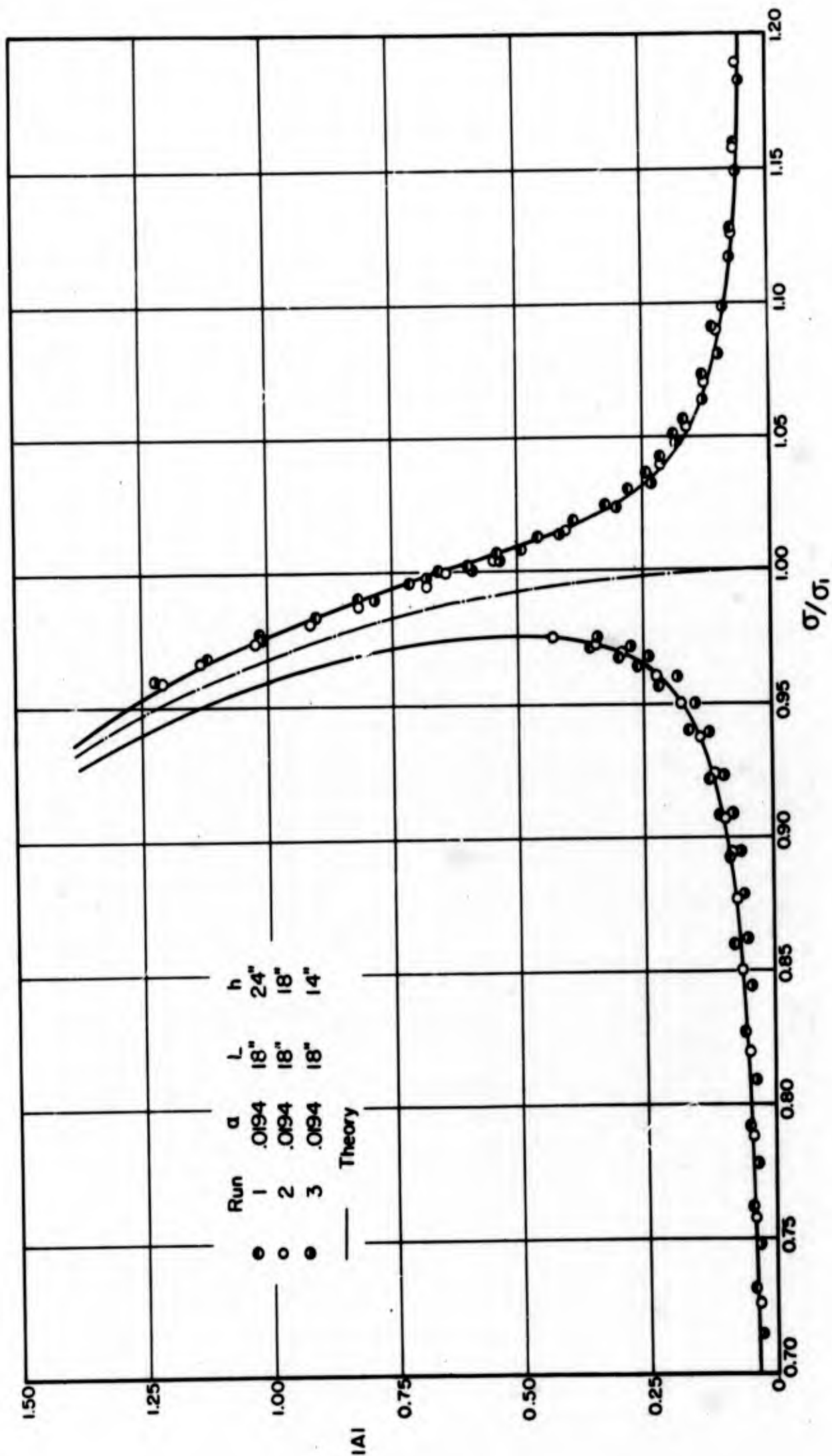
FIG. 8.1 The Effect of Finite Depth. Frequency Correction

8.3 Forced Two-Dimensional Standing Waves

1. Frequency-Amplitude Curves of the First Mode

A series of experiments was carried out for the frequency-amplitude relation of forced two-dimensional standing waves. Two different amplitudes of the wave maker were used to investigate the non-linear effect and several depth/length ratios were tested (Runs 1 to 9 in Table 8.1). The frequency of the wave maker, equal to that of the standing waves, was measured against the amplitude of standing waves near the point of symmetry (about 3/8" from the end wall). The experimental results in dimensionless quantities, shown in Fig. 8.2, indicate satisfactory agreement with the theoretical prediction. A careful choice of the length/width ratio is required to ensure the stability of the standing waves. As a result of the analysis in Sec. V, no cross waves can be excited if the half-frequency of the wave maker is smaller than the resonance frequency of cross waves of the fundamental mode. If the half-frequency of the wave maker is nearly equal to the resonance frequency, the fundamental mode of cross waves can always be excited with $\ell = n/4$, but for $\ell \neq n/4$ it can only be excited with a critical amplitude of wave maker depending on ℓ. In this light, the length/width ratio was deliberately kept away from $n/4$ and the half-frequency of wave maker was smaller than the resonance frequency for all runs in the experiment.

The test was started at a frequency much smaller than the resonance frequency of the first mode and then the frequency of the wave maker was slowly increased toward the resonance frequency. The phase relation between the wave maker and standing waves is shown in Fig. 7.3(a), which confirms the prediction in Fig. 4.1. The amplitude of standing waves increases rapidly as the frequency approaches close to the resonance frequency; then the jump of amplitude from the left to the right branch of the frequency-amplitude curve occurred at a critical frequency near the vertical tangent accompanied by a change of phase. The critical frequency for the jump depends on the amplitude of the wave maker. This phenomenon is very well demonstrated by Fig. 8.2. Again, the phase relation agrees with Fig. 4.1 as shown in Fig. 7.3(b). A further increase of frequency led to a decrease of amplitude until it reached the point of transition to the second mode.

The test was continued by decreasing the frequency back to the path just passed and building up the amplitude of standing waves as high as possible. During

the test, each adjustment of the frequency of the wave
maker caused some disturbance on the free surface due to
the difference in frequency and a period of time was re-
quired to reach a steady state. The experimental points
shown in Fig. 8.2 are steady two-dimensional standing
waves and so are the rest in Figs. 8.1, 8.4. A measure-
ment was not attempted for the highest standing waves
possible due to the fact that the disburbance caused by
the wave maker would not decay even for a longer period
of time and the wall effect became significant at such
a high amplitude. It is believed that this disturbance
causes the instability of the free surface in the form
of small breaking wavelets. The whole system remained
essentially two-dimensional in that no cross waves of
appreciable amplitude would develop even for a long
period of time, however, this instability makes the
measurement of amplitude at a particular point meaning-
less. Taylor [1] had the same kind of difficulties in
his experiment and the profile of the highest standing
waves was taken within a very short period of time be-
fore the instability developed. The three-dimensional
or conical type standing waves observed in Taylor's
experiment did not appear in the experiment because of
the particular length/width ratio chosen. A run with
the length/width ratio equal to 0.97 (L=23.5 inches)
was tried. It was found that the two-dimensional
standing waves of small amplitude was stable, but the
system became unstable as the frequency reached the
region of non-linear effects and three-dimensional
waves of finite amplitude with full frequency were
observed. The oscillation was along one of the di-
agonals with half wave length and full frequency of the
wave maker. Its nature is similar to that of the cross
wave case which will be described in detail in the next
section.

2. Profiles of Two-dimensional Standing Waves of the First Mode

Two profiles of two-dimensional standing waves on each branch of the frequency-amplitude curves for α=0.0194 were made to test the error involved in the second order computation presented in Sec. 4.5. (Runs 10 and 11). The comparison shown in Fig. 8.3 indicates a better agreement for σ=0.965 than σ=1.000 and the error which appeared in the amplitudes near x=0 and π is about 5% for the latter and less than 1% for the former. The disagreement near $\zeta \doteq 0$ for σ =1.000 is due to the fact that the measurement is actually the envelope of standing waves rather than the instantaneous profile as computed, while the good agreement for σ =0.965 indicates that its profile is not far from the simple harmonic oscillation. The experimental difficulty involved in obtaining a profile of higher amplitude is that the amplitude becomes very sensitive to the variation of the frequency which could not be kept within the limit required for the duration of a run due to the characteristics of the motor. The crest-height/trough-depth ratio for σ=1.000 is equal to 1.43 as compared with the maximum value 1.84 found by Penney and Price. The photograph of the two-dimensional standing wave is shown in Fig. 8.5 for the first and second modes.

3. Frequency-amplitude Curve for the Second Mode

Since the solution for the second mode has not been carried out, it would be instructive to see how the amplitude of the wave maker affects the second mode of oscillation as well as the frequency-amplitude curve in a dimensionless plot to compare with the first mode. Runs 8 and 9 with two different lengths of the tank but the same dimensionless amplitude of wave maker α were made for the purpose. The result indicates (See Fig. 8.4) that the second mode differs slightly from the first mode at large amplitude in the neighborhood of the resonance frequency; while for small amplitude it agrees with the rough estimation based on the linear theory in Sec. 3.6, i.e. the amplitude of the second mode is about 20% higher. The important implication of the result is that the amplitude increases with increase of the mode of oscillation at the same value of σ/σ_n and the range of frequency of higher modes becomes narrower. The non-linear frequency range for the second mode is approximately $0.88 < \sigma/\sigma_2 < 1.10$ as compared with the non-linear range for the first mode $0.93 < \sigma/\sigma_1 < 1.05$ for the particular α. Therefore, the high mode of oscillation in the system is essentially non-linear in characteristic for a sufficiently large α.
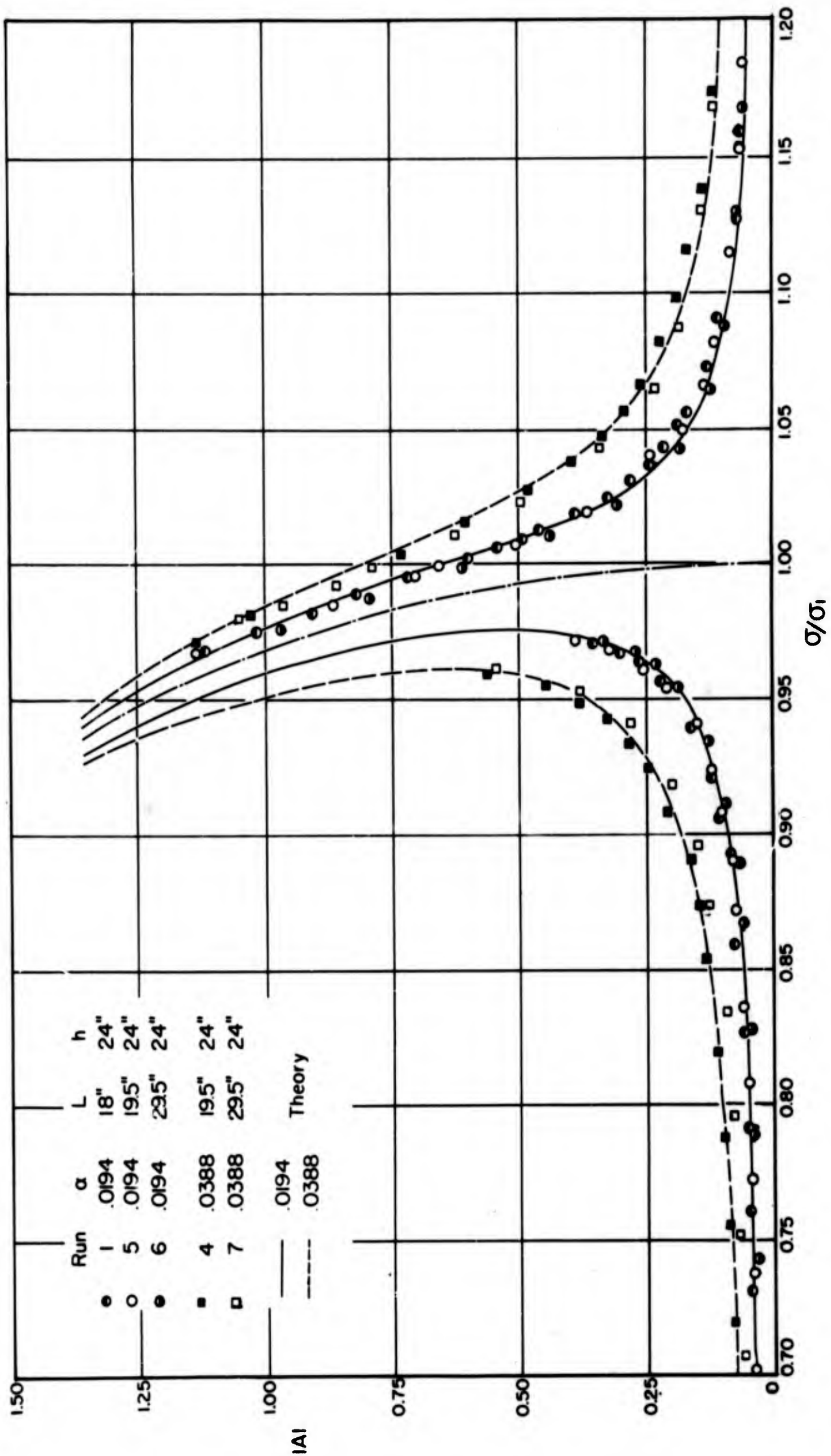
FIG. 8.2 Comparison of Theoretical and Experimental Results for Frequency-Amplitude Curves of Forced Two-dimensional Standing Waves

Table 8.1

Summary of Experiments on Two-Dimensional Standing Waves

Run	L	h	$\pi h/L$	$[\tanh \frac{\pi h}{L}]^{1/2}$	2θ	2α	$f_1 = (\frac{g}{4\pi L})^{1/2}$ inf. depth
1	18	24	4.189	0.9998	0.566°	0.0387	1.3070
.2	18	18	3.142	0.9982	0.775°	0.0388	1.3070
3	18	14	2.443	0.9932	1.024°	0.0387	1.3070
4	19.5	24	3.867	0.9996	1.233°	0.0778	1.2558
5	19.5	24	3.867	0.9996	1.022°	0.0388	1.2558
6	29.5	24	2.556	0.9940	0.935°	0.0389	1.0209
7	29.5	24	2.556	0.9940	1.962°	0.0778	1.0209
*8	29.5	24	5.112	1.0000	0.935°	0.0390	1.0209
*9	35.5	24	4.248	0.9998	1.127°	0.0389	0.9307
10	27.5	24	2.742	0.9955	0.868°	0.0388	1.0574
11	27.5	24	2.742	0.9955	0.868°	0.0388	1.0574

* The second mode.
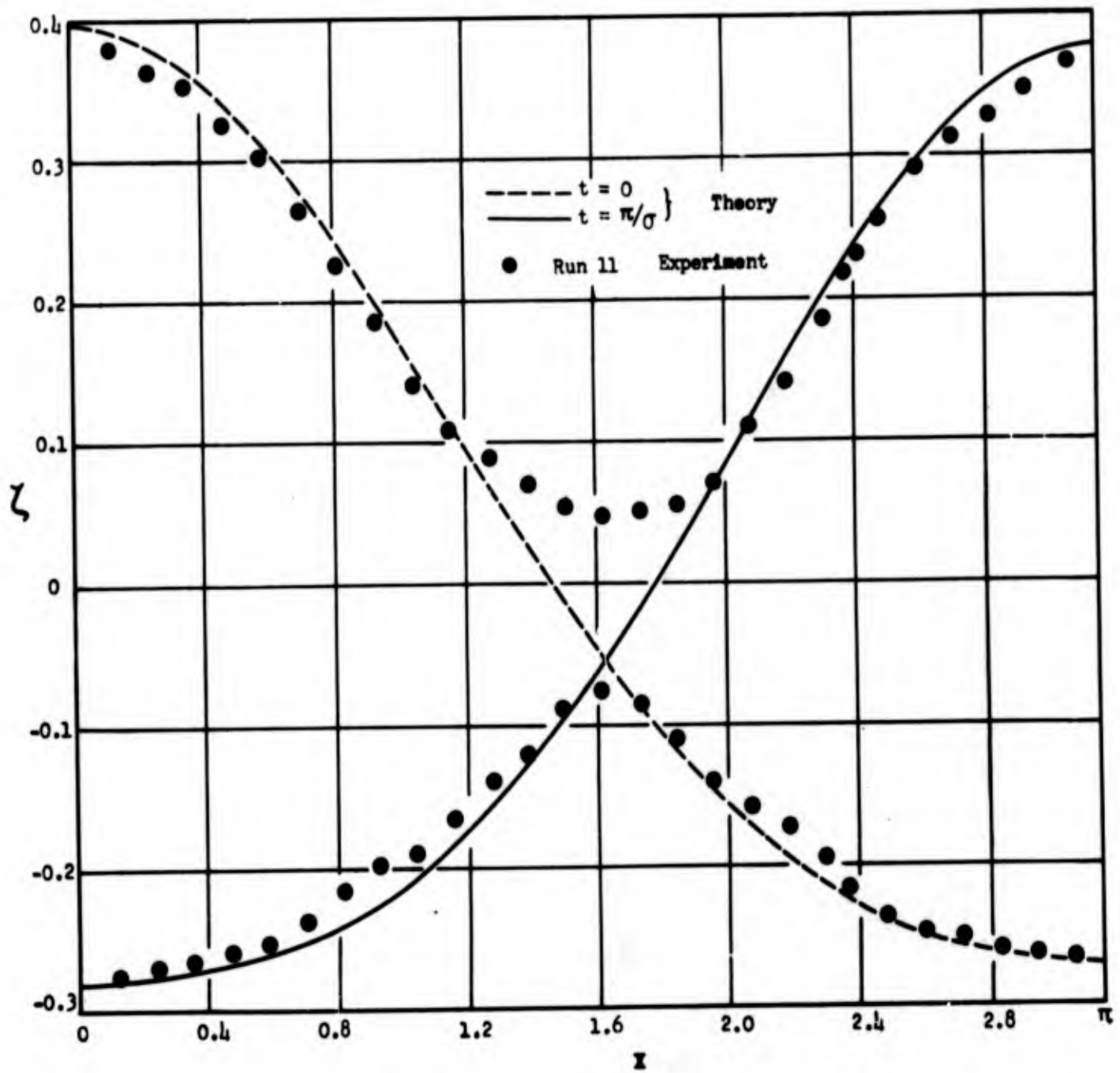
(a) $\sigma = 0.965$

FIG. 8.3 Comparison of Theoretical and Experimental Results for Profiles of
Two-dimensional Standing Waves, $\alpha = 0.0194$
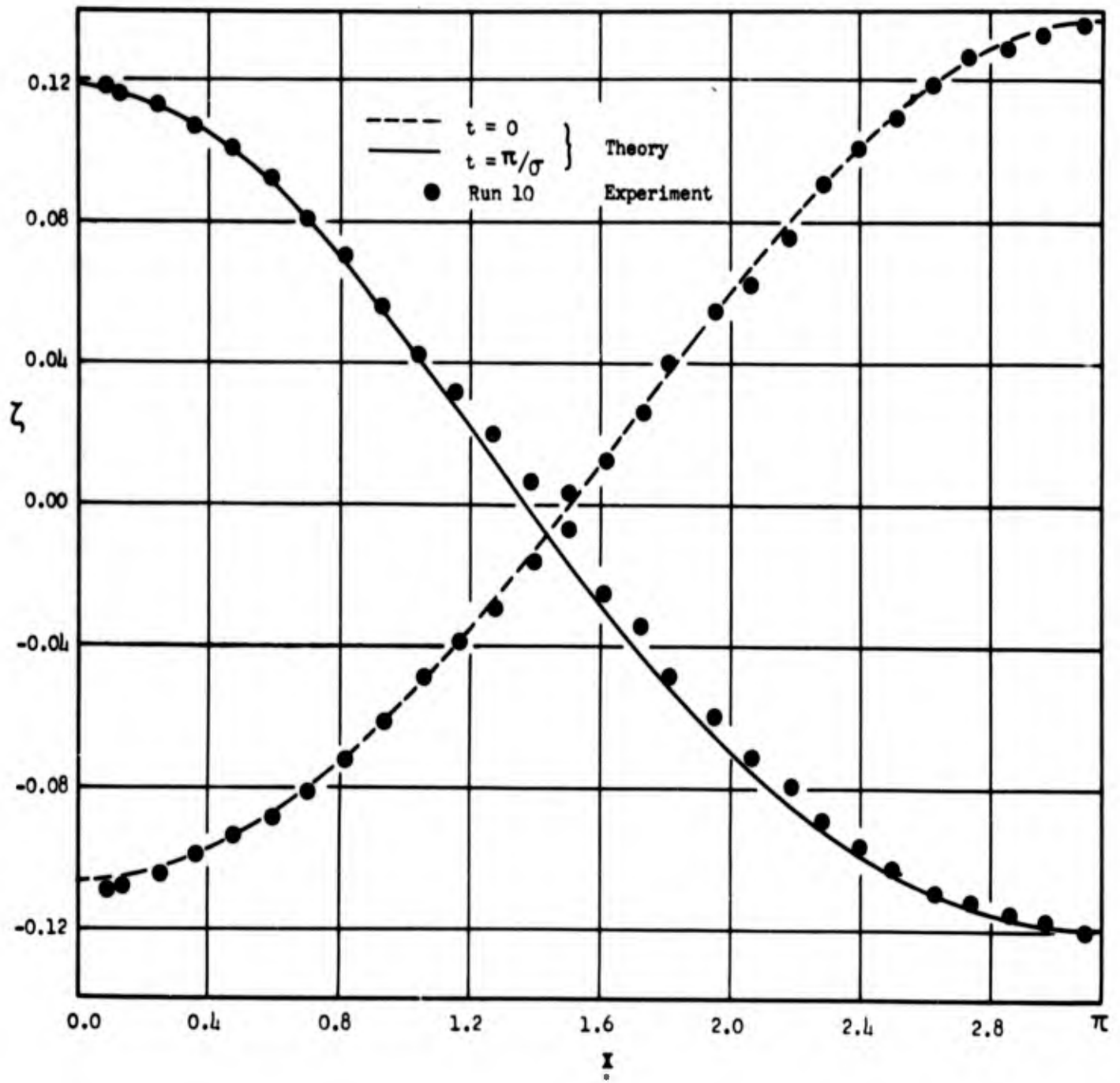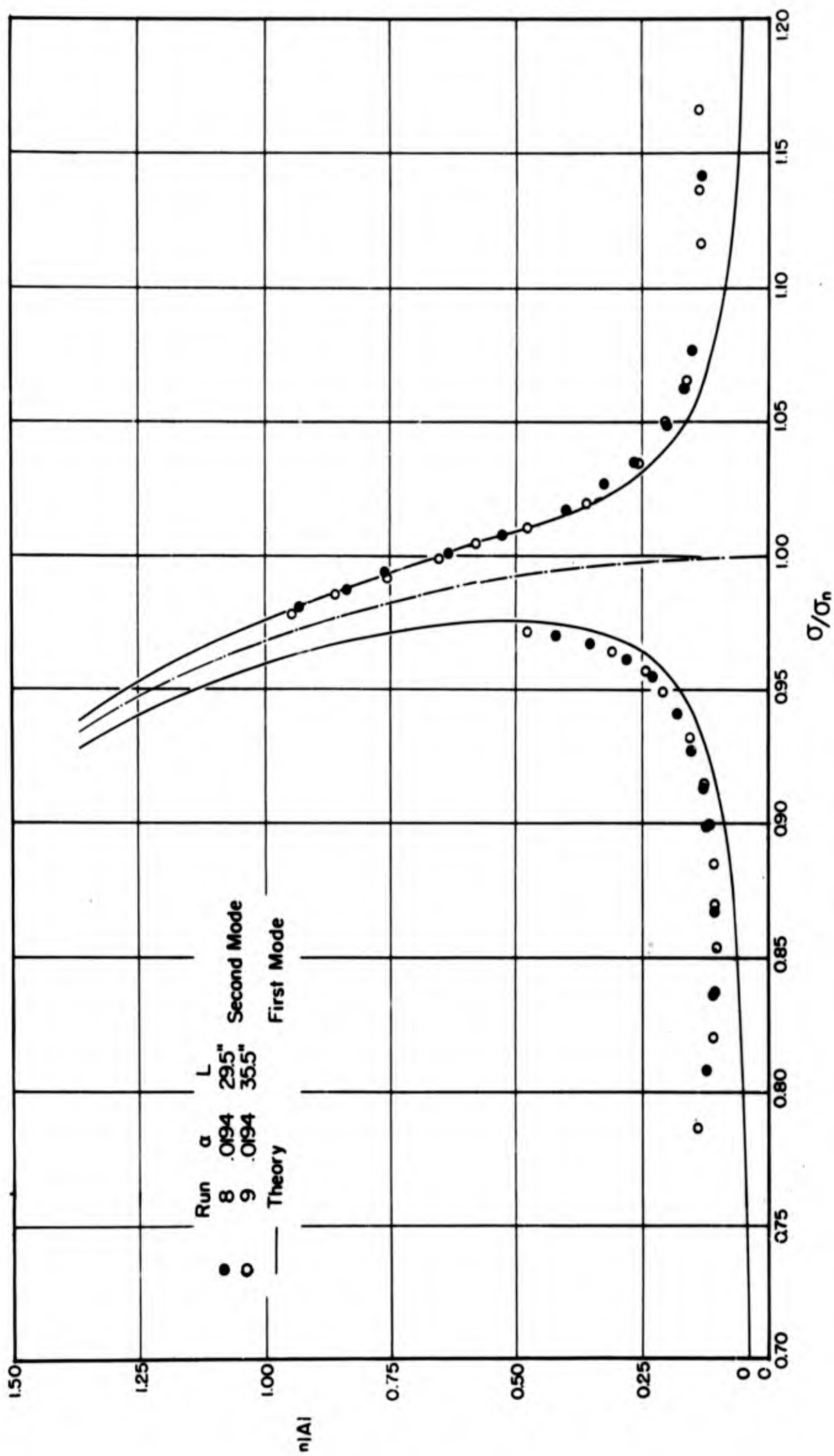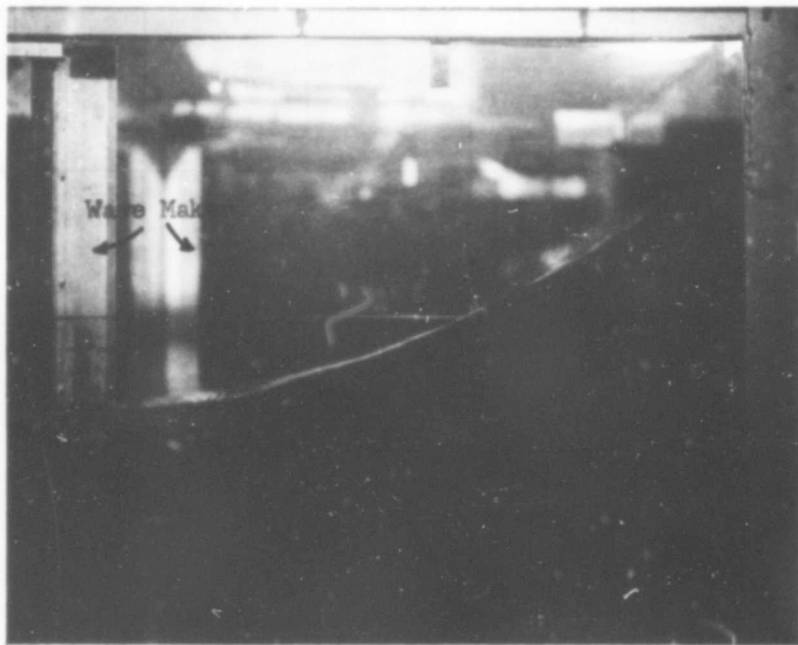
FIG. 8.3(b) $\sigma = 1.000$

FIG. 8.4 Frequency-Amplitude Curve of the Second Mode of Forced Two-dimensional Standing Waves

-71-

(a) The First Mode

(b) The Second Mode

FIG. 8.5 Photographs of Two-dimensional Standing Waves

8.4 Cross Waves

The experimental program on cross waves is aimed at investigating the possibility of exciting the fundamental mode of cross waves under the conditions predicted by the theoretical analysis in Sec. V as well as obtaining the frequency-amplitude curve of cross waves. Two series of experiments were made: first, at the length/width ratio $\ell = \frac{n}{4}$ with the smallest amplitude of the wave maker available and second, at $\ell \neq \frac{n}{4}$ with a critical amplitude of wave maker for excitation. The experimental conditions are summarized in Table 8.2. Two photographs of cross waves are shown in Fig. 8.8.

(1) The experiment for $\ell = \frac{n}{4}$

With the smallest amplitude of wave maker available it was possible to excite the cross waves at the frequency $\omega/2\pi$ as $\omega^2 \approx \ell$. The frequency-amplitude curves plotted in Fig. 8.6 are in agreement with the resonance curve of free oscillation. The absence of the data near $\omega/\omega_1 = 1$ is due to the fact that near this frequency the amplitude of cross waves became smaller than that of the longitudinal mode, both of which are very sensitive to the variation of the driving frequency of the wave maker; therefore, the system of waves is very unstable. The cross waves were always started at the frequency nearly equal to but smaller than $\omega/\omega_1 = 1$ and were not visible until the amplitude of cross waves is comparable with that of the longitudinal component of standing waves. The amplitude increased rapidly with a small decrease in the frequency of wave maker. The amplitude of the longitudinal component of the standing waves decreased as the amplitude of cross waves increased, the surface approaching a two-dimensional form at high amplitude. The violent type of instability due to splashy wavelets similar to the two-dimensional case mentioned in the previous section was also observed. This disturbance which appeared at $\ell |A| > 1.0$ depended on the amplitude of the wave maker and made it difficult to obtain accurate measurements.

For $\ell = 1$ several trials were made to generate cross waves, but without success; instead of the type observed above, three-dimensional standing waves with half wave length and half frequency of the wave maker oscillating along one of the diagonals of the tank were observed. The oscillation appeared to be stable; but, by a slight adjustment of the adjusting string at the top of the

wave maker (which changes the effective length of the tank on two sides near the top of the wave maker) the amplitude of the standing waves may change or the oscillation may shift to the other one of the diagonals. As the tank was not square, the oscillation was along the longer diagonal, since the oscillation for the first mode of cross waves is associated with the fourth mode of the longitudinal component of the standing waves at $\ell = 1$. The possibility of the half-frequency mode of the longitudinal component in oscillation has to be considered. A run with $\ell \neq 1$ was made with the frequency of the wave maker operated near $\sigma = 2$ which is not in the range of the resonance frequency for cross waves; but no half-frequency mode was observed. Together with the similar standing waves of full-frequency mentioned in the previous section, it suggests that this peculiar type of oscillation might be caused by the fact that the wave maker is not perfectly parallel to the end wall.

(2) The experiment for $\ell \neq {}^{n}/4$

Three different length/width ratios with several amplitudes of wave maker were tested. For $\ell = 0.289$ and 0.362, the cross waves could be excited with the smallest wave maker amplitude; however, for $\ell = 0.562$ a critical amplitude was found to be $\alpha = 0.0121$. The frequency-amplitude curves are shown in Fig. 8.7. These curves are in the form of a parabola similar to the resonance curve and their vertices lie on the right of the resonance curve. In this case, it was possible to have the cross waves of small amplitude and to determine the onset frequency, which depends on the amplitude of wave maker. The result of Howard's analysis [21], based on the quadratic theory and $\ell \approx 1/4$, indicates that the critical amplitude of the wave maker has the following relation with the frequency:

$$\alpha_0^2 \sim (\sigma^2 - 1)^2 \left(1 - \frac{\omega^2}{\omega_1^2}\right)$$

By approximating this relation to correlate the data, then for $\ell \neq {}^{n}/4$ and $\sigma^2 \neq 1$. α_0 is essentially proportional to $\left| 1 - \omega^2/\omega_1^2 \right|$ as plotted in Fig. 8.9.

(3) The Phase Relation

The phase angle between the cross waves and the wave maker is measured by a wave gage at $y = 0$ and the displacement gage at the top of the wave maker. A sample of measurement is shown in Fig. 7.4, which gives the phase angle ϵ in Eq. (5.31) equal to $\pi/2$.

Table 8.2   Summary of Experiments on Cross Waves

Run	L	2θ	2α	h	$[\tanh \frac{\pi h}{W}]^{1/2}$	ℓ
101	6	0.279°	0.0571	24	0.9981	1/4
102	12	0.990°	0.0832	20	0.9945	1/2
103	12	0.443°	0.0454	24	0.9981	1/2
104	18	0.835°	0.0571	24	0.9981	3/4
105	18.14	0.279°	0.0203	24	0.9981	3/4
111	7	0.287°	0.0504	24	0.9981	0.289
112	7	0.366°	0.0642	24	0.9981	0.289
113	7	0.447°	0.0785	24	0.9981	0.289
114	8.75	0.279°	0.0392	24	0.9981	0.362
115	8.75	0.448°	0.0630	24	0.9981	0.362
116	8.75	0.604°	0.0848	24	0.9981	0.362
117	14.5	0.286°	0.0242	24	0.9981	0.560
118	14.5	0.364°	0.0308	24	0.9981	0.560
119	14.5	0.443°	0.0376	24	0.9981	0.560
120	14.5	0.609°	0.0515	24	0.9981	0.560

(a) 1 = 1/4
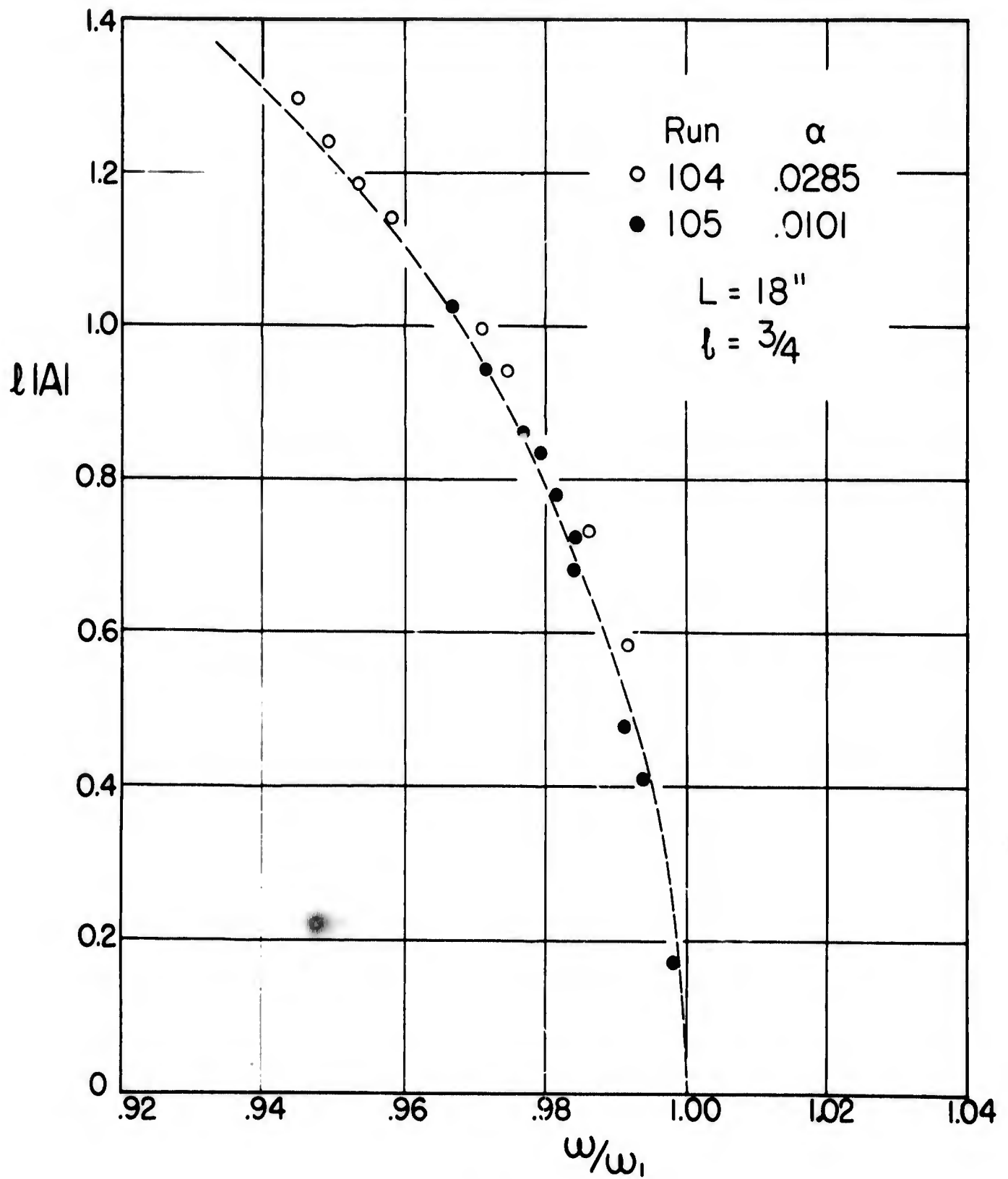
FIG. 8.6 Frequency-Amplitude Curves of Cross Waves for 1 = n/4

FIG. 8.6(b) 1 = 1/2

FIG. 8.6(c) l = 3/4

(a) 1 = 0.289

FIG. 8.7 Frequency-Amplitude Curves of Cross Waves for $1 \neq n/4$

FIG. 8.7(b) l = 0.362

FIG. 8.7(c) 1 - 0.560

(a) End View

(b) View from Corner

FIG. 8.8 Photograph of Cross Waves

FIG. 8.9 $\omega^2/\omega_1^2 - 1$ versus α_0^2

8.5 The Stability of Two-Dimensional Standing Waves and Excitation of the Fundamental Mode of Cross Waves

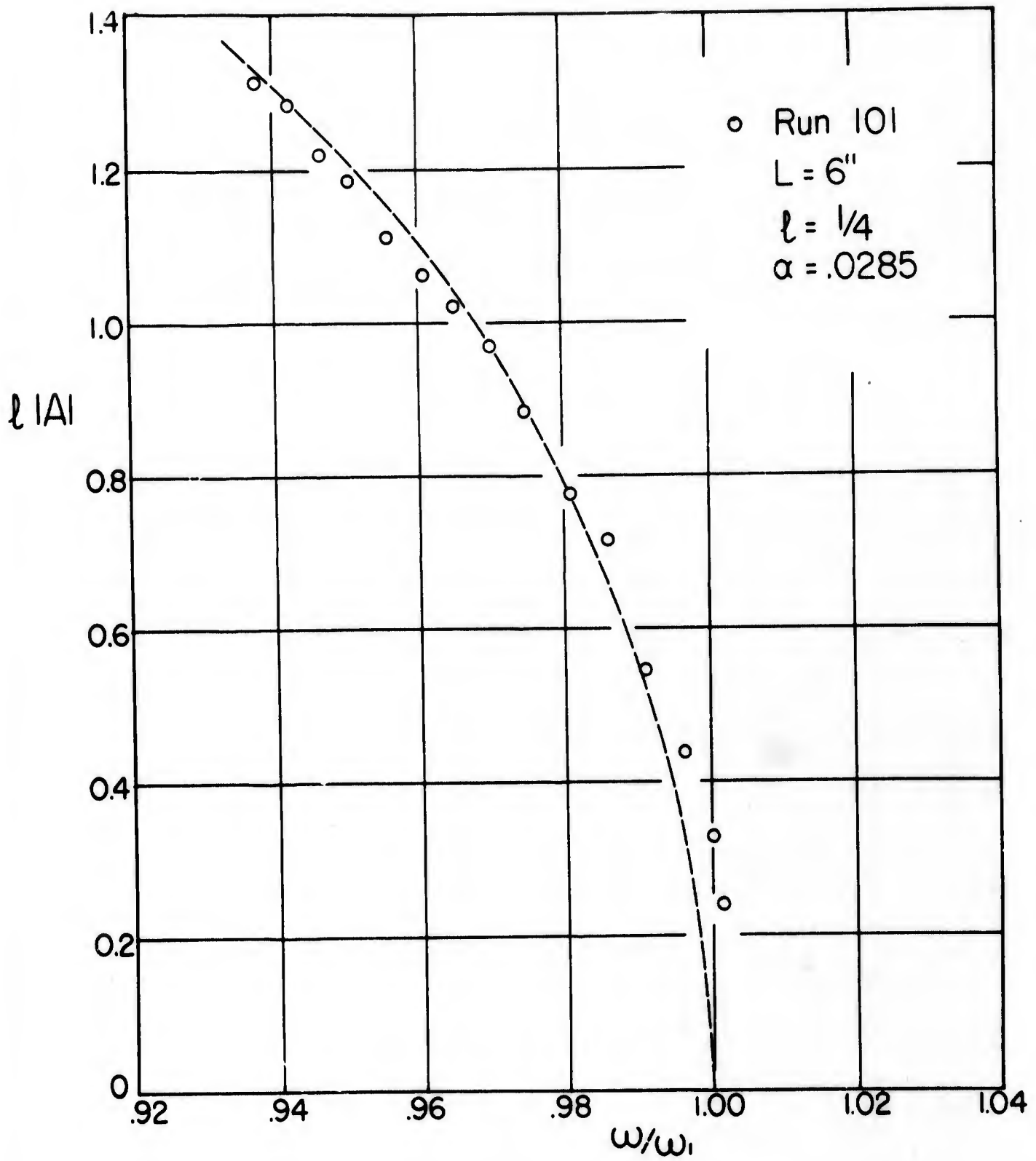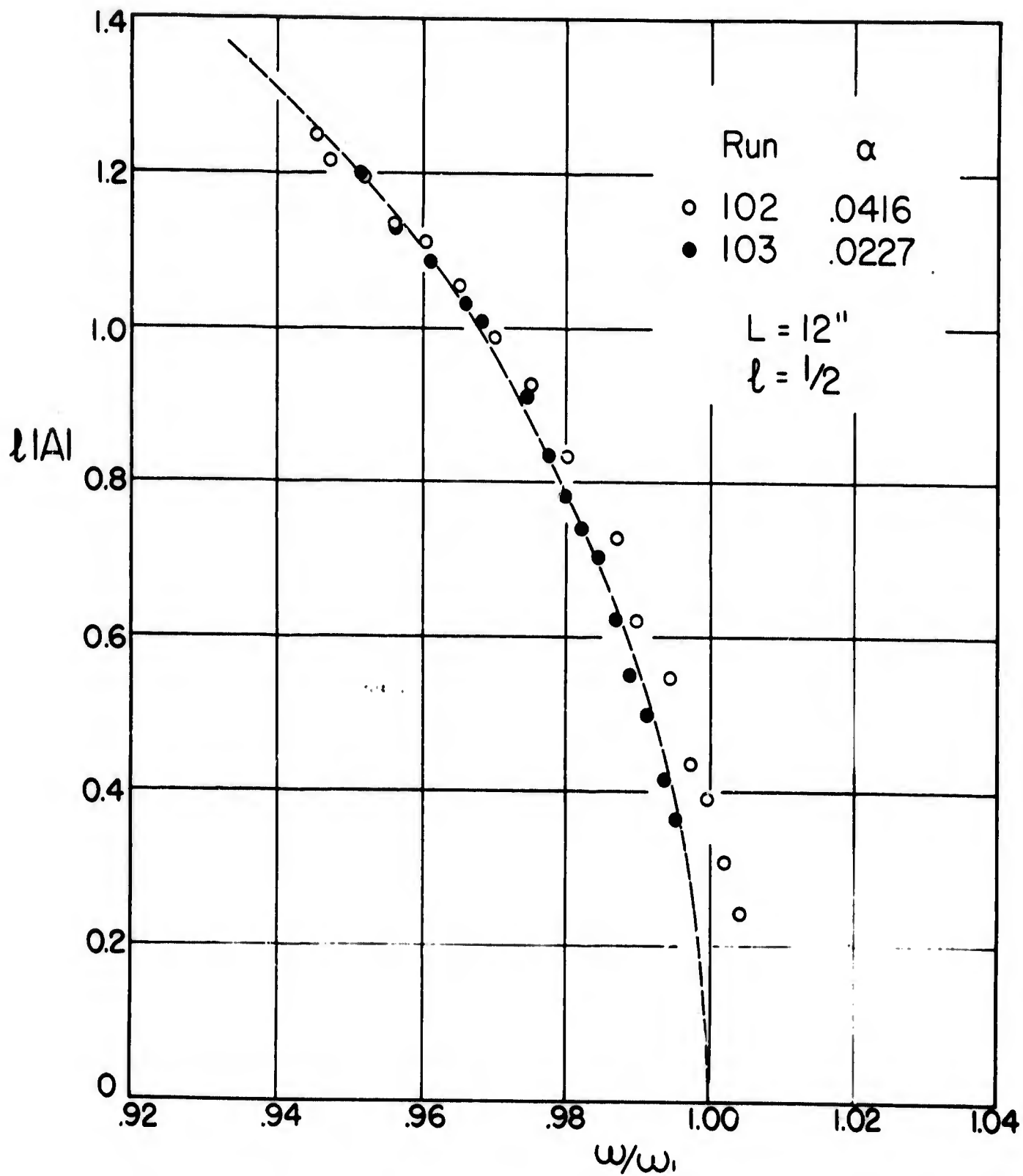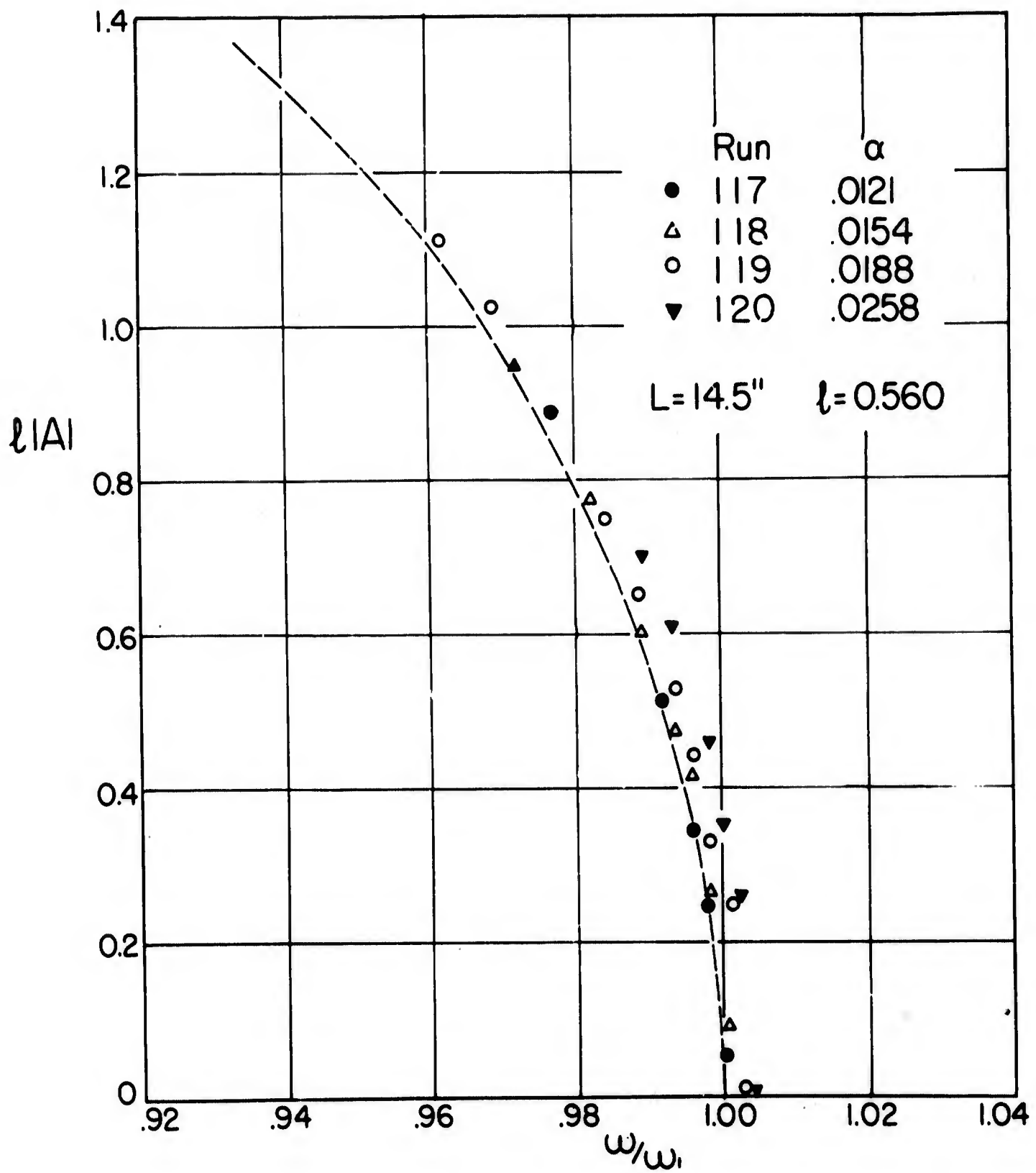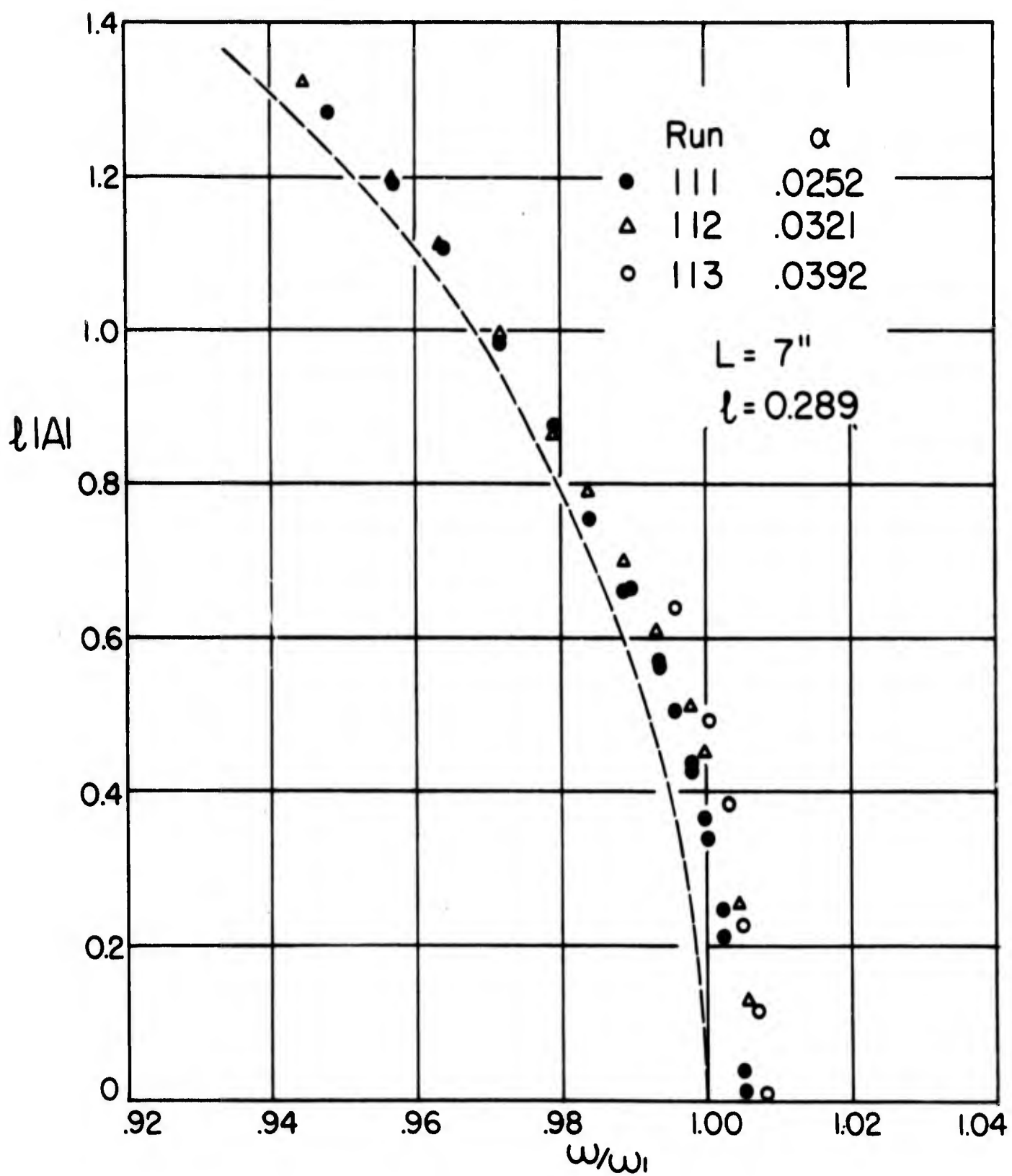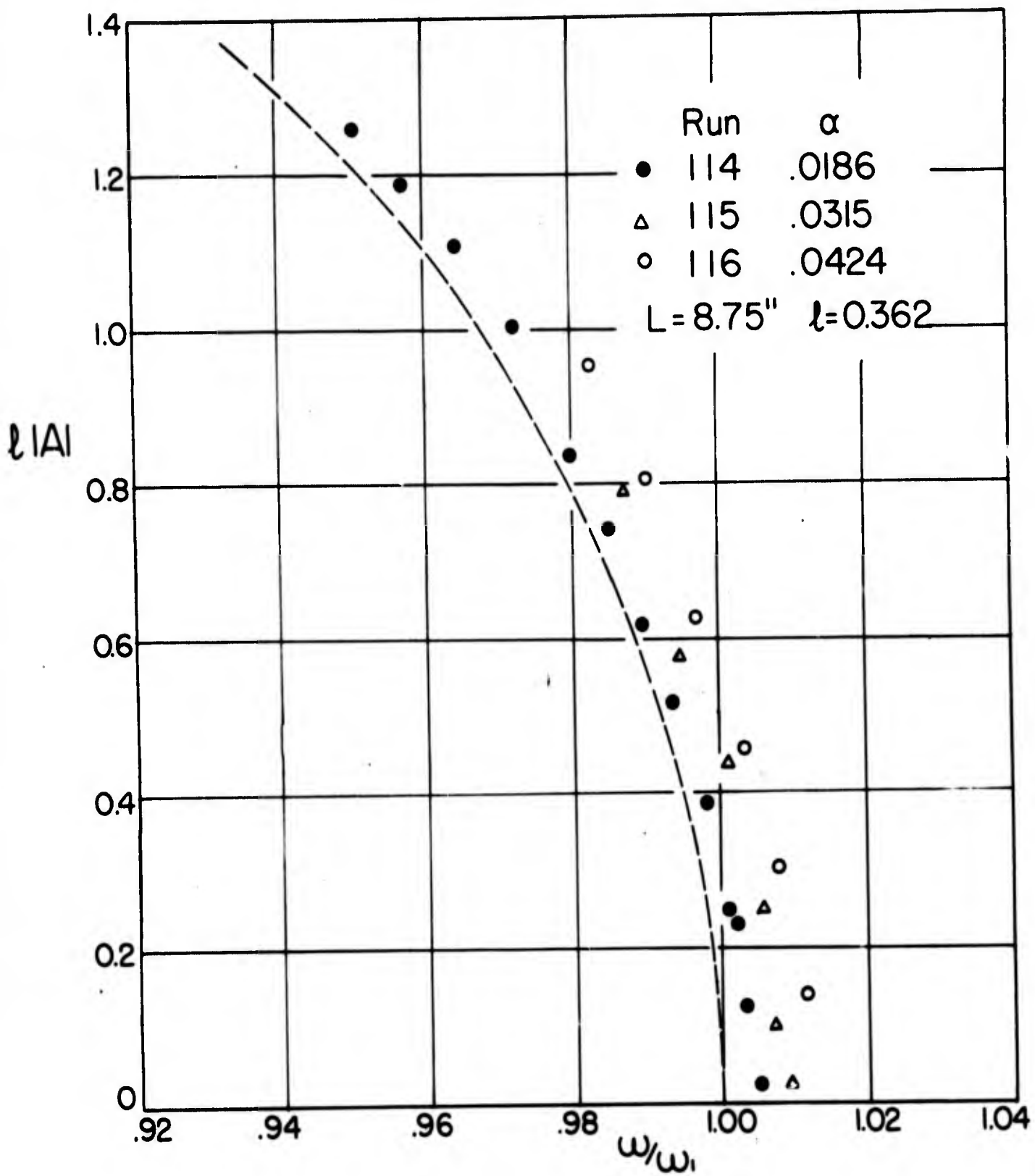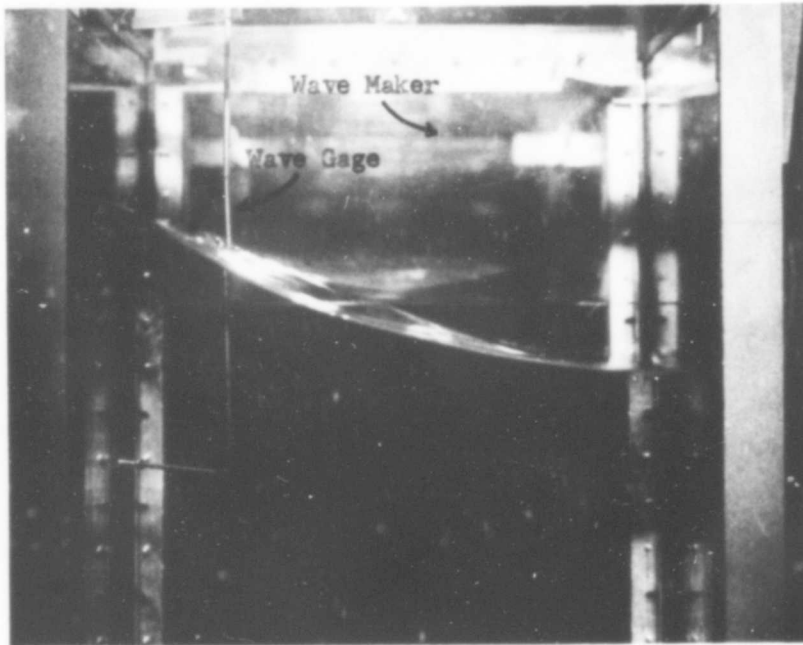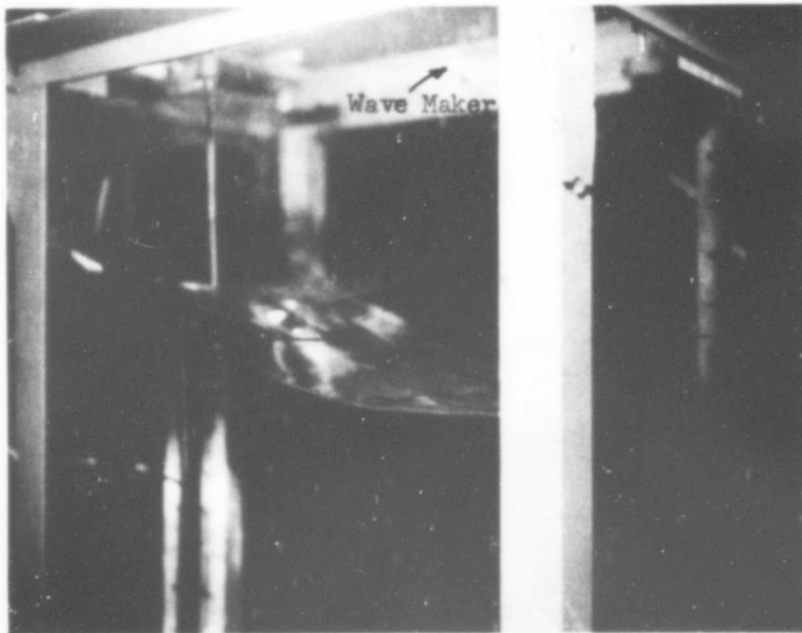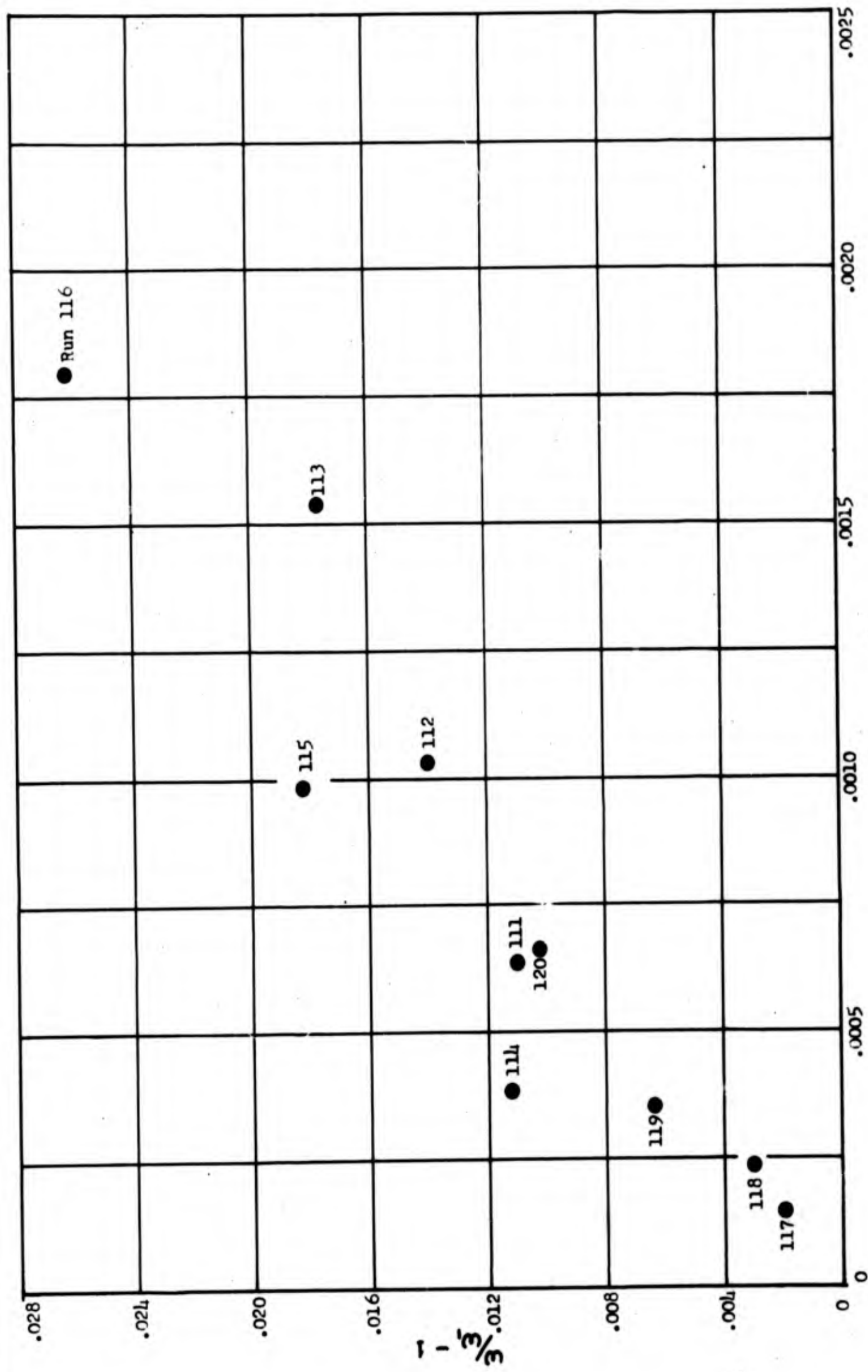The linearized version of the problem is basically two-dimensional and thus the two-dimensional standing waves of small amplitude are always stable. Since the linear solution does not apply in the neighborhood of a resonance frequency, a non-linear solution has to be solved in each neighborhood. By means of comparing the linear and non-linear solutions in Fig. 4.5 for the first mode of two-dimensional standing waves, the range of significant non-linear effects can be approximately determined; it depends on the amplitude of the wave maker. For the particular values of α in the experiment, they were found as:

$$0.93 < \sigma/\sigma_1 < 1.05 \qquad \text{for } \alpha = 0.0194$$
$$0.92 < \sigma/\sigma_1 < 1.08 \qquad \text{for } \alpha = 0.0388$$

The exact range of non-linear effects cannot be determined by the comparison; however, the limiting case for $\alpha \to 0$ is of interest. For $\alpha \to 0$ (Free oscillation), the non-linear range can be determined as $0.93 < \sigma/\sigma_n < 1.00$ where the frequency 0.93 is determined by the highest possible free standing waves based on the results of Penney and Price [14]. The spacing of the discrete resonance frequencies becomes closer as the mode of oscillation increases; therefore, higher modes of standing waves are essentially non-linear in their characteristics. Both non-linear two-dimensional and three-dimensional standing waves may exist in this range and the stability of two-dimensional standing waves in general is extremely difficult to investigate for there are infinitely-many modes of three-dimensional oscillation. However, the interest centers only on the stability of two-dimensional standing waves in relation to the excitation of the fundamental mode of cross waves. The result of Sec. V indicates that the cross waves can be excited at the half-frequency of the wave maker nearly equal to the resonance frequency of the first mode in the transverse direction by an infinitesimal amplitude of wave maker with $\ell = {}^n/4$ (n is an integer). The experimental result indicates that for $\ell \neq {}^n/4$, there exists a critical amplitude of wave maker for excitation depending on ℓ. In the light of these results, a stability diagram is constructed in Fig. 8.10 for the half-frequency of wave maker near or smaller than the fundamental mode of cross waves as $\alpha \approx 0$. In the dark area, the cross waves exist with $\alpha \approx 0$ and in the shaded area the cross waves can be excited with a critical value of α. The extent of the shaded area depends on the magnitude of α. The region above $\omega/\omega_1 \approx 1$ is unexplored. The ray through the origin has a slope, $\dfrac{\omega/\omega_1}{\sigma/\sigma_1} = \frac{1}{2}(\sigma_1/\omega_1) = \frac{1}{2}(\frac{w}{L})^{1/2} = \frac{1}{\sqrt{4\ell}}$; hence, it represents a particular value of ℓ.
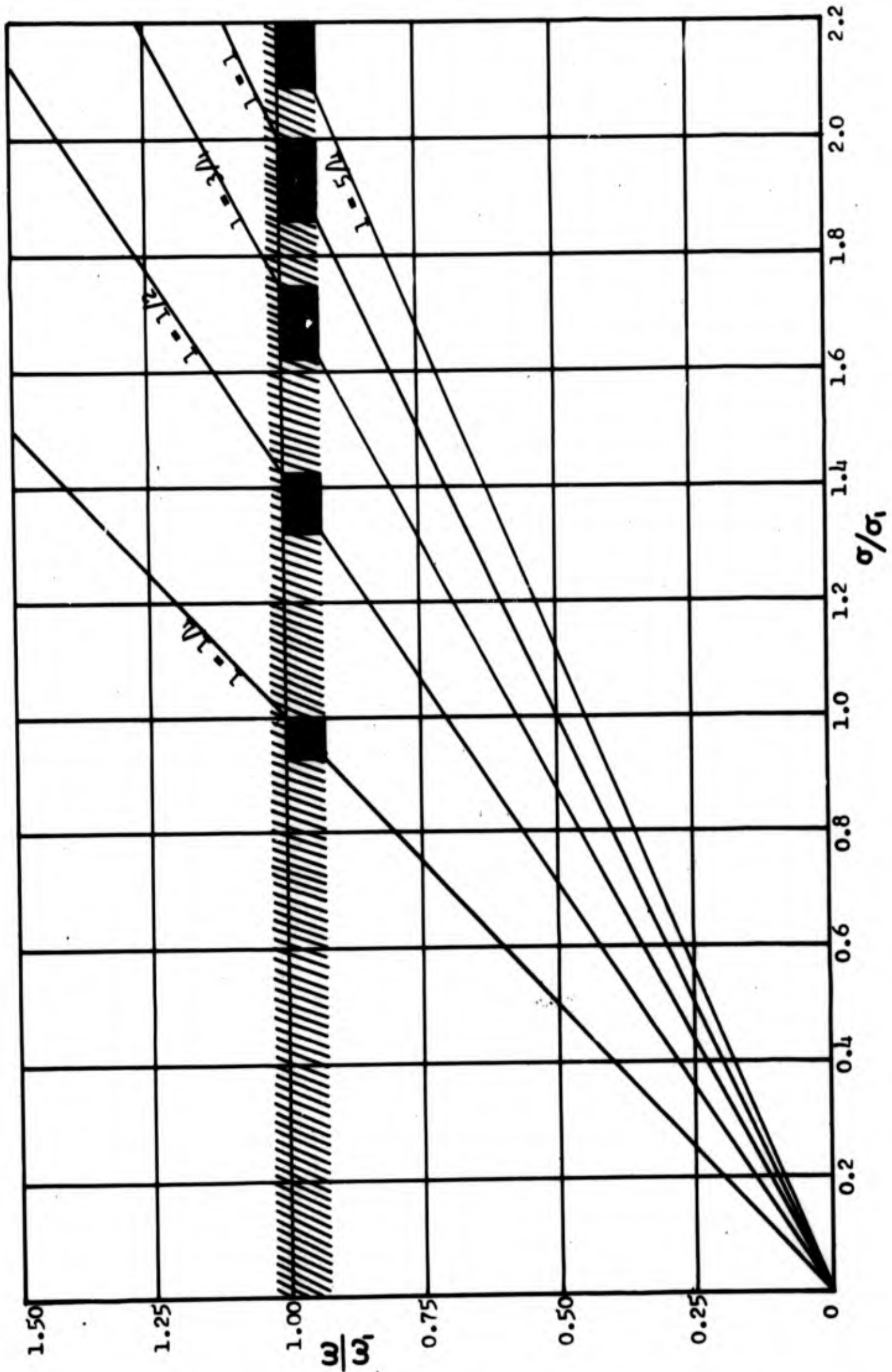
FIG. 8.10 Stability Diagram for Infinitesimal Amplitude of Wave Maker

IX. CONCLUSIONS

From these theoretical and experimental investigations, the following conclusions can be drawn:

(1) The linearized version of the problem of forced standing waves generated in a rectangular tank by a two-dimensional wave maker is basically two-dimensional and the solution for forced two-dimensional standing waves of small amplitude is always stable. The linear solution is not valid in a neighborhood of a resonance frequency of the system; therefore, a non-linear solution has to be obtained, in each of these neighborhoods. By means of comparing the linear and non-linear solutions, the range of significant non-linear effects can be approximately determined for a particular α. In this range, infinitely many non-linear solutions may exist. Since the non-linear range depends on α and since the spacing of the resonance frequency becomes closer at higher modes, standing waves of higher-modes with sufficiently large amplitudes of the wave maker are essentially non-linear in character.

(2) Forced two-dimensional standing waves of finite amplitude were obtained as a family of particular solutions in the non-linear range in the three-dimensional system. Two non-intersecting branches of oscillation were found theoretically and experimentally for the frequency-amplitude curve relation. The third-order solution obtained by the method of iteration used in Sec. IV is in good agreement with the experimental result. In the experiment, stable two-dimensional standing waves could be generated if the half-frequency of the wave maker is smaller than the resonance frequency in the transverse direction and the length/width ratio of the tank is not equal to a multiple of 1/4.

(3) The stability of two-dimensional standing waves of finite amplitude in the sense of avoiding the excitation of the fundamental mode of cross waves was investigated by means of finding the possible solution of the cross waves. The analysis shows that the cross waves have a frequency equal to half that of the wave maker and can be excited near the resonance frequency in the transverse direction with infinitesimal amplitude ($\alpha \approx o$) at $\ell = n/4$ and with a critical amplitude as $\ell \neq n/4$.

(4) The frequency-amplitude curve of cross waves for in-
finitesimal amplitude of wave maker at $\ell = n/4$ was found
experimentally in agreement with the non-linear resonance
curve of free oscillation for the two-dimensional case.
For a finite amplitude of the wave maker at $\ell \neq n/4$, it
is essentially parabolic in shape with its vertex on the
right of the former and similar to the resonance curve.
Hence, the frequency-amplitude curve for cross waves can
in general can be described approximately by the resonance
curve for the two-dimensional case.

REFERENCES

[1] Taylor, G.I. "An Experimental Study of Standing Waves", Proc. Roy. Soc. A, <u>218</u> (1953), pp. 44-59.

[2] Schuler, M. "Der Umschlag von Oberflächenwellen", ZAMM Band 13, Heft 6 (1933), pp. 443-446.

[3] Ursell, F. "Edge Waves on Sloping Beach", Proc. Roy. Soc. A, <u>214</u> (1952), pp. 79-98.

[4] McKernan, J.C. "The Use of Transverse Standing Waves to Simulate Short Crested Head Seas", Course XIII, M.S. Thesis M.I.T. 1958.

[5] Russell, J.S. "Wave of Translation", Frubner & Co. London, 1885.

[6] Stokes, G.G. "On the Theory of Oscillatory Waves", Math. & Phys. Papers V. 1 (1880), pp. 197-229 & pp. 314-326.

[7] Rayleigh, J.W.S., Lord "On Progressive Waves", Scientific Papers V. 1, p. 261 & p. 322; V. 6, p. 11, p. 306 & p. 419 (1869-1919).

[8] Mitchell, J.H. "On the Highest Waves in Water", Phil. Mag. (5), <u>36</u> (1893) pp. 430-437.

[9] Havelock, E.T. "Periodic Irrotational Waves of Finite Height", Proc. Roy. Soc. A, <u>95</u> (1918), pp. 38-51.

[10] Levi-Civita, T. "Determination rigoureuse des ondes d'ampleur finie", Math. Ann. Vol. 93 (1925), pp. 264-314.

[11] Struik, D.J. "Determination rigoureuse des ondes irrotationelles periodiques dans un canal á profondeur finie", Math. Ann. Vol. 95 (1926), pp. 595-634.

[12] De, S.C. "Contributions to the Theory of Stokes Waves", Proc. Camb. Phil. Soc., <u>51</u> (1955), pp. 713-736.

[13] Benjamin, T.B. & Lighthill, M. J. "On Cnoidal Waves and Bores", Proc. Roy. Soc. A, <u>224</u> (1954), pp. 448-460.

[14]   Penney, W.G. and Price, A.T.   "Finite Periodic
       Stationary Gravity Waves in a Perfect Liquid",
       Phil. Trans. A, 244 (1952), pp. 254-284.

[15]   Faraday, M.   "On the Forms and States Assumed
       by Fluid in Contact with Vibrating Elastic
       Surfaces", Phil. Trans. Roy. Soc. 31 (1831),
       p. 319.

[16]   Matthiessen, L.   "Akustische Versuche, die
       Kleinsten Transversal-Wellen der Flüssigkeiten
       betreffend", Ann. Phys. Lpz., 134 (1868), p.107.

[17]   Matthiessen, L.   "Über die Transversalschwingun-
       gen tonender tropfbarer und elastischer Flüssig-
       keiten", Ann. Phys. Lpz., 141, (1870), p. 375.

[18]   Rayleigh, J.W.S., Lord   "On Maintained Vibrations",
       Phil. Mag. (5), 15 (1883), p. 235.

[19]   Rayleigh, J.W.S., Lord   "On the Crispations of
       Fluid Resting Upon a Vibrating Support", Phil.
       Mag. (5), 16 (1883), p. 50.

[20]   Benjamin, T.B. and Ursell, F.   "The Stability
       of Plane Free Surface of a Liquid in Vertical
       Periodic Motion", Proc. Roy. Soc. A, 225
       (1954), pp. 505-515.

[21]   Howard, L.   "Cross Waves", Reported at Nov. 1959
       Meeting of Division of Fluid Dynamics, American
       Physical Society, Unpublished.

[22]   Lamb, H.   "Hydrodynamics", Cambridge University
       Press, 6th Ed. 1932.

[23]   Coulson, C.A.   "Waves", Oliver and Boyd, London,
       7th Ed. 1955.

[24]   Havelock, T.H.   "Forced Progressive Waves on
       Water", Phil. Mag. (7), 8 (1929), pp. 569-576.

[25]   Minorsky, N.   "Non-Linear Mechanics", Edwards,
       Ann Arbor, Michigan, 1947.

[26]   Stoker, J.J.   "Non-Linear Vibration", Inter-
       science Publishers, 1950.

[27] McLachlan, N.W. "Ordinary Non-Linear Differential Equations in Engineering and Physical Science", Oxford University Press, 1950.

[28] Dean, R.G. and Ursell, F. "Interaction of a Fixed Semi-immersed Circular Cylinder with a Train of Surface Waves", Tech. Rep. No. 37, Hydrodynamics Lab. M.I.T. 1959.

[29] Stoker, J.J. "Water Waves", Interscience Publishers, Inc., New York, 1957.

Appendix A. $\underline{E(\lambda,\mu)}$ and $\underline{S_N(s)}$ Functions for
the Expansion of $e^{\lambda\zeta}$ $\underline{Cos\mu x}$

Rewrite Eq. (4.2) as the following:

$$\zeta = \frac{1}{2}\sum_{n=-\infty}^{\infty} a_n e^{inx} \quad , \quad \text{where} \quad a_n = a_{-n} \quad (A.1)$$

If
$$\eta = \frac{1}{2}\sum_{n=-\infty}^{\infty} b_n e^{inx} \quad ,$$

then
$$\zeta\eta = \frac{1}{4}\sum_{m=0}^{\infty}\sum_{n=-\infty}^{\infty} a_m b_n e^{i(m+n)x} = \frac{1}{4}\sum_{s=-\infty}^{\infty}\left(\sum_{m=0}^{\infty} a_m b_{s-m}\right)e^{isx} \quad (A.2)$$

or
$$\zeta^2 = \frac{1}{4}\sum_{s=-\infty}^{\infty} S_2(s)e^{isx}, \quad \text{where} \quad S_2(s) = \sum_{m=-\infty}^{\infty} a_m a_{s-m} \quad .(A.3)$$

Let
$$\zeta^N = \frac{1}{2^N}\sum_{s=-\infty}^{\infty} S_N(s)e^{isx} \quad ; \quad (A.4)$$

and
$$\zeta^N = \zeta\,\zeta^{N-1} = \frac{1}{2^N}\sum_{s=-\infty}^{\infty}\sum_{m=-\infty}^{\infty} a_m S_{N-1}(s-m)e^{isx} \quad , \quad (A.5)$$

hence
$$S_N(s) = \sum_{m=-\infty}^{\infty} a_m S_{N-1}(s-m) \quad . \quad (A.6)$$

Continued application of Eq. (A.6) leads to

$$S_N(s) = \sum_{m=-\infty}^{\infty}\sum_{n=-\infty}^{\infty}\sum_{p=-\infty}^{\infty}\cdots a_m a_n a_p \cdots a_{s-m-n-p\cdots} \quad (A.7$$

It will be observed that $S_N(s) = S_N(-s)$ since $a_n = a_{-n}$.
Also

$$S_0(0) = 1 \,, \; S_0(s) = 0 \quad \text{for} \quad s \neq 0$$
and
$$S_1(s) = a_s \quad \text{for all} \; s. \quad (A.8)$$

Now, we write

$$e^{\lambda\zeta} = \sum_{N=0}^{\infty}\frac{\lambda^N}{N!}\zeta^N = \sum_{N=0}^{\infty}\frac{\lambda^N}{2^N N!}\sum_{s=-\infty}^{\infty} S_N(s)e^{isx} = \sum_{s=-\infty}^{\infty} E(\lambda,s)e^{isx} \quad (A.9)$$

where

$$E(\lambda,s) = E(\lambda,-s) = \sum_{N=0}^{\infty}\frac{\lambda^N}{2^N N!} S_N(s) \quad (A.10)$$

and therefore

$$e^{\lambda z}\cos\mu x = \frac{1}{2}\sum_{s=-\infty}^{\infty}E(\lambda,s)\left[e^{i(s+\mu)x}+e^{i(s-\mu)x}\right]$$

$$= \frac{1}{2}\sum_{s=-\infty}^{\infty}\left[E(\lambda,s-\mu)+E(\lambda,s+\mu)\right]e^{isx}$$

$$= E(\lambda,\mu)+\sum_{s=1}^{\infty}\cos sx\left[E(\lambda,s-\mu)+E(\lambda,s+\mu)\right]. \qquad (A.11)$$

Values of $S_N(s)$ to Third Order

$S_0(0)=1$, $S_0(s)=0$ for all $s\geq 1$

$S_1(s)=a_s$ for all s

$S_2(0)=a_0^2+2a_1^2$

$S_2(1)=2a_0a_1+2a_1a_2$

$S_2(2)=2a_1a_2$

$S_2(3)=2a_1a_2$

$S_3(0)=a_0^3+6a_0a_1^2$

$S_3(1)=3a_0^2a_1+3a_1^3$

$S_3(2)=3a_0a_1^2$

$S_3(3)=a_1^3$

Values of $E(\lambda,\mu)$ to Third Order

$$E(\lambda,0)=\left(1+\frac{\lambda}{2}a_0+\frac{\lambda^2}{8}a_0^2+\frac{\lambda^3}{48}a_0^3\right)+\frac{\lambda^2}{4}\left(1+\frac{\lambda}{2}a_0\right)a_1^2$$

$$E(\lambda,1)=\frac{\lambda}{2}\left(1+\frac{\lambda}{2}a_0+\frac{\lambda^2}{8}a_0^2\right)a_1+\frac{\lambda^2}{4}a_1a_2+\frac{\lambda^3}{16}a_1^3$$

$$E(\lambda,2)=\frac{\lambda}{2}\left(1+\frac{\lambda}{2}a_0\right)a_2+\frac{\lambda^2}{8}\left(1+\frac{\lambda}{2}a_0\right)a_1^2$$

$$E(\lambda,3)=\frac{\lambda}{2}a_3+\frac{\lambda^2}{4}a_1a_2+\frac{\lambda^3}{48}a_1^3$$

Appendix B. $F(\lambda, \mu)$ and $T_N(s)$ Functions for the Expansion of $e^{\lambda \zeta_2}$ $\cos \mu \ell y$

Rewrite Eq. (5.7) as the following:

$$\zeta_2 = \frac{1}{2} \sum_{n=-\infty}^{\infty} C_n e^{inx} \cos \ell y \quad , \text{ where } \quad C_n = C_{-n} \qquad (B.1)$$

Consider ℓy as x, $\frac{1}{2} \sum_{n=-\infty}^{\infty} C_n e^{inx}$ as a_1 and $a_n = 0$ for $n \neq 1$ in Eq. (A.1), then Eq. (A.11) leads to

$$e^{\lambda \zeta_2} \cos \mu \ell y = F(\lambda, \mu) + \sum_{s=1}^{\infty} \cos s \ell y \left[F(\lambda, s-\mu) + F(\lambda, s+\mu) \right] \qquad (B.2)$$

where

$$F(\lambda, s) = F(\lambda, -s) = \sum_{N=0}^{\infty} \frac{\lambda^N}{2^N N!} T_N(s) \qquad (B.3)$$

with

$$T_N(s) = T_{-N}(s) \qquad \text{(See Appendix A)} \qquad (B.4)$$

By the use of Eq. (A.8), we have

$$T_0(0) = 1, \quad T_0(s) = 0 \quad \text{for all } s \neq 0 \qquad (B.5)$$

and

$$T_1(1) = \frac{1}{2} \sum_{n=-\infty}^{\infty} C_n e^{inx}, \quad T_1(s) = 0 \text{ for all } s \neq 1 \qquad (B.6)$$

Now, Eq. (A.6) leads to

$$T_N(s) = \sum_{m=-\infty}^{\infty} T_1(m) T_{N-1}(s-m) \qquad (B.7)$$

with, in addition to Eq. (B.4),

$$T_N(-s) = T_N(s) \qquad (B.8)$$

due to Eq. (B.3).

Hence,

$$T_2(s) = \sum_{m=-\infty}^{\infty} T_1(m) T_1(s-m) = T_1(1)\left[T_1(s-1) + T_1(s+1)\right] ,$$

$$T_2(0) = 2T_1^2(1) \quad T_2(1) = 0 \quad T_2(2) = T_1^2(1) \quad T_2(s) = 0 \text{ for } s \geq 3$$

$$T_3(s) = \sum_{m=-\infty}^{\infty} T_1(m) T_2(s-m) = T_1(1)\left[T_2(s-1) + T_2(s+1)\right] ,$$

$$T_3(0) = 0 \quad T_3(1) = 3T_1^3(1) \quad T_3(2) = 0 \quad T_3(3) = T_1^3(1)$$

$$T_3(s) = 0 \quad \text{for} \quad s \geq 4 \tag{B.9}$$

$$T_4(s) = \sum_{m=-\infty}^{\infty} T_1(m) T_3(s-m) = T_1(1)\left[T_3(s-1) + T_3(s+1)\right] ,$$

$$T_4(0) = 6T_1^4(1) \quad T_4(1) = 0 \quad T_4(2) = 4T_1^2(1) \quad T_4(3) = 0$$

$$T_4(4) = T_1^4(1) \quad T_4(s) = 0 \quad \text{for} \quad s \geq 5 .$$

Also

$$T_1(1) = \frac{1}{2}\sum_{n=-\infty}^{\infty} C_n e^{inx} = \frac{1}{2}\sum_{n=-\infty}^{\infty} C_n \cos nx = \frac{1}{2}\sum_{s=-\infty}^{\infty} S_1'(s) e^{isx} ; \tag{B.10}$$

$$T_1^2(1) = \frac{1}{4}\sum_{m=-\infty}^{\infty}\sum_{n=-\infty}^{\infty} C_m C_n e^{i(m+n)x} = \frac{1}{4}\sum_{s=-\infty}^{\infty}\sum_{m=-\infty}^{\infty} C_m C_{s-m} e^{isx}$$

$$= \frac{1}{4}\sum_{s=-\infty}^{\infty} S_2'(s) e^{isx} \tag{B.11}$$

where

$$S_2'(s) = \sum_{m=-\infty}^{\infty} C_m C_{s-m} . \tag{B.12}$$

Then

$$T_1^N(1) = \frac{1}{2^N}\sum_{s=-\infty}^{\infty} S_N'(s) e^{isx} \tag{B.13}$$

where

$$S_N'(s) = \sum_{m=-\infty}^{\infty} C_m S_{N-1}'(s-m) \tag{B.14}$$

with

$$S_0'(0) = 1 , \quad S_0'(s) = 0 \quad \text{for} \quad s \neq 0 \tag{B.15}$$

and

$$S_1'(s) = C_s \quad \text{for all } s .$$

Now, $F(\lambda, S)$ in terms of $T_1(1)$ is

$$F(\lambda, S) = T_0(s) + \frac{\lambda}{2} T_1(s) + \frac{\lambda^2}{8} T_2(s) + \frac{\lambda^3}{48} T_3(s) + \frac{\lambda^4}{384} T_4(s) + \cdots \tag{B.16}$$

-94-

For $S = 0, 1, 2, 3, \cdots$

$$F(\lambda, 0) = T_0(0) + \frac{\lambda}{2}T_1(0) + \frac{\lambda^2}{8}T_2(0) + \frac{\lambda^3}{48}T_3(0) + \cdots = T_0(0) + \frac{\lambda^2}{4}T_1^2(1) + \cdots$$

$$F(\lambda, 1) = T_0(1) + \frac{\lambda}{2}T_1(1) + \frac{\lambda^2}{8}T_2(1) + \frac{\lambda^3}{48}T_3(1) + \cdots = \frac{\lambda}{2}T_1(1) + \frac{\lambda^3}{16}T_1^3(1) + \cdots$$

$$F(\lambda, 2) = T_0(2) + \frac{\lambda}{2}T_1(2) + \frac{\lambda^2}{8}T_2(2) + \frac{\lambda^3}{48}T_3(2) + \cdots = \frac{\lambda^2}{8}T_1^2(1) + \cdots \qquad \text{(B.17)}$$

$$F(\lambda, 3) = T_0(3) + \frac{\lambda}{2}T_1(3) + \frac{\lambda^2}{8}T_2(3) + \frac{\lambda^3}{48}T_3(3) + \cdots = \frac{\lambda^3}{48}T_1^3(1) + \cdots$$

By using Eqs. (B.10) to (B.15),

$$F(\lambda, 0) = 1 + \frac{\lambda^2}{16}\sum_{s=-\infty}^{\infty} S_2'(s)e^{isx} + \cdots = \sum_{s=-\infty}^{\infty}\left[S_0'(s) + \frac{\lambda^2}{16}S_2'(s) + \cdots\right]e^{isx}$$

$$F(\lambda, 1) = \frac{\lambda}{4}\sum_{s=-\infty}^{\infty} S_1'(s)e^{isx} + \frac{\lambda^3}{128}\sum_{s=-\infty}^{\infty} S_3'(s)e^{isx} + \cdots = \sum_{s=-\infty}^{\infty}\left[\frac{\lambda}{4}S_1'(s) + \frac{\lambda^3}{128}S_3'(s) + \cdots\right]e^{isx}$$

$$F(\lambda, 2) = \frac{\lambda^2}{32}\sum_{s=-\infty}^{\infty} S_2'(s)e^{isx} + \cdots = \sum_{s=-\infty}^{\infty}\left[\frac{\lambda^2}{32}S_2'(s) + \cdots\right]e^{isx} \qquad \text{(B.18)}$$

$$F(\lambda, 3) = \frac{\lambda^3}{128}\sum_{s=-\infty}^{\infty} S_3'(s)e^{isx} + \cdots = \sum_{s=-\infty}^{\infty}\left[\frac{\lambda^3}{128}S_3'(s) + \cdots\right]e^{isx}$$

and let

$$F(\lambda, \mu) = \sum_{s=-\infty}^{\infty} f_s(\lambda, \mu)\cos sx \qquad \text{(B.19)}$$

with

$$f_s(\lambda, \mu) = f_{-s}(\lambda, \mu) \qquad \text{(B.20)}$$

because of

$$S_N'(s) = S_N'(-s)$$

Hence, by comparing the coefficients of $\cos sx$ on the right-hand-sides of Eqs. (B.18) and (B.19), we have

$$f_s(\lambda, 0) = S_0'(s) + \frac{\lambda^2}{16}S_2'(s) + \cdots$$

$$f_s(\lambda, 1) = \frac{\lambda}{4}S_1'(s) + \frac{\lambda^3}{128}S_3'(s) + \cdots \qquad \text{(B.21)}$$

$$f_s(\lambda, 2) = \frac{\lambda^2}{32}S_2'(s) + \cdots$$

$$f_s(\lambda, 3) = \frac{\lambda^3}{128}S_3'(s) + \cdots$$

Values of $S'_N(s)$ to the Third Order

$S'_0(0) = 1$, $\quad S'_0(s) = 0$ for all $\quad s \geq 1$

$S'_1(s) = C_s \qquad$ for all $\quad s$

$S'_2(0) = C_0^2 \qquad\qquad S'_2(1) = 2C_0 C_1 \qquad S'_2(2) = C_1^2$

$S'_3(0) = C_0^3 \qquad\qquad S'_3(1) = 0$

Values of $f_s(\lambda, \mu)$ to the Third Order

$f_0(\lambda, 0) = S'_0(0) + \dfrac{\lambda}{16} S'_2(0) + \cdots = 1 + \dfrac{\lambda^2}{16} C_0^2$

$f_1(\lambda, 0) = S'_0(1) + \dfrac{\lambda}{16} S'_2(1) + \cdots = \dfrac{\lambda^2}{8} C_0 C_1$

$f_2(\lambda, 0) = 0$

$f_0(\lambda, 1) = \dfrac{\lambda}{4} S'_1(0) + \dfrac{\lambda^3}{128} S'_3(0) + \cdots = \dfrac{\lambda}{4} C_0$

$f_1(\lambda, 1) = \dfrac{\lambda}{4} S'_1(1) + \dfrac{\lambda^3}{128} S'_3(1) + \cdots = \dfrac{\lambda}{4} C_1$

$f_2(\lambda, 1) = \dfrac{\lambda}{4} S'_1(2) + \dfrac{\lambda^3}{128} S'_3(2) + \cdots = \dfrac{\lambda}{4} C_2$

$f_0(\lambda, 2) = \dfrac{\lambda^2}{32} S'_2(0) + \cdots = \dfrac{\lambda^2}{32} C_0^2$

$f_1(\lambda, 2) = \dfrac{\lambda^2}{32} S'_2(1) + \cdots = \dfrac{\lambda^2}{16} C_0 C_1$

$f_2(\lambda, 2) = 0$

$f_0(\lambda, 3) = \dfrac{\lambda^3}{128} S'_3(0) + \cdots = \dfrac{\lambda^3}{128} C_0^3$

$f_1(\lambda, 3) = 0$

$f_2(\lambda, 3) = 0$

Appendix C. Expansions of the Product of Fourier Series

It is desirable to expand the following products:

$$P_1 = \sum_{m=0}^{\infty} A_m \cos mx \sum_{n=0}^{\infty} B_n \cos nx \qquad \text{for} \quad B_n = B_{-n} \qquad (C.1)$$

and

$$P_2 = \sum_{m=1}^{\infty} A_m \cos mx \sum_{n=-\infty}^{\infty} B_n \cos nx \qquad \text{for} \quad B_n = B_{-n} \qquad (C.2)$$

into Fourier Series. For Eq. (C.1),

$$P_1 = \frac{1}{2} \sum_{m=0}^{\infty} \sum_{n=0}^{\infty} A_m B_n \left[\cos(m+n)x + \cos(m-n)x \right]$$

in which

$$\sum_{m=0}^{\infty} \sum_{n=0}^{\infty} A_m B_n \cos(m+n)x = \sum_{s=0}^{\infty} \cos sx \sum_{\substack{m=0 \\ s-m \geq 0}}^{\infty} A_m B_{s-m}$$

and

$$\sum_{m=0}^{\infty} \sum_{n=0}^{\infty} A_m B_n \cos(m-n)x$$

$$= \sum_{m=0}^{\infty} A_m B_m + \sum_{\substack{s=m-n \geq 1 \\ m \neq n, m > n}}^{\infty} \cos sx \sum_{n=0}^{\infty} A_{s+n} B_n + \sum_{\substack{s=n-m \geq 1 \\ m \neq n, n > m}}^{\infty} \cos sx \sum_{m=0}^{\infty} A_m B_{s+m}$$

Then,

$$2P_1 = \sum_{m=0}^{\infty} A_m B_m + \sum_{s=0}^{\infty} \cos sx \sum_{m=0}^{\infty} A_m B_{s-m} + \sum_{s=1}^{\infty} \cos sx \sum_{m=0}^{\infty} A_{s+m} B_n + \sum_{s=1}^{\infty} \cos sx \sum_{m=0}^{\infty} A_m B_{s+m}$$

$$= \sum_{m=0}^{\infty} A_m B_m + B_0 \sum_{s=1}^{\infty} A_s \cos sx + \sum_{s=1}^{\infty} \cos sx \sum_{m=0}^{\infty} A_m B_{s-m} + \sum_{s=1}^{\infty} \cos sx \sum_{m=s}^{\infty} A_m B_{m-s} + \sum_{s=1}^{\infty} \cos sx \sum_{m=0}^{\infty} A_m B_{s-m}$$

$$= \sum_{m=0}^{\infty} A_m B_m + B_0 \sum_{s=0}^{\infty} A_s \cos sx + \sum_{s=1}^{\infty} \cos sx \sum_{m=0}^{\infty} A_m (B_{s-m} + B_{s+m}) \qquad (C.3)$$

For Eq. (C.2),

$$P_2 = \left[\sum_{m=0}^{\infty} A_m \cos mx - A_0 \right] \left[2 \sum_{m=0}^{\infty} B_n \cos nx - B_0 \right]$$

$$= \sum_{m=1}^{\infty} A_m B_m - 2A_0 \sum_{s=1}^{\infty} B_s \cos sx + \sum_{s=1}^{\infty} \cos sx \sum_{m=0}^{\infty} A_m (B_{s-m} + B_{s+m})$$

$$= \sum_{m=1}^{\infty} A_m B_m - \sum_{s=1}^{\infty} \cos sx \sum_{m=1}^{\infty} A_m (B_{s-m} + B_{s+m}) \qquad (C.4)$$

Appendix D. The System of Ordinary Differential Equations
for Cross Waves

Coefficients of $Cos0x Cos0\ell y$:

$$\frac{\dot{a_0}}{2} = \sum_{n=0}^{\infty} \dot{b}_n E(n,n) f_0(n,0) + \sum_{m=1}^{\infty}\sum_{n=0}^{\infty} \dot{b}_n [E(n,m-n)+E(n,m+n)] f_m(n,0)$$

$$+ \sum_{n=0}^{\infty} \dot{d}_n E(\nu_n,n) f_0(\nu_n,1) + \sum_{m=1}^{\infty}\sum_{n=0}^{\infty} \dot{d}_n [E(\nu_n,m-n)+E(\nu_n,m+n)] f_m(\nu_n,1)$$

$$- \frac{1}{2} \sum_{m=0}^{\infty}\sum_{n=0}^{\infty} mn b_m b_n E(m+n,m-n) f_0(m+n,0) - \frac{1}{2}\sum_{m=0}^{\infty}\sum_{n=0}^{\infty}\sum_{p=1}^{\infty} mn b_m b_n [E(m+n,p-m+n)+E(m+n,p+m-n)] f_p(m+n,0)$$

$$+ \frac{1}{8} \sum_{m=0}^{\infty}\sum_{n=0}^{\infty} mn d_m d_n [E(\nu_m+\nu_n,m+n)-E(\nu_m+\nu_n,m-n)][f_0(\nu_m+\nu_n,0)+f_0(\nu_m+\nu_n,2)]$$

$$+ \frac{1}{8} \sum_{m=0}^{\infty}\sum_{n=0}^{\infty}\sum_{p=1}^{\infty} mn d_m d_n [E(\nu_m+\nu_n,p-m-n)+E(\nu_m+\nu_n,p+m+n)-E(\nu_m+\nu_n,p+m-n)-E(\nu_m+\nu_n,p-m+n)][f_p(\nu_m+\nu_n,0)+f_p(\nu_m+\nu_n,2)]$$

$$- \frac{1}{8} \sum_{m=0}^{\infty}\sum_{n=0}^{\infty} d_m d_n [E(\nu_m+\nu_n,m+n)+E(\nu_m+\nu_n,m-n)][f_0(\nu_m+\nu_n,0)-f_0(\nu_m+\nu_n,2)]$$

$$- \frac{1}{8} \sum_{m=0}^{\infty}\sum_{n=0}^{\infty}\sum_{p=1}^{\infty} d_m d_n [E(\nu_m+\nu_n,p-m-n)+E(\nu_m+\nu_n,p+m+n)+E(\nu_m+\nu_n,p-m+n)+E(\nu_m+\nu_n,p+m-n)][f_p(\nu_m+\nu_n,0)-f_p(\nu_m+\nu_n,2)]$$

$$- \frac{1}{8} \sum_{m=0}^{\infty}\sum_{n=0}^{\infty} \nu_m \nu_n d_m d_n [E(\nu_m+\nu_n,m+n)+E(\nu_m+\nu_n,m-n)][f_0(\nu_m+\nu_n,0)+f_0(\nu_m+\nu_n,2)]$$

$$- \frac{1}{8} \sum_{m=0}^{\infty}\sum_{n=0}^{\infty}\sum_{p=1}^{\infty} \nu_m \nu_n d_m d_n [E(\nu_m+\nu_n,p-m-n)+E(\nu_m+\nu_n,p+m+n)+E(\nu_m+\nu_n,p+m+n)+E(\nu_m+\nu_n,p+m-n)][f_p(\nu_m+\nu_n,0)+f_p(\nu_m+\nu_n,2)]$$

$$+ \frac{1}{2} \sum_{m=0}^{\infty}\sum_{n=0}^{\infty} m(n-\nu_n) b_m d_n E(m+\nu_n,m+n) f_0(m+\nu_n,1)$$

$$+ \frac{1}{2} \sum_{m=0}^{\infty}\sum_{n=0}^{\infty}\sum_{p=1}^{\infty} m(n-\nu_n) b_m d_n [E(m+\nu_n,p-m-n)+E(m+\nu_n,p+m+n)] f_p(m+\nu_n,1)$$

$$- \frac{1}{2} \sum_{m=0}^{\infty}\sum_{n=0}^{\infty} m(n+\nu_n) b_m d_n E(m+\nu_n,m-n) f_0(m+\nu_n,1)$$

$$- \frac{1}{2} \sum_{m=0}^{\infty}\sum_{n=0}^{\infty}\sum_{p=1}^{\infty} m(n+\nu_n) b_m d_n [E(m+\nu_n,p-m-n)+E(m+\nu_n,p+m-n)] f_p(m+\nu_n,1)$$

$$+ \frac{2\alpha\sigma}{\pi} Sin\sigma t \left\{ \sum_{m=0}^{\infty}\sum_{n=0}^{\infty} \frac{2mn b_n}{4m^2-1} [E(n+\tfrac{1}{2},m-n)-E(n+\tfrac{1}{2},m+n)] f_0(n+\tfrac{1}{2},0) \right.$$

$$+ \sum_{m=0}^{\infty}\sum_{n=0}^{\infty}\sum_{p=1}^{\infty} \frac{2mn b_n}{4m^2-1} [E(n+\tfrac{1}{2},p+m+n)+E(n+\tfrac{1}{2},p+m-n)-E(n+\tfrac{1}{2},p-m-n)-E(n+\tfrac{1}{2},p+m+n)] f_p(n+\tfrac{1}{2},0)$$

$$+ \sum_{m=0}^{\infty}\sum_{n=0}^{\infty} \frac{2mn d_n}{4m^2-1} [E(\nu_n+\tfrac{1}{2},m-n)-E(\nu_n+\tfrac{1}{2},m+n)] f_0(\nu_n+\tfrac{1}{2},1)$$

$$+ \sum_{m=0}^{\infty}\sum_{n=0}^{\infty}\sum_{p=1}^{\infty} \frac{2mndn}{4m^2-1}\left[E(\nu_n+\tfrac{1}{2}, p-m+n)+E(\nu_n+\tfrac{1}{2}, p+m-n)-E(\nu_n+\tfrac{1}{2}, p-m-n)-E(\nu_n+\tfrac{1}{2}, p+m+n)\right]$$
$$f_p(\nu_n+\tfrac{1}{2}, 1)$$

$$- \sum_{n=0}^{\infty} nb_n E(n+\tfrac{1}{2}, n) f_0(n+\tfrac{1}{2}, 0) - \sum_{m=1}^{\infty}\sum_{n=0}^{\infty} nb_n\left[E(n+\tfrac{1}{2}, m-n)+E(n+\tfrac{1}{2}, m+n)\right] f_m(n+\tfrac{1}{2}, 0)$$

$$+ \sum_{m=1}^{\infty}\sum_{n=1}^{\infty} \frac{nb_n}{4m^2-1}\left[E(n+\tfrac{1}{2}, m+n)+E(n+\tfrac{1}{2}, m-n)\right] f_0(n+\tfrac{1}{2}, 0)$$

$$+ \sum_{m=1}^{\infty}\sum_{n=1}^{\infty}\sum_{p=1}^{\infty} \frac{nb_n}{4m^2-1}\left[E(n+\tfrac{1}{2}, p-m-n)+E(n+\tfrac{1}{2}, p+m-n)+E(n+\tfrac{1}{2}, p-m+n)+E(n+\tfrac{1}{2}, p+m+n)\right] f_p(n+\tfrac{1}{2}, 0)$$

$$- \sum_{n=0}^{\infty} \nu_n d_n E(\nu_n+\tfrac{1}{2}, n) f_0(\nu_n+\tfrac{1}{2}, 1) - \sum_{m=1}^{\infty}\sum_{n=0}^{\infty} \nu_n d_n\left[E(\nu_n+\tfrac{1}{2}, m-n)+E(\nu_n+\tfrac{1}{2}, m+n)\right] f_m(\nu_n+\tfrac{1}{2}, 1)$$

$$+ \sum_{m=1}^{\infty}\sum_{n=0}^{\infty} \frac{\nu_n d_n}{4m^2-1}\left[E(\nu_n+\tfrac{1}{2}, m+n)+E(\nu_n+\tfrac{1}{2}, m-n)\right] f_0(\nu_n+\tfrac{1}{2}, 1)$$

$$+ \sum_{m=1}^{\infty}\sum_{n=0}^{\infty}\sum_{p=1}^{\infty} \frac{\nu_n d_n}{4m^2-1}\left[E(\nu_n+\tfrac{1}{2}, p-m-n)+E(\nu_n+\tfrac{1}{2}, p+m-n)+E(\nu_n+\tfrac{1}{2}, p-m+n)+E(\nu_n+\tfrac{1}{2}, p+m+n)\right]f_p(\nu_n+\tfrac{1}{2}, 1) \Big\}$$

$$+ \frac{8\alpha\sigma^2}{\pi}\cos\sigma t\left\{\tfrac{1}{2}E(\tfrac{1}{2}, 0)f_0(\tfrac{1}{2}, 0)+\sum_{m=1}^{\infty}E(\tfrac{1}{2}, m)f_m(\tfrac{1}{2}, 0)-\sum_{n=1}^{\infty}\frac{1}{4n^2-1}E(\tfrac{1}{2}, n)f_0(\tfrac{1}{2}, 0)\right.$$

$$\left. - \sum_{m=1}^{\infty}\sum_{n=1}^{\infty}\frac{1}{4n^2-1}\left[E(\tfrac{1}{2}, m+n)+E(\tfrac{1}{2}, m-n)\right]f_m(\tfrac{1}{2}, 0)\right\}$$

$$- \tfrac{1}{2}\alpha^2\sigma^2\sin^2\sigma t\left\{E(1, 0)f_0(1, 0)+2\sum_{m=1}^{\infty}E(1, m)f_m(1, 0)\right\} \tag{D.1}$$

Coefficients of Cos sx Cos 0ℓy, for $s \geq 1$:

$$a_s = 2\sum_{n=0}^{\infty}\dot{b}_n E(n, n)f_0(n, 0)+\sum_{m=1}^{\infty}\sum_{n=0}^{\infty}\dot{b}_n\left[E(n, m-n)+E(n, m+n)\right]\left[f_{s-m}(n, 0)+f_{s+m}(n, 0)\right]$$

$$+ 2\sum_{n=0}^{\infty}\dot{d}_n E(\nu_n, n)f_s(\nu_n, 1)+\sum_{m=1}^{\infty}\sum_{n=0}^{\infty}\dot{d}_n\left[E(\nu_n, m-n)+E(\nu_n, m+n)\right]\left[f_{s-m}(\nu_n, 1)+f_{s+m}(\nu_n, 1)\right]$$

$$- \sum_{m=0}^{\infty}\sum_{n=0}^{\infty} mnb_m b_n E(m+n, m-n)f_s(m+n, 0)$$

$$- \tfrac{1}{2}\sum_{m=0}^{\infty}\sum_{n=0}^{\infty}\sum_{p=1}^{\infty} mnb_m b_n\left[E(m+n, p-m+n)+E(m+n, p+m-n)\right]\left[f_{s-p}(m+n, 0)+f_{s+p}(m+n, 0)\right]$$

$$+ \tfrac{1}{4}\sum_{m=0}^{\infty}\sum_{n=0}^{\infty} mnd_m d_n\left[E(\nu_m+\nu_n, m+n)-E(\nu_m+\nu_n, m-n)\right]\left[f_s(\nu_m+\nu_n, 0)+f_s(\nu_m+\nu_n, 2)\right]$$

$$+ \tfrac{1}{8}\sum_{m=0}^{\infty}\sum_{n=0}^{\infty}\sum_{p=1}^{\infty} mnd_m d_n\left[E(\nu_m+\nu_n, p-m-n)+E(\nu_m+\nu_n, p+m+n)-E(\nu_m+\nu_n, p-m+n)-E(\nu_m+\nu_n, p+m-n)\right]$$
$$\left[f_{s-p}(\nu_m+\nu_n, 0)+f_{s+p}(\nu_m+\nu_n, 0)+f_{s-p}(\nu_m+\nu_n, 2)+f_{s+p}(\nu_m+\nu_n, 2)\right]$$

$$- \tfrac{\lambda^2}{4}\sum_{m=0}^{\infty}\sum_{n=0}^{\infty} d_m d_n\left[E(\nu_m+\nu_n, m+n)+E(\nu_m+\nu_n, m-n)\right]\left[f_s(\nu_m+\nu_n, 0)-f_s(\nu_m+\nu_n, 2)\right]$$

$$- \tfrac{\lambda^2}{8}\sum_{m=0}^{\infty}\sum_{n=0}^{\infty}\sum_{p=1}^{\infty} d_m d_n\left[E(\nu_m+\nu_n, p-m-n)+E(\nu_m+\nu_n, p+m+n)+E(\nu_m+\nu_n, p-m+n)+E(\nu_m+\nu_n, p+m-n)\right]$$
$$\left[f_{s-p}(\nu_m+\nu_n, 0)+f_{s+p}(\nu_m+\nu_n, 0)-f_{s-p}(\nu_m+\nu_n, 2)-f_{s+p}(\nu_m+\nu_n, 2)\right]$$

$$-\frac{1}{4}\sum_{m=0}^{\infty}\sum_{n=0}^{\infty}\nu_m\nu_n d_m d_n\left[E(\nu_m+\nu_n,m+n)+E(\nu_m+\nu_n,m-n)\right]\left[f_s(\nu_m+\nu_n,0)+f_s(\nu_m+\nu_n,2)\right]$$

$$-\frac{1}{8}\sum_{m=0}^{\infty}\sum_{n=0}^{\infty}\sum_{p=1}^{\infty}\nu_m\nu_n d_m d_n\left[E(\nu_m+\nu_n,p-m-n)+E(\nu_m+\nu_n,p+m+n)+E(\nu_m+\nu_n,p-m+n)+E(\nu_m+\nu_n,p+m-n)\right]$$
$$\left[f_{s-p}(\nu_m+\nu_n,0)+f_{s+p}(\nu_m+\nu_n,0)+f_{s-p}(\nu_m+\nu_n,2)+f_{s+p}(\nu_m+\nu_n,2)\right]$$

$$+\sum_{m=0}^{\infty}\sum_{n=0}^{\infty}m(n-\nu_n)b_m d_n\,E(m+\nu_n,m+n)\,f_s(m+\nu_n,1)$$

$$+\frac{1}{2}\sum_{m=0}^{\infty}\sum_{n=0}^{\infty}\sum_{p=1}^{\infty}m(n-\nu_n)b_m d_n\left[E(m+\nu_n,p-m-n)+E(m+\nu_n,p+m+n)\right]\left[f_{s-p}(m+\nu_n,1)+f_{s+p}(m+\nu_n,1)\right]$$

$$-\frac{1}{2}\sum_{m=0}^{\infty}\sum_{n=0}^{\infty}m(n+\nu_n)b_m d_n\,E(m+\nu_n,m-n)\,f_s(m+\nu_n,1)$$

$$-\frac{1}{2}\sum_{m=0}^{\infty}\sum_{n=0}^{\infty}\sum_{p=1}^{\infty}m(n+\nu_n)b_m d_n\left[E(m+\nu_n,p-m+n)+E(m+\nu_n,p+m-n)\right]\left[f_{s-p}(m+\nu_n,1)+f_{s+p}(m+\nu_n,1)\right]$$

$$+\frac{2\alpha\sigma}{\pi}\sin\sigma t\left\{\sum_{m=0}^{\infty}\sum_{n=0}^{\infty}\frac{4mn\,b_n}{4m^2-1}\left[E(n+\tfrac{1}{2},m-n)-E(n+\tfrac{1}{2},m+n)\right]f_s(n+\tfrac{1}{2},0)\right.$$

$$+\sum_{m=0}^{\infty}\sum_{n=0}^{\infty}\sum_{p=1}^{\infty}\frac{2mn\,b_n}{4m^2-1}\left[E(n+\tfrac{1}{2},p-m+n)+E(n+\tfrac{1}{2},p+m-n)-E(n+\tfrac{1}{2},p-m-n)-E(n+\tfrac{1}{2},p+m+n)\right]$$
$$\left[f_{s-p}(n+\tfrac{1}{2},0)+f_{s+p}(n+\tfrac{1}{2},0)\right]$$

$$+\sum_{m=0}^{\infty}\sum_{n=0}^{\infty}\frac{4mn\,d_n}{4m^2-1}\left[E(\nu_n+\tfrac{1}{2},m-n)-E(\nu_n+\tfrac{1}{2},m+n)\right]f_s(\nu_n+\tfrac{1}{2},1)$$

$$+\sum_{m=0}^{\infty}\sum_{n=0}^{\infty}\sum_{p=1}^{\infty}\frac{2mn\,d_n}{4m^2-1}\left[E(\nu_n+\tfrac{1}{2},p-m+n)+E(\nu_n+\tfrac{1}{2},p+m-n)-E(\nu_n+\tfrac{1}{2},p-m-n)-E(\nu_n+\tfrac{1}{2},p+m+n)\right]$$
$$\left[f_{s-p}(\nu_n+\tfrac{1}{2},1)+f_{s+p}(\nu_n+\tfrac{1}{2},1)\right]$$

$$-\sum_{n=0}^{\infty}2n\,b_n\,E(n+\tfrac{1}{2},n)\,f_s(n+\tfrac{1}{2},0)-\sum_{m=1}^{\infty}\sum_{n=0}^{\infty}n\,b_n\left[E(n+\tfrac{1}{2},m-n)+E(n+\tfrac{1}{2},m+n)\right]\left[f_{s-m}(n+\tfrac{1}{2},0)+f_{s+m}(n+\tfrac{1}{2},0)\right]$$

$$+\sum_{m=1}^{\infty}\sum_{n=1}^{\infty}\frac{2n\,b_n}{4m^2-1}\left[E(n+\tfrac{1}{2},m+n)+E(n+\tfrac{1}{2},m-n)\right]f_s(n+\tfrac{1}{2},0)$$

$$+\sum_{m=1}^{\infty}\sum_{n=1}^{\infty}\sum_{p=1}^{\infty}\frac{n\,b_n}{4m^2-1}\left[E(n+\tfrac{1}{2},p-m-n)+E(n+\tfrac{1}{2},p+m+n)+E(n+\tfrac{1}{2},p-m+n)+E(n+\tfrac{1}{2},p+m-n)\right]$$
$$\left[f_{s-p}(n+\tfrac{1}{2},0)+f_{s+p}(n+\tfrac{1}{2},0)\right]$$

$$-\sum_{n=0}^{\infty}2\nu_n\,d_n\,E(\nu_n+\tfrac{1}{2},n)\,f_s(\nu_n+\tfrac{1}{2},1)-\sum_{m=1}^{\infty}\sum_{n=0}^{\infty}\nu_n\,d_n\left[E(\nu_n+\tfrac{1}{2},m-n)+E(\nu_n+\tfrac{1}{2},m+n)\right]\left[f_{s-m}(\nu_n+\tfrac{1}{2},1)+f_{s+m}(\nu_n+\tfrac{1}{2},1)\right]$$

$$+\sum_{m=1}^{\infty}\sum_{n=0}^{\infty}\frac{2\nu_n\,d_n}{4m^2-1}\left[E(\nu_n+\tfrac{1}{2},m+n)+E(\nu_n+\tfrac{1}{2},m-n)\right]f_0(\nu_n+\tfrac{1}{2},1)$$

$$+\sum_{m=1}^{\infty}\sum_{n=0}^{\infty}\sum_{p=1}^{\infty}\frac{\nu_n\,d_n}{4m^2-1}\left[E(\nu_n+\tfrac{1}{2},p-m-n)+E(\nu_n+\tfrac{1}{2},p+m+n)+E(\nu_n+\tfrac{1}{2},p-m+n)+E(\nu_n+\tfrac{1}{2},p+m-n)\right]$$
$$\left.\left[f_{s-p}(\nu_n+\tfrac{1}{2},1)+f_{s+p}(\nu_n+\tfrac{1}{2},1)\right]\right\}$$

$$+\frac{8\alpha\sigma^2}{\pi}\cos\sigma t\left\{E(\tfrac{1}{2},0)f_s(\tfrac{1}{2},0)+\sum_{m=1}^{\infty}E(\tfrac{1}{2},m)\left[f_{s-m}(\tfrac{1}{2},0)+f_{s+m}(\tfrac{1}{2},0)\right]-\sum_{n=1}^{\infty}\frac{2}{4n^2-1}E(\tfrac{1}{2},n)f_s(\tfrac{1}{2},0)\right.$$
$$\left.-\sum_{m=1}^{\infty}\sum_{n=1}^{\infty}\frac{1}{4n^2-1}\left[E(\tfrac{1}{2},m-n)+E(\tfrac{1}{2},m+n)\right]\left[f_{s-m}(\tfrac{1}{2},0)+f_{s+m}(\tfrac{1}{2},0)\right]\right\}$$

$$-\alpha^2\sigma^2\sin^2\sigma t\left\{E(1,0)f_s(1,0)+\sum_{m=1}^{\infty}E(1,m)\left[f_{s-m}(1,0)+f_{s+m}(1,0)\right]\right\} \tag{D.2}$$

Coefficients of Cos θx Cos ℓy:

$$\frac{C_0}{2} = 2\sum_{n=0}^{\infty}\dot{b}_n E(n,n)f_0(n,1) + 2\sum_{m=1}^{\infty}\sum_{n=0}^{\infty}\dot{b}_n[E(n,m-n)+E(n,m+n)]f_m(n,1)$$

$$+\sum_{n=0}^{\infty}\dot{d}_n E(\nu_n,n)[f_0(\nu_n,0)+f_0(\nu_n,2)] + \sum_{m=1}^{\infty}\sum_{n=0}^{\infty}\dot{d}_n[E(\nu_n,m-n)+E(\nu_n,m+n)][f_m(\nu_n,0)+f_m(\nu_n,2)]$$

$$-\sum_{m=0}^{\infty}\sum_{n=0}^{\infty}mn\,b_m b_n E(m+n,m-n)f_0(m+n,1) - \sum_{m=0}^{\infty}\sum_{n=0}^{\infty}\sum_{p=1}^{\infty}mn\,b_m b_n[E(m+n,p-m-n)+E(m+n,p+m+n)]f_p(m+n,1)$$

$$+\frac{1}{8}\sum_{m=0}^{\infty}\sum_{n=0}^{\infty}mn\,d_m d_n[E(\nu_m+\nu_n,m+n)-E(\nu_m+\nu_n,m-n)][3f_0(\nu_m+\nu_n,1)+f_0(\nu_m+\nu_n,3)]$$

$$+\frac{1}{8}\sum_{m=0}^{\infty}\sum_{n=0}^{\infty}\sum_{p=1}^{\infty}mn\,d_m d_n[E(\nu_m+\nu_n,p-m-n)+E(\nu_m+\nu_n,p+m+n)-E(\nu_m+\nu_n,p+m-n)-E(\nu_m+\nu_n,p-m+n)]$$
$$[3f_p(\nu_m+\nu_n,1)+f_p(\nu_m+\nu_n,3)]$$

$$-\frac{\theta^2}{8}\sum_{m=0}^{\infty}\sum_{n=0}^{\infty}d_m d_n[E(\nu_m+\nu_n,m+n)+E(\nu_m+\nu_n,m-n)][f_0(\nu_m+\nu_n,1)-f_0(\nu_m+\nu_n,3)]$$

$$-\frac{\theta^2}{8}\sum_{m=0}^{\infty}\sum_{n=0}^{\infty}\sum_{p=1}^{\infty}d_m d_n[E(\nu_m+\nu_n,p+m+n)+E(\nu_m+\nu_n,p-m-n)+E(\nu_m+\nu_n,p+m-n)+E(\nu_m+\nu_n,p-m+n)]$$
$$[f_p(\nu_m+\nu_n,1)-f_p(\nu_m+\nu_n,3)]$$

$$-\frac{1}{8}\sum_{m=0}^{\infty}\sum_{n=0}^{\infty}\nu_m\nu_n d_m d_n[E(\nu_m+\nu_n,m+n)+E(\nu_m+\nu_n,m-n)][3f_0(\nu_m+\nu_n,1)+f_0(\nu_m+\nu_n,3)]$$

$$-\frac{1}{8}\sum_{m=0}^{\infty}\sum_{n=0}^{\infty}\sum_{p=1}^{\infty}\nu_m\nu_n d_m d_n[E(\nu_m+\nu_n,p-m-n)+E(\nu_m+\nu_n,p+m+n)+E(\nu_m+\nu_n,p+m-n)+E(\nu_m+\nu_n,p-m+n)]$$
$$[3f_p(\nu_m+\nu_n,1)+f_p(\nu_m+\nu_n,3)]$$

$$+\frac{1}{2}\sum_{m=0}^{\infty}\sum_{n=0}^{\infty}mn\,b_m d_n[E(m+\nu_n,m+n)-E(m+\nu_n,m-n)][f_0(m+\nu_n,0)+f_0(m+\nu_n,2)]$$

$$+\frac{1}{2}\sum_{m=0}^{\infty}\sum_{n=0}^{\infty}\sum_{p=1}^{\infty}mn\,b_m d_n[E(m+\nu_n,p-m-n)+E(m+\nu_n,p+m+n)-E(m+\nu_n,p+m-n)-E(m+\nu_n,p-m+n)]$$
$$[f_p(m+\nu_n,0)+f_p(m+\nu_n,2)]$$

$$-\frac{1}{2}\sum_{m=0}^{\infty}\sum_{n=0}^{\infty}m\nu_n b_m d_n[E(m+\nu_n,m+n)+E(m+\nu_n,m-n)][f_0(m+\nu_n,0)+f_0(m+\nu_n,2)]$$

$$-\frac{1}{2}\sum_{m=0}^{\infty}\sum_{n=0}^{\infty}\sum_{p=1}^{\infty}m\nu_n b_m d_n[E(m+\nu_n,p-m-n)+E(m+\nu_n,p+m+n)+E(m+\nu_n,p+m+n)+E(m+\nu_n,p-m-n)]$$
$$[f_p(m+\nu_n,0)+f_p(m+\nu_n,2)]$$

$$+\frac{2d\sigma}{\pi}\sin\sigma t\left\{\sum_{m=0}^{\infty}\sum_{n=0}^{\infty}\frac{4mn\,b_n}{4m^2-1}[E(n+\tfrac{1}{2},m-n)-E(n+\tfrac{1}{2},m+n)]f_0(n+\tfrac{1}{2},1)\right.$$

$$+\sum_{m=0}^{\infty}\sum_{n=0}^{\infty}\sum_{p=1}^{\infty}\frac{4mn\,b_n}{4m^2-1}[E(n+\tfrac{1}{2},p-m+n)+E(n+\tfrac{1}{2},p+m-n)-E(n+\tfrac{1}{2},p-m-n)-E(n+\tfrac{1}{2},p+m+n)]$$
$$f_p(n+\tfrac{1}{2},1)$$

$$+\sum_{m=0}^{\infty}\sum_{n=0}^{\infty}\frac{2mn\,d_n}{4m^2-1}[E(\nu_n+\tfrac{1}{2},m-n)-E(\nu_n+\tfrac{1}{2},m+n)][f_0(\nu_n+\tfrac{1}{2},0)+f_0(\nu_n+\tfrac{1}{2},2)]$$

$$+\sum_{m=0}^{\infty}\sum_{n=0}^{\infty}\sum_{p=1}^{\infty}\frac{2mn\,d_n}{4m^2-1}[E(\nu_n+\tfrac{1}{2},p-m+n)+E(\nu_n+\tfrac{1}{2},p+m-n)-E(\nu_n+\tfrac{1}{2},p+m+n)-E(\nu_n+\tfrac{1}{2},p-m-n)]$$
$$\left.[f_p(\nu_n+\tfrac{1}{2},0)+f_p(\nu_n+\tfrac{1}{2},2)]\right.$$

$$-\sum_{n=0}^{\infty} 2nb_n E(n+\tfrac{1}{2},n) f_0(n+\tfrac{1}{2},1) - \sum_{m=1}^{\infty}\sum_{n=0}^{\infty} 2nb_n \left[E(n+\tfrac{1}{2},m-n)+E(n+\tfrac{1}{2},m+n)\right] f_m(n+\tfrac{1}{2},1)$$

$$+\sum_{m=1}^{\infty}\sum_{n=0}^{\infty} \frac{2nb_n}{4m^2-1}\left[E(n+\tfrac{1}{2},m+n)+E(n+\tfrac{1}{2},m-n)\right] f_0(n+\tfrac{1}{2},1)$$

$$+\sum_{m=1}^{\infty}\sum_{n=0}^{\infty}\sum_{p=1}^{\infty} \frac{2nb_n}{4m^2-1}\left[E(n+\tfrac{1}{2},p-m-n)+E(n+\tfrac{1}{2},p+m+n)+E(n+\tfrac{1}{2},p-m+n)+E(n+\tfrac{1}{2},p+m-n)\right] f_p(n+\tfrac{1}{2},1)$$

$$-\sum_{n=0}^{\infty} \mathcal{U}_n d_n E(\mathcal{U}_n+\tfrac{1}{2},n)\left[f_0(\mathcal{U}_n+\tfrac{1}{2},0)+f_0(\mathcal{U}_n+\tfrac{1}{2},2)\right] - \sum_{m=1}^{\infty}\sum_{n=0}^{\infty} \mathcal{U}_n d_n \left[E(\mathcal{U}_n+\tfrac{1}{2},m-n)+E(\mathcal{U}_n+\tfrac{1}{2},m+n)\right]$$
$$\left[f_m(\mathcal{U}_n+\tfrac{1}{2},0)+f_m(\mathcal{U}_n+\tfrac{1}{2},2)\right]$$

$$+\sum_{m=1}^{\infty}\sum_{n=0}^{\infty} \frac{\mathcal{U}_n d_n}{4m^2-1}\left[E(\mathcal{U}_n+\tfrac{1}{2},m+n)+E(\mathcal{U}_n+\tfrac{1}{2},m-n)\right]\left[f_0(\mathcal{U}_n+\tfrac{1}{2},0)+f_0(\mathcal{U}_n+\tfrac{1}{2},2)\right]$$

$$+\sum_{m=1}^{\infty}\sum_{n=0}^{\infty}\sum_{p=1}^{\infty} \frac{\mathcal{U}_n d_n}{4m^2-1}\left[E(\mathcal{U}_n+\tfrac{1}{2},p-m-n)+E(\mathcal{U}_n+\tfrac{1}{2},p+m+n)+E(\mathcal{U}_n+\tfrac{1}{2},p-m+n)+E(\mathcal{U}_n+\tfrac{1}{2},p+m-n)\right]$$
$$\left[f_p(\mathcal{U}_n+\tfrac{1}{2},0)+f_p(\mathcal{U}_n+\tfrac{1}{2},2)\right] \Big\}$$

$$-\frac{8\alpha\sigma^2}{\pi}\cos\sigma t\Big\{\sum_{n=1}^{\infty}\frac{1}{4n^2-1}E(\tfrac{1}{2},n)f_0(\tfrac{1}{2},1)+\sum_{m=1}^{\infty}\sum_{n=1}^{\infty}\frac{1}{4n^2-1}\left[E(\tfrac{1}{2},m+n)+E(\tfrac{1}{2},m-n)\right]f_m(\tfrac{1}{2},1)$$

$$-E(\tfrac{1}{2},0)f_0(\tfrac{1}{2},1)-\sum_{m=1}^{\infty}2E(\tfrac{1}{2},m)f_m(\tfrac{1}{2},1)\Big\}$$

$$-\alpha^2\sigma^2\sin^2\sigma t\Big\{E(1,0)f_0(1,1)+\sum_{m=1}^{\infty}E(1,m)f_m(1,1)\Big\} \tag{D.3}$$

Coefficients of $\cos sx \cos \ell y$, for $s\geq 1$:

$$C_s = 4\sum_{n=0}^{\infty} \dot{b}_n E(n,n) f_s(n,1) + 2\sum_{m=1}^{\infty}\sum_{n=0}^{\infty} \dot{b}_n \left[E(n,m-n)+E(n,m+n)\right]\left[f_{s-m}(n,1)+f_{s+m}(n,1)\right]$$

$$+2\sum_{n=0}^{\infty}\dot{d}_n E(\mathcal{U}_n,n)\left[f_s(\mathcal{U}_n,0)+f_s(\mathcal{U}_n,2)\right] - 2\sum_{m=0}^{\infty}\sum_{n=0}^{\infty} mn\, b_m b_n E(m+n,m-n) f_s(m+n,1)$$

$$+\sum_{m=1}^{\infty}\sum_{n=0}^{\infty} \dot{d}_n \left[E(\mathcal{U}_n,m-n)+E(\mathcal{U}_n,m+n)\right]\left[f_{s-m}(\mathcal{U}_n,0)+f_{s+m}(\mathcal{U}_n,0)+f_{s-m}(\mathcal{U}_n,2)+f_{s+m}(\mathcal{U}_n,2)\right]$$

$$-\sum_{m=0}^{\infty}\sum_{n=0}^{\infty}\sum_{p=1}^{\infty} mn\, b_m b_n \left[E(m+n,p-m+n)+E(m+n,p+m-n)\right]\left[f_{s-p}(m+n,1)+f_{s+p}(m+n,1)\right]$$

$$+\frac{1}{4}\sum_{m=0}^{\infty}\sum_{n=0}^{\infty} mn\, d_m d_n \left[E(\mathcal{U}_m+\mathcal{U}_n,m+n)-E(\mathcal{U}_m+\mathcal{U}_n,m-n)\right]\left[3f_s(\mathcal{U}_m+\mathcal{U}_n,1)+f_s(\mathcal{U}_m+\mathcal{U}_n,3)\right]$$

$$+\frac{1}{8}\sum_{m=0}^{\infty}\sum_{n=0}^{\infty}\sum_{p=1}^{\infty} mn\, d_m d_n \left[E(\mathcal{U}_m+\mathcal{U}_n,p-m-n)+E(\mathcal{U}_m+\mathcal{U}_n,p+m+n)-E(\mathcal{U}_m+\mathcal{U}_n,p-m+n)-E(\mathcal{U}_m+\mathcal{U}_n,p+m-n)\right]$$
$$\left[3f_{s-p}(\mathcal{U}_m+\mathcal{U}_n,1)+3f_{s+p}(\mathcal{U}_m+\mathcal{U}_n,1)+f_{s-p}(\mathcal{U}_m+\mathcal{U}_n,3)+f_{s+p}(\mathcal{U}_m+\mathcal{U}_n,3)\right]$$

$$-\frac{\ell^2}{4}\sum_{m=0}^{\infty}\sum_{n=0}^{\infty} d_m d_n \left[E(\mathcal{U}_m+\mathcal{U}_n,m+n)+E(\mathcal{U}_m+\mathcal{U}_n,m-n)\right]\left[f_s(\mathcal{U}_m+\mathcal{U}_n,1)-f_s(\mathcal{U}_m+\mathcal{U}_n,3)\right]$$

$$-\frac{\ell^2}{8}\sum_{m=0}^{\infty}\sum_{n=0}^{\infty}\sum_{p=1}^{\infty} d_m d_n \left[E(\mathcal{U}_m+\mathcal{U}_n,p-m-n)+E(\mathcal{U}_m+\mathcal{U}_n,p+m+n)+E(\mathcal{U}_m+\mathcal{U}_n,p-m+n)+E(\mathcal{U}_m+\mathcal{U}_n,p+m-n)\right]$$
$$\left[f_{s-p}(\mathcal{U}_m+\mathcal{U}_n,1)+f_{s-p}(\mathcal{U}_m+\mathcal{U}_n,1)-f_{s-p}(\mathcal{U}_m+\mathcal{U}_n,3)-f_{s-p}(\mathcal{U}_m+\mathcal{U}_n,3)\right]$$

$$-\frac{1}{4}\sum_{m=0}^{\infty}\sum_{n=0}^{\infty}v_m v_n d_m d_n \left[E(v_m+v_n, m+n)+E(v_m+v_n, m-n)\right]\left[3f_s(v_m+v_n,1)+f_s(v_m+v_n,3)\right]$$

$$-\frac{1}{8}\sum_{m=0}^{\infty}\sum_{n=0}^{\infty}\sum_{p=1}^{\infty}v_m v_n d_m d_n \left[E(v_m+v_n, p-m-n)+E(v_m+v_n, p+m+n)+E(v_m+v_n, p-m+n)+E(v_m+v_n, p+m-n)\right]$$
$$\left[3f_{s-p}(v_m+v_n,1)+3f_{s+p}(v_m+v_n,1)+f_{s-p}(v_m+v_n,3)+f_{s+p}(v_m+v_n,3)\right]$$

$$+\sum_{m=0}^{\infty}\sum_{n=0}^{\infty}mn\, d_m d_n \left[E(m+v_n, m+n)-E(m+v_n, m-n)\right]\left[f_s(m+v_n,0)+f_s(m+v_n,2)\right]$$

$$+\frac{1}{2}\sum_{m=0}^{\infty}\sum_{n=0}^{\infty}\sum_{p=1}^{\infty}mn\, d_m d_n \left[E(m+v_n, p-m-n)+E(m+v_n, p+m+n)-E(m+v_n, p-m+n)-E(m+v_n, p+m-n)\right]$$
$$\left[f_{s-p}(m+v_n,0)+f_{s+p}(m+v_n,0)+f_{s-p}(m+v_n,2)+f_{s+p}(m+v_n,2)\right]$$

$$-\sum_{m=0}^{\infty}\sum_{n=0}^{\infty}m v_n b_m d_n \left[E(m+v_n, m+n)+E(m+v_n, m-n)\right]\left[f_s(m+v_n,0)+f_s(m+v_n,2)\right]$$

$$-\frac{1}{2}\sum_{m=0}^{\infty}\sum_{n=0}^{\infty}\sum_{p=1}^{\infty}m v_n b_m d_n \left[E(m+v_n, p-m-n)+E(m+v_n, p+m+n)+E(m+v_n, p-m+n)+E(m+v_n, p+m-n)\right]$$
$$\left[f_{s-p}(m+v_n,0)+f_{s+p}(m+v_n,0)+f_{s-p}(m+v_n,2)+f_{s+p}(m+v_n,2)\right]$$

$$+\frac{2\alpha_0}{\pi}\sin\alpha t\left\{\sum_{m=0}^{\infty}\sum_{n=0}^{\infty}\frac{8mn\,b_n}{4m^2-1}\left[E(n+\tfrac{1}{2}, m-n)-E(n+\tfrac{1}{2}, m-n)\right]f_s(n+\tfrac{1}{2},1)\right.$$

$$+\sum_{m=0}^{\infty}\sum_{n=0}^{\infty}\sum_{p=1}^{\infty}\frac{4mn\,b_n}{4m^2-1}\left[E(n+\tfrac{1}{2}, p-m+n)+E(n+\tfrac{1}{2}, p+m-n)-E(n+\tfrac{1}{2}, p-m-n)-E(n+\tfrac{1}{2}, p+m+n)\right]$$
$$\left[f_{s-p}(n+\tfrac{1}{2},1)+f_{s+p}(n+\tfrac{1}{2},1)\right]$$

$$+\sum_{m=0}^{\infty}\sum_{n=0}^{\infty}\frac{4mn\,d_n}{4m^2-1}\left[E(v_n+\tfrac{1}{2}, m-n)-E(v_n+\tfrac{1}{2}, m+n)\right]\left[f_s(v_n+\tfrac{1}{2},0)+f_s(v_n+\tfrac{1}{2},2)\right]$$

$$+\sum_{m=0}^{\infty}\sum_{n=0}^{\infty}\sum_{p=1}^{\infty}\frac{2mn\,d_n}{4m^2-1}\left[E(v_n+\tfrac{1}{2}, p-m-n)+E(v_n+\tfrac{1}{2}, p+m+n)-E(v_n+\tfrac{1}{2}, p-m+n)-E(v_n+\tfrac{1}{2}, p+m+n)\right]$$
$$\left[f_{s-p}(v_n+\tfrac{1}{2},0)+f_{s+p}(v_n+\tfrac{1}{2},0)+f_{s-p}(v_n+\tfrac{1}{2},2)+f_{s+p}(v_n+\tfrac{1}{2},2)\right]$$

$$-\sum_{n=0}^{\infty}4n b_n E(n+\tfrac{1}{2}, n)f_s(n+\tfrac{1}{2},1)+\sum_{m=1}^{\infty}\sum_{n=0}^{\infty}\frac{4n b_n}{4m^2-1}\left[E(n+\tfrac{1}{2}, m+n)+E(n+\tfrac{1}{2}, m-n)\right]f_s(n+\tfrac{1}{2},1)$$

$$-\sum_{m=1}^{\infty}\sum_{n=0}^{\infty}2n b_n \left[E(n+\tfrac{1}{2}, m-n)+E(n+\tfrac{1}{2}, m+n)\right]\left[f_{s-m}(n+\tfrac{1}{2},1)+f_{s+m}(n+\tfrac{1}{2},1)\right]$$

$$+\sum_{m=1}^{\infty}\sum_{n=0}^{\infty}\sum_{p=1}^{\infty}\frac{2n b_n}{4m^2-1}\left[E(n+\tfrac{1}{2}, p-m-n)+E(n+\tfrac{1}{2}, p+m+n)+E(n+\tfrac{1}{2}, p-m+n)+E(n+\tfrac{1}{2}, p+m-n)\right]$$
$$\left[f_{s-p}(n+\tfrac{1}{2},1)+f_{s+p}(n+\tfrac{1}{2},1)\right]$$

$$-\sum_{n=0}^{\infty}2v_n d_n E(v_n+\tfrac{1}{2}, n)\left[f_s(v_n+\tfrac{1}{2},0)+f_s(v_n+\tfrac{1}{2},2)\right]$$

$$-\sum_{m=1}^{\infty}\sum_{n=0}^{\infty}v_n d_n \left[E(v_n+\tfrac{1}{2}, m-n)+E(v_n+\tfrac{1}{2}, m+n)\right]\left[f_{s-m}(v_n+\tfrac{1}{2},0)+f_{s+m}(v_n+\tfrac{1}{2},0)\right.$$
$$\left.+f_{s-m}(v_n+\tfrac{1}{2},2)+f_{s+m}(v_n+\tfrac{1}{2},2)\right]$$

$$+\sum_{m=1}^{\infty}\sum_{n=0}^{\infty}\frac{2v_n d_n}{4m^2-1}\left[E(v_n+\tfrac{1}{2}, m+n)+E(v_n+\tfrac{1}{2}, m-n)\right]\left[f_s(v_n+\tfrac{1}{2},0)+f_s(v_n+\tfrac{1}{2},2)\right]$$

$$+ \sum_{m=1}^{\infty}\sum_{n=0}^{\infty}\sum_{p=1}^{\infty} \frac{\nu_n d_n}{4m^2-1}\left[E(\nu_n+\tfrac{1}{2},p-m-n)+E(\nu_n+\tfrac{1}{2},p+m+n)+E(\nu_n+\tfrac{1}{2},p-m+n)+E(\nu_n+\tfrac{1}{2},p+m-n)\right]$$

$$\left[f_{s-p}(\nu_n+\tfrac{1}{2},0)+f_{s+p}(\nu_n+\tfrac{1}{2},0)+f_{s-p}(\nu_n+\tfrac{1}{2},2)+f_{s+p}(\nu_n+\tfrac{1}{2},2)\right]\Big\}$$

$$-\frac{8\alpha\sigma^2}{\pi}\cos\sigma t\left\{\sum_{n=1}^{\infty}\frac{2}{4n^2-1}E(\tfrac{1}{2},n)f_s(\tfrac{1}{2},1)+\sum_{m=1}^{\infty}\sum_{n=1}^{\infty}\frac{1}{4n^2-1}\left[E(\tfrac{1}{2},m+n)+E(\tfrac{1}{2},m-n)\right]\left[f_{s-m}(\tfrac{1}{2},1)+f_{s+m}(\tfrac{1}{2},1)\right]\right.$$

$$\left.-2E(\tfrac{1}{2},0)f_s(\tfrac{1}{2},1)-\sum_{m=1}^{\infty}2E(\tfrac{1}{2},m)\left[f_{s-m}(\tfrac{1}{2},1)+f_{s+m}(\tfrac{1}{2},1)\right]\right\}$$

$$-2\alpha^2\sigma^2\sin^2\sigma t\left\{E(1,0)f_s(1,1)+\sum_{m=1}^{\infty}E(1,m)\left[f_{s-m}(1,1)+f_{s+m}(1,1)\right]\right\}\Big\} \qquad (D.4)$$

Coefficients of Cos 0x Cos 0 ℓ y:

$$\frac{\dot{a}_0}{2}=\frac{1}{2}\sum_{m=0}^{\infty}\sum_{n=0}^{\infty}mn\,a_m b_n\left[E(n,m-n)-E(n,m+n)\right]f_0(n,0)$$

$$+\frac{1}{2}\sum_{m=0}^{\infty}\sum_{n=0}^{\infty}\sum_{p=1}^{\infty}mn\,a_m b_n\left[E(n,p-m+n)+E(n,p+m-n)-E(n,p-m-n)-E(n,p+m+n)\right]f_p(n,0)$$

$$+\frac{1}{2}\sum_{m=0}^{\infty}\sum_{n=0}^{\infty}mn\,C_m b_n\left[E(n,m-n)-E(n,m+n)\right]f_0(n,1)$$

$$+\frac{1}{2}\sum_{m=0}^{\infty}\sum_{n=0}^{\infty}\sum_{p=1}^{\infty}mn\,C_m b_n\left[E(n,p-m+n)+E(n,p+m+n)-E(n,p-m-n)-E(n,p+m+n)\right]f_p(n,1)$$

$$+\frac{1}{2}\sum_{m=0}^{\infty}\sum_{n=0}^{\infty}mn\,a_m d_n\left[E(\nu_n,m-n)-E(\nu_n,m+n)\right]f_0(\nu_n,1)$$

$$+\frac{1}{2}\sum_{m=0}^{\infty}\sum_{n=0}^{\infty}\sum_{p=1}^{\infty}mn\,a_m d_n\left[E(\nu_n,p-m+n)+E(\nu_n,p+m-n)-E(\nu_n,p-m-n)-E(\nu_n,p+m+n)\right]f_p(\nu_n,1)$$

$$+\frac{1}{4}\sum_{m=0}^{\infty}\sum_{n=0}^{\infty}mn\,C_m d_n\left[E(\nu_n,m-n)-E(\nu_n,m+n)\right]\left[f_0(\nu_n,0)+f_0(\nu_n,2)\right]$$

$$+\frac{1}{4}\sum_{m=0}^{\infty}\sum_{n=0}^{\infty}\sum_{p=1}^{\infty}mn\,C_m d_n\left[E(\nu_n,p-m+n)+E(\nu_n,p+m-n)-E(\nu_n,p-m-n)-E(\nu_n,p+m+n)\right]$$
$$\left[f_p(\nu_n,0)+f_p(\nu_n,2)\right]$$

$$+\frac{l^2 C_0}{4}\sum_{n=0}^{\infty}d_n E(\nu_n,n)\left[f_0(\nu_n,0)-f_0(\nu_n,2)\right]$$

$$+\frac{l^2 C_0}{4}\sum_{m=1}^{\infty}\sum_{n=0}^{\infty}d_n\left[E(\nu_n,m-n)+E(\nu_n,m+n)\right]\left[f_m(\nu_n,0)-f_m(\nu_n,2)\right]$$

$$+\frac{l^2}{4}\sum_{m=1}^{\infty}\sum_{n=0}^{\infty}C_m d_n\left[E(\nu_n,m+n)+E(\nu_n,m-n)\right]\left[f_0(\nu_n,0)-f_0(\nu_n,2)\right]$$

$$+\frac{l^2}{4}\sum_{m=1}^{\infty}\sum_{n=0}^{\infty}\sum_{p=1}^{\infty}C_m d_n\left[E(\nu_n,p-m+n)+E(\nu_n,p+m+n)+E(\nu_n,p-m-n)+E(\nu_n,p+m+n)\right]$$
$$\left[f_p(\nu_n,0)-f_p(\nu_n,2)\right]$$

$$-\sum_{n=0}^{\infty}n b_n E(n,n)f_0(n,0)-\sum_{m=1}^{\infty}\sum_{n=0}^{\infty}\nu_n d_n\left[E(\nu_n,m-n)+E(\nu_n,m+n)\right]f_m(n,0)$$

$$-\sum_{n=0}^{\infty}\nu_n d_n E(\nu_n,n)f_0(\nu_n,1)-\sum_{m=1}^{\infty}\sum_{n=0}^{\infty}\nu_n d_n\left[E(\nu_n,m-n)+E(\nu_n,m+n)\right]f_m(\nu_n,1)$$

$$+\frac{4\alpha\sigma}{\pi}\sin\sigma t\left\{\sum_{m=0}^{\infty}\sum_{n=0}^{\infty}\frac{mn\,a_n}{4m^2-1}\left[E(\tfrac{1}{2},m+n)-E(\tfrac{1}{2},m-n)\right]f_0(\tfrac{1}{2},0)+\sum_{m=0}^{\infty}\sum_{n=0}^{\infty}\frac{mn\,C_n}{4m^2-1}\left[E(\tfrac{1}{2},m+n)-E(\tfrac{1}{2},m-n)\right]f_0(\tfrac{1}{2},1)\right.$$

$$\left.+\sum_{m=0}^{\infty}\sum_{n=0}^{\infty}\sum_{p=1}^{\infty}\frac{mn\,a_n}{4m^2-1}\left[E(\tfrac{1}{2},p-m-n)+E(\tfrac{1}{2},p+m+n)-E(\tfrac{1}{2},p-m+n)-E(\tfrac{1}{2},p+m-n)\right]f_p(\tfrac{1}{2},0)\right.$$

-104-

$$+ \sum_{m=0}\sum_{n=0}\sum_{p=1} \frac{mnC_n}{4m^2-1}\left[E(\tfrac{1}{2},p-m-n)+E(\tfrac{1}{2},p+m+n)-E(\tfrac{1}{2},p-m+n)-E(\tfrac{1}{2},p+m-n)\right]f_p(\tfrac{1}{2},1)$$

$$-\tfrac{1}{2}E(\tfrac{1}{2},0)f_0(\tfrac{1}{2},0)-\sum_{m=1}^{\infty}E(\tfrac{1}{2},m)f_m(\tfrac{1}{2},0)+\sum_{n=1}^{\infty}\frac{1}{4n^2-1}E(\tfrac{1}{2},n)f_0(\tfrac{1}{2},0)$$

$$+\sum_{m=1}^{\infty}\sum_{n=1}^{\infty}\frac{1}{4n^2-1}\left[E(\tfrac{1}{2},m+n)+E(\tfrac{1}{2},m-n)\right]f_m(\tfrac{1}{2},0)\Big\} \tag{D.5}$$

Coefficients of $\cos sx \cos 0\, \ell y$, for $s \ge 1$:

$$\dot{a}_s = \sum_{m=0}^{\infty}\sum_{n=0}^{\infty} mn\, a_m b_n \left[E(n,m-n)-E(n,m+n)\right]f_s(n,0)$$

$$+\tfrac{1}{2}\sum_{m=0}^{\infty}\sum_{n=0}^{\infty}\sum_{p=1}^{\infty} mn\, a_m b_n\left[E(n,p-m+n)+E(n,p+m-n)-E(n,p-m-n)-E(n,p+m+n)\right]$$
$$\left[f_{s-p}(n,0)+f_{s+p}(n,0)\right]$$

$$+\sum_{m=0}^{\infty}\sum_{n=0}^{\infty} mn\, C_m b_n\left[E(n,m-n)-E(n,m+n)\right]f_s(n,1)$$

$$+\tfrac{1}{2}\sum_{m=0}^{\infty}\sum_{n=0}^{\infty}\sum_{p=1}^{\infty} mn\, C_m b_n\left[E(n,p-m+n)+E(n,p+m-n)-E(n,p-m-n)-E(n,p+m+n)\right]$$
$$\left[f_{s-p}(n,1)+f_{s+p}(n,1)\right]$$

$$+\sum_{m=0}^{\infty}\sum_{n=0}^{\infty} mn\, a_m d_n\left[E(\nu_n,m-n)-E(\nu_n,m+n)\right]f_s(\nu_n,1)$$

$$+\tfrac{1}{2}\sum_{m=0}^{\infty}\sum_{n=0}^{\infty}\sum_{p=1}^{\infty} mn\, a_m d_n\left[E(\nu_n,p-m+n)+E(\nu_n,p+m-n)-E(\nu_n,p-m-n)-E(\nu_n,p+m+n)\right]$$
$$\left[f_{s-p}(\nu_n,1)+f_{s+p}(\nu_n,1)\right]$$

$$+\tfrac{1}{2}\sum_{m=0}^{\infty}\sum_{n=0}^{\infty} mn\, C_m d_n\left[E(\nu_n,m-n)-E(\nu_n,m+n)\right]\left[f_s(\nu_n,0)+f_s(\nu_n,2)\right]$$

$$+\tfrac{1}{4}\sum_{m=0}^{\infty}\sum_{n=0}^{\infty}\sum_{p=1}^{\infty} mn\, C_m d_n\left[E(\nu_n,p-m+n)+E(\nu_n,p+m-n)-E(\nu_n,p-m-n)-E(\nu_n,p+m+n)\right]$$
$$\left[f_{s-p}(\nu_n,0)+f_{s+p}(\nu_n,0)+f_{s-p}(\nu_n,2)+f_{s+p}(\nu_n,2)\right]$$

$$+\frac{\ell^2 C_0}{2}\sum_{n=0}^{\infty} d_n E(\nu_n,n)\left[f_s(\nu_n,0)-f_s(\nu_n,2)\right]$$

$$+\frac{\ell^2 C_0}{4}\sum_{m=1}^{\infty}\sum_{n=0}^{\infty} d_n\left[E(\nu_n,m-n)+E(\nu_n,m+n)\right]\left[f_{s-m}(\nu_n,0)+f_{s+m}(\nu_n,0)-f_{s-m}(\nu_n,2)-f_{s+m}(\nu_n,2)\right]$$

$$+\frac{\ell^2}{2}\sum_{m=1}^{\infty}\sum_{n=0}^{\infty} C_m d_n\left[E(\nu_n,m+n)+E(\nu_n,m-n)\right]\left[f_s(\nu_n,0)-f_s(\nu_n,2)\right]$$

$$+\frac{\ell^2}{4}\sum_{m=1}^{\infty}\sum_{n=0}^{\infty}\sum_{p=1}^{\infty} C_m d_n\left[E(\nu_n,p-m-n)+E(\nu_n,p+m+n)+E(\nu_n,p-m+n)+E(\nu_n,p+m-n)\right]$$
$$\left[f_{s-p}(\nu_n,0)+f_{s+p}(\nu_n,0)-f_{s-p}(\nu_n,2)-f_{s+p}(\nu_n,2)\right]$$

$$-2\sum_{n=0}^{\infty} n b_n E(n,n) f_s(n,0)-\sum_{m=1}^{\infty}\sum_{n=0}^{\infty} n b_n\left[E(n,m-n)+E(n,m+n)\right]\left[f_{s-m}(n,0)+f_{s+m}(n,0)\right]$$

$$-2\sum_{n=0}^{\infty}\nu_n d_n E(\nu_n,n) f_s(\nu_n,1)-\sum_{m=1}^{\infty}\sum_{n=0}^{\infty}\nu_n d_n\left[E(\nu_n,m-n)+E(\nu_n,m+n)\right]\left[f_{s-m}(\nu_n,1)+f_{s+m}(\nu_n,1)\right]$$

-105-

$$+ \frac{400}{\pi} \sin \alpha t \left\{ \sum_{m=0}^{\infty} \sum_{n=0}^{\infty} \frac{2mn a_n}{4m^2-1} \left[E(\tfrac{1}{2}, m+n) - E(\tfrac{1}{2}, m-n) \right] f_s(\tfrac{1}{2}, 0) \right.$$

$$+ \sum_{m=0}^{\infty} \sum_{n=0}^{\infty} \sum_{p=1}^{\infty} \frac{mn a_n}{4m^2-1} \left[E(\tfrac{1}{2}, p-m-n) + E(\tfrac{1}{2}, p+m+n) - E(\tfrac{1}{2}, p-m+n) - E(\tfrac{1}{2}, p+m-n) \right]$$

$$\left[f_{s-p}(\tfrac{1}{2}, 0) + f_{s+p}(\tfrac{1}{2}, 0) \right]$$

$$+ \sum_{m=0}^{\infty} \sum_{n=0}^{\infty} \frac{2mn C_n}{4m^2-1} \left[E(\tfrac{1}{2}, m+n) - E(\tfrac{1}{2}, m-n) \right] f_s(\tfrac{1}{2}, 1)$$

$$+ \sum_{m=0}^{\infty} \sum_{n=0}^{\infty} \sum_{p=1}^{\infty} \frac{mn C_n}{4m^2-1} \left[E(\tfrac{1}{2}, p-m-n) + E(\tfrac{1}{2}, p+m+n) - E(\tfrac{1}{2}, p-m+n) - E(\tfrac{1}{2}, p+m-n) \right]$$

$$\left[f_{s-p}(\tfrac{1}{2}, 1) + f_{s+p}(\tfrac{1}{2}, 1) \right]$$

$$- E(\tfrac{1}{2}, 0) f_s(\tfrac{1}{2}, 0) - \sum_{m=1}^{\infty} E(\tfrac{1}{2}, m) \left[f_{s-m}(\tfrac{1}{2}, 0) + f_{s+m}(\tfrac{1}{2}, 0) \right]$$

$$+ \sum_{n=1}^{\infty} \frac{2}{4n^2-1} E(\tfrac{1}{2}, n) f_s(\tfrac{1}{2}, 0) + \sum_{m=1}^{\infty} \sum_{n=1}^{\infty} \frac{1}{4n^2-1} \left[E(\tfrac{1}{2}, m-n) + E(\tfrac{1}{2}, m+n) \right] \left[f_{s-m}(\tfrac{1}{2}, 0) + f_{s+m}(\tfrac{1}{2}, 0) \right] \Bigg\}$$

$$(D.6)$$

Coefficients of Cos Ox Cos ly:

$$\frac{\dot{C}_0}{2} = \sum_{m=0}^{\infty} \sum_{n=0}^{\infty} mn b_n \left[E(n, m-n) - E(n, m+n) \right] \left\{ a_m f_0(n, 1) + \tfrac{1}{2} C_m \left[f_0(n, 0) + f_0(n, 2) \right] \right\}$$

$$+ \sum_{m=0}^{\infty} \sum_{n=0}^{\infty} \sum_{p=1}^{\infty} mn b_n \left[E(n, p-m+n) + E(n, p+m-n) - E(n, p-m-n) - E(n, p+m+n) \right]$$

$$\left\{ a_m f_p(n, 1) + \tfrac{1}{2} C_m \left[f_p(n, 0) + f_p(n, 2) \right] \right\}$$

$$+ \tfrac{1}{2} \sum_{m=0}^{\infty} \sum_{n=0}^{\infty} mn d_n \left[E(\nu_n, m-n) - E(\nu_n, m+n) \right] \left\{ a_m \left[f_0(\nu_n, 0) + f_0(\nu_n, 2) \right] + \tfrac{1}{2} C_m \left[3 f_0(\nu_n, 1) + f_0(\nu_n, 3) \right] \right\}$$

$$+ \tfrac{1}{2} \sum_{m=0}^{\infty} \sum_{n=0}^{\infty} \sum_{p=1}^{\infty} mn d_n \left[E(\nu_n, p-m+n) + E(\nu_n, p+m-n) - E(\nu_n, p-m-n) - E(\nu_n, p+m+n) \right]$$

$$\left\{ a_m \left[f_p(\nu_n, 0) + f_p(\nu_n, 2) \right] + \tfrac{1}{2} C_m \left[f_p(\nu_n, 1) + f_p(\nu_n, 3) \right] \right\}$$

$$+ \frac{l^2 C_0}{4} \sum_{n=0}^{\infty} d_n E(\nu_n, n) \left[f_0(\nu_n, 1) - f_0(\nu_n, 3) \right]$$

$$+ \frac{l^2 C_0}{4} \sum_{m=1}^{\infty} \sum_{n=0}^{\infty} d_n \left[E(\nu_n, m-n) + E(\nu_n, m+n) \right] \left[f_m(\nu_n, 1) - f_m(\nu_n, 3) \right]$$

$$+ \frac{l^2}{4} \sum_{m=1}^{\infty} \sum_{n=0}^{\infty} C_m d_n \left[E(\nu_n, m+n) + E(\nu_n, m-n) \right] \left[f_0(\nu_n, 1) - f_0(\nu_n, 3) \right]$$

$$+ \frac{l^2}{4} \sum_{m=1}^{\infty} \sum_{n=0}^{\infty} \sum_{p=1}^{\infty} C_m d_n \left[E(\nu_n, p-m-n) + E(\nu_n, p+m+n) + E(\nu_n, p-m+n) + E(\nu_n, p+m-n) \right]$$

$$\left[f_p(\nu_n, 1) - f_p(\nu_n, 3) \right]$$

$$- 2 \sum_{n=0}^{\infty} n b_n E(n, n) f_0(n, 1) - 2 \sum_{m=1}^{\infty} \sum_{n=0}^{\infty} n b_n \left[E(n, m-n) + (n, m+n) \right] f_m(n, 1)$$

$$-\sum_{n=0}^{\infty} \nu_n d_n \, E(\nu_n, n)\left[f_0(\nu_n, 0) + f_0(\nu_n, 2)\right]$$

$$-\sum_{m=1}^{\infty}\sum_{n=0}^{\infty} \nu_n d_n \left[E(\nu_n, m-n) + E(\nu_n, m+n)\right]\left[f_m(\nu_n, 0) + f_m(\nu_n, 2)\right]$$

$$+\frac{4\alpha\sigma}{\pi}\sin\omega t\left\{\sum_{m=0}^{\infty}\sum_{n=0}^{\infty}\frac{2mn a_n}{4m^2-1}\left[E(\tfrac{1}{2}, m+n) - E(\tfrac{1}{2}, m-n)\right]f_0(\tfrac{1}{2}, 1)\right.$$

$$+\sum_{m=0}^{\infty}\sum_{n=0}^{\infty}\sum_{p=1}^{\infty}\frac{2mn a_n}{4m^2-1}\left[E(\tfrac{1}{2}, p-m-n) + E(\tfrac{1}{2}, p+m+n) - E(\tfrac{1}{2}, p-m+n) - E(\tfrac{1}{2}, p+m-n)\right]$$
$$f_p(\tfrac{1}{2}, 1)$$

$$+\sum_{m=0}^{\infty}\sum_{n=0}^{\infty}\frac{mn C_n}{4m^2-1}\left[E(\tfrac{1}{2}, m+n) - E(\tfrac{1}{2}, m-n)\right]\left[f_0(\tfrac{1}{2}, 0) + f_0(\tfrac{1}{2}, 2)\right]$$

$$+\sum_{m=0}^{\infty}\sum_{n=0}^{\infty}\sum_{p=1}^{\infty}\frac{mn C_n}{4m^2-1}\left[E(\tfrac{1}{2}, p-m-n) + E(\tfrac{1}{2}, p+m+n) - E(\tfrac{1}{2}, p-m+n) - E(\tfrac{1}{2}, p+m-n)\right]$$
$$\left[f_p(\tfrac{1}{2}, 0) + f_p(\tfrac{1}{2}, 2)\right]$$

$$-E(\tfrac{1}{2}, 0)f_0(\tfrac{1}{2}, 1) - 2\sum_{m=1}^{\infty}E(\tfrac{1}{2}, m)f_m(\tfrac{1}{2}, 1) + \sum_{n=1}^{\infty}\frac{2}{4n^2-1}E(\tfrac{1}{2}, n)f_0(\tfrac{1}{2}, 1)$$

$$\left.+\sum_{m=1}^{\infty}\sum_{n=1}^{\infty}\frac{2}{4n^2-1}\left[E(\tfrac{1}{2}, m-n) + E(\tfrac{1}{2}, m+n)\right]f_m(\tfrac{1}{2}, 1)\right\}$$

$$\text{(D.7)}$$

Coefficients of Cos sx Cos ℓy, for $s \geq 1$:

$$\dot{C}_s = \sum_{m=0}^{\infty}\sum_{n=0}^{\infty} mn b_n \left[E(n, m-n) - E(n, m+n)\right]\left\{2a_m f_s(n, 1) + C_m\left[f_s(n, 0) + f_s(n, 2)\right]\right\}$$

$$+\frac{1}{2}\sum_{m=0}^{\infty}\sum_{n=0}^{\infty}\sum_{p=1}^{\infty} mn b_n \left[E(n, p-m+n) + E(n, p+m-n) - E(n, p-m-n) - E(n, p+m+n)\right]$$
$$\left\{2a_m\left[f_{s-p}(n, 1) + f_{s+p}(n, 1)\right] + C_m\left[f_{s-p}(n, 0) + f_{s+p}(n, 0) + f_{s-p}(n, 2) + f_{s+p}(n, 2)\right]\right\}$$

$$+\frac{1}{2}\sum_{m=0}^{\infty}\sum_{n=0}^{\infty} mn d_n \left[E(\nu_n, m-n) - E(\nu_n, m+n)\right]$$
$$\left\{2a_m\left[f_s(\nu_n, 0) + f_s(\nu_n, 2)\right] + C_m\left[3f_s(\nu_n, 1) + f_s(\nu_n, 3)\right]\right\}$$

$$+\frac{1}{4}\sum_{m=0}^{\infty}\sum_{n=0}^{\infty}\sum_{p=1}^{\infty} mn d_n \left[E(\nu_n, p-m+n) + E(\nu_n, p+m-n) - E(\nu_n, p-m-n) - E(\nu_n, p+m+n)\right]$$
$$\left\{2a_m\left[f_{s-p}(\nu_n, 0) + f_{s+p}(\nu_n, 0) + f_{s-p}(\nu_n, 2) + f_{s+p}(\nu_n, 2)\right]\right.$$
$$\left.+ C_m\left[3f_{s-p}(\nu_n, 1) + 3f_{s+p}(\nu_n, 1) + f_{s-p}(\nu_n, 3) + f_{s+p}(\nu_n, 3)\right]\right\}$$

$$+\frac{\ell^2 C_0}{2}\sum_{n=0}^{\infty} d_n E(\nu_n, n)\left[f_s(\nu_n, 1) - f_s(\nu_n, 3)\right]$$

$$+\frac{\ell^2 C_0}{4}\sum_{m=1}^{\infty}\sum_{n=0}^{\infty} d_n \left[E(\nu_n, m-n) - E(\nu_n, m+n)\right]\left[f_{s-m}(\nu_n, 1) + f_{s+m}(\nu_n, 1) - f_{s-m}(\nu_n, 3) - f_{s+m}(\nu_n, 3)\right]$$

$$+\frac{1}{2}\sum_{m=1}^{\infty}\sum_{n=0}^{\infty} c_m d_n \left[E(v_n, m+n) + E(v_n, m-n)\right]\left[f_s(v_n,1) - f_s(v_n,3)\right]$$

$$+\frac{1}{4}\sum_{m=1}^{\infty}\sum_{n=0}^{\infty}\sum_{p=1}^{\infty} c_m d_n \left[E(v_n, p-m-n) + E(v_n, p+m+n) + E(v_n, p-m+n) + E(v_n, p+m-n)\right]$$
$$\left[f_{s-p}(v_n,1) + f_{s+p}(v_n,1) + f_{s-p}(v_n,3) + f_{s+p}(v_n,3)\right]$$

$$-4\sum_{n=0}^{\infty} n b_n E(n,n) f_s(n,1) - 2\sum_{m=1}^{\infty}\sum_{n=0}^{\infty} n b_n \left[E(n,m-n)+E(n,m+n)\right]\left[f_{s-m}(n,1)+f_{s+m}(n,1)\right]$$

$$-2\sum_{n=0}^{\infty} v_n d_n E(v_n,n)\left[f_s(v_n,0)+f_s(v_n,2)\right] - \sum_{m=1}^{\infty}\sum_{n=0}^{\infty} v_n d_n \left[E(v_n,m-n)+E(v_n,m+n)\right]$$
$$\left[f_{s-m}(v_n,0)+f_{s+m}(v_n,0)+f_{s-m}(v_n,2)+f_{s+m}(v_n,2)\right]$$

$$+\frac{4\alpha\sigma}{\pi}\sin\omega t \left\{ \sum_{m=0}^{\infty}\sum_{n=0}^{\infty} \frac{4mn\, a_n}{4m^2-1}\left[E(\tfrac{1}{2}, m+n) - E(\tfrac{1}{2}, m-n)\right] f_s(\tfrac{1}{2},1)\right.$$

$$+ \sum_{m=0}^{\infty}\sum_{n=0}^{\infty}\sum_{p=1}^{\infty} \frac{2mn\, a_n}{4m^2-1}\left[E(\tfrac{1}{2}, p-m-n)+E(\tfrac{1}{2}, p+m+n)-E(\tfrac{1}{2}, p-m+n)-E(\tfrac{1}{2}, p+m-n)\right]$$
$$\left[f_{s-p}(\tfrac{1}{2},1) + f_{s+p}(\tfrac{1}{2},1)\right]$$

$$+ \sum_{m=0}^{\infty}\sum_{n=0}^{\infty} \frac{2mn\, c_n}{4m^2-1}\left[E(\tfrac{1}{2}, m+n)-E(\tfrac{1}{2}, m-n)\right]\left[f_s(\tfrac{1}{2},0)+f_s(\tfrac{1}{2},2)\right]$$

$$+ \sum_{m=0}^{\infty}\sum_{n=0}^{\infty}\sum_{p=1}^{\infty} \frac{mn\, c_n}{4m^2-1}\left[E(\tfrac{1}{2}, p-m-n)+E(\tfrac{1}{2}, p+m+n)-E(\tfrac{1}{2}, p-m+n)-E(\tfrac{1}{2}, p+m-n)\right]$$
$$\left[f_{s-p}(\tfrac{1}{2},0)+f_{s+p}(\tfrac{1}{2},0)+f_{s-p}(\tfrac{1}{2},2)+f_{s+p}(\tfrac{1}{2},2)\right]$$

$$-2E(\tfrac{1}{2},0)f_s(\tfrac{1}{2},1) - 2\sum_{m=1}^{\infty} E(\tfrac{1}{2},m)\left[f_{s-m}(\tfrac{1}{2},1)+f_{s+m}(\tfrac{1}{2},1)\right]$$

$$+\sum_{n=1}^{\infty} \frac{4}{4n^2-1} E(\tfrac{1}{2},n) f_s(\tfrac{1}{2},1)$$

$$\left.+\sum_{m=1}^{\infty}\sum_{n=1}^{\infty} \frac{2}{4n^2-1}\left[E(\tfrac{1}{2},m-n)+E(\tfrac{1}{2},m+n)\right]\left[f_{s-m}(\tfrac{1}{2},1)+f_{s+m}(\tfrac{1}{2},1)\right]\right\}$$

(D.8)